The Influence of Mechanical and Neural Coupling on Electromyography Signals of the Extrinsic Hand Muscles

by

Carl Richard Beringer III

BS, Drexel University, 2014

Submitted to the Graduate Faculty of the

Swanson School of Engineering in partial fulfillment

of the requirements for the degree of

Doctor of Philosophy

University of Pittsburgh

2020

UNIVERSITY OF PITTSBURGH

SWANSON SCHOOL OF ENGINEERING

This dissertation was presented

by

Carl Richard Beringer III

It was defended on

May 4, 2020

and approved by

Aaron Batista, Ph.D., Associate Professor, Department of Bioengineering

Jennifer Collinger, Ph.D., Assistant Professor, Department of Physical Medicine and Rehabilitation

Doug Weber, Ph.D., Associate Professor, Departments of Bioengineering and Physical Medicine and Rehabilitation

Dissertation Director: Robert A. Gaunt, Ph.D., Assistant Professor, Department of Physical Medicine and Rehabilitation

The Influence of Mechanical and Neural Coupling on Electromyography Signals of the Extrinsic Hand Muscles

Carl Richard Beringer III, PhD

University of Pittsburgh, 2020

Dexterous control of a myoelectric prosthetic hand has been the subject of decades of research and effort but remains an unsolved challenge. In part, it is because dexterous prosthetic control relies upon products from multidisciplinary fields: an articulated high degree-of-freedom (DOF) robotic limb, stable electrodes to capture high-resolution biosignals, the portable computational power to run control algorithms in real-time, and a decoder founded on a strong understanding of how the hand is controlled. Our scientific understanding of muscle activations coordinate to enable skilled and dexterous movements of the hand has not kept pace with the rapid development of technology which may be leveraged to develop a prosthetic hand. Dexterous control of the hand is a complex endeavor which requires simultaneous control over numerous muscles which span multiple joints. These muscles do not act independently and are coupled through mechanical means, such as shared tendons, and neural mechanisms, including diverging descending motor commands. Understanding how the coupling in the hand is present and manifested, particularly through the lens of electromyography, is a vital endeavor which is a necessary step towards development of dexterous prostheses.

In this manuscript, I present my research that uses electromyography to characterize the mechanical and neural coupling within the extrinsic hand muscles. I begin with how the EMG activity of the extrinsic finger muscles, which span across the wrist, is affected by the posture of the wrist and contributes to wrist movements. In the next section, I demonstrate the neural coupling present during movements of the digits and develop a series of generalized models of coactivation and stabilization for the extrinsic finger flexors and extensors. Finally, using the EMG data collected I present the development of an optimization environment to test methods of EMG-to-activation and simulate the forward dynamics of a 17 DOF model of the hand to replicate dexterous movements. These results provide an insight on control of the hand which may prove useful for development of prosthetic control algorithms and demonstrate a testing environment for EMG-to-activation signal processing protocols.

Table of Contents

List of Tables

List of Figures

Preface

"Each one, as a good manager of God's different gifts, must use for the good of others the special gift he has received from God." – 1 Peter 4:10

Over 10 years ago, I was a cavalry scout hunkered down in Baghdad, Iraq wondering what I was going to do with my life after I came home and left the Army. I knew I was going to put my GI Bill to good use, so I just needed to figure out what degree I wanted to pursue. I was always fascinated with biology but also pulled towards engineering. While weighing the pros and cons of both fields, I stumbled upon a newly offered degree program in 'biomedical engineering' and heard about the incredible work being done in brain-machine interfaces. I was instantly hooked and applied to Drexel University in Philadelphia to pursue biomedical engineering.

A year later, I met a wonderful woman named Laura that was simultaneously pursuing her bachelor's and master's degrees while performing research. I was inspired by her drive and ambition, and began pursuing research in the Moxon Neurorobotics Laboratory. Over the next few years, I watched and supported Laura as she graduated with a BS/MS, and then went on to continue her work towards a PhD. I realized that I also wanted to pursue research and make a difference in the world, so I began applying to PhD programs as well.

In 2014, I was accepted to Pitt and offered a position funded by the Defense Advanced Research Projects Agency focused towards restoring wounded warriors known as HAPTIX. For nearly six years, I have poured my heart and soul into this project. There is no greater honor for me than to have been a part of this project and given back to my brothers and sisters in the military, as well as to have tried to make the world a better place. It has been my goal ever since I first heard about biomedical engineering.

There have been many people who have supported me on this journey. In no particular order, I would like to acknowledge and thank them them.

To my amazing wife Laura, the first Dr. Beringer, who has continually served as an inspiration and role model to me. Thank you for supporting and encouraging me all these years; for understanding the crunch times before big meetings, and for all your love.

To my mother for supporting me and letting me vent to her about anything and everything under the sun.

To my advisor and committee members for their support and mentorship.

To the members of Ghost platoon, HHC, 1-18 Infantry, 2nd Brigade, 1st Infantry Division. My brothers-in-arms who made me understand the meaning of sacrifice and teamwork. To the leadership for pushing me as far as I could go. To SFC Brown, for inspiring me to do better because I could be better.

To my son Benjamin, and any more who follow. You motivate me to do and be my best so that I may set a standard that you will follow.

1.0 General Introduction

The human hand is a wondrous appendage that allows us to interact and manipulate the environment around us. It is amazingly versatile and capable of strong, gross movements as well as performing delicate manipulations that require a fine touch. It can even be argued that the hand has become vital for communication in the digital age thanks to texting and e-mail. Achieving such a level of motor control requires the coordination of the many hand muscles which may span across four joints. Further compounding this complexity is the mechanical and neural coupling present in the hand, which prevents the muscles which actuate the digits from acting independently. Because of these factors, the hand should be considered as a complete system rather than an assembly of the palm, thumb, and four fingers.

The loss of a hand is a devastating injury that affects the daily lives of more than 540,000 Americans (Ziegler-Graham, MacKenzie, Ephraim, Travison, & Brookmeyer, 2008). In order to restore function and independence to amputees, prosthetic devices that use electromyographic (EMG) activity collected by surface electrodes from the residual muscles as a control signal are often prescribed. Despite an explosion in research and development of prosthetic control algorithms, myoelectric prosthetic hands have rejection rates of up to 33%, with many users complaining of poor control (Mcfarland, Winkler, Heinemann, Jones, & Esquenazi, 2010). A review of upper limb amputee needs has shown that many patients desire increased independent control of the fingers, a feature not offered by present control systems, so that they may perform activities of daily living such as tying their shoes or buttoning a shirt (Cordella et al., 2016).

The difficulty in developing a prosthetic control system that can completely replicate intended hand movements is due to the complexity of the hand and a gap in understanding of how the hand coordinates movements. Previous studies of the hand, particularly those examining the extrinsic finger muscles, have often only focused on a single muscle during simple movements (Birdwell, Hargrove, Kuiken, & Weir, 2013; Butler, Kilbreath, Gorman, & Gandevia, 2005; Johanson et al., 1990; Kilbreath & Gandevia, 1994; Leijnse, Campbell-Kyureghyan, Spektor, & Quesada, 2008; Reilly & Schieber, 2003; van Duinen, Yu, & Gandevia, 2009). Across these studies, different tasks are used which makes comparison difficult.

In this work, I have sought to understand and characterize the extrinsic hand muscles during a broad range of movements and postures. In Chapter 2, I describe changes in the extrinsic finger muscles EMG activity during different wrist postures and how these muscles assist in wrist movements of able-bodied subjects. In Chapter 3, I examine the behavior of the extrinsic finger muscles during movements of neighboring digits in able-bodied subjects. After this, in Chapter 4 I compare these patterns of EMG activity in trans-radial amputees to the results in the previous chapters.

1.1 Control of the Hand

1.1.1 Skeletal Muscle Tissue and Modeling

Muscle is a form of tissue which generate forces through contraction of the tissue for the production of movements, stabilization of joints, and generation of heat. Muscle tissue is divided into several subtypes, but all muscle tissue has four properties which enable this function: electrical excitability, contractibility, extensibility, and elasticity (Tortora & Derrickson, 2018). Skeletal muscle tissue is a type of muscle tissue responsible for volitional movements of the body through the generation of force. Skeletal muscles are composed of hundreds to thousands of cells (muscle fibers) responsible for force generation. These muscle fibers are further composed of cylindrical structures known as myofibrils, which are comprised of thick and thin filaments. The filaments are organized in longitudinal compartments known as sarcomeres and act as a functional unit. The generation of force via muscle contraction originates within these sarcomeres through the sliding filament mechanism: thick filaments walk along the lengths of neighboring thin filaments, which are attached to the walls of each sarcomere, generating force through the shortening of the muscle. The force generation of muscles as a muscle-tendon unit has been modeled based on its physical properties in Hill-type muscle models described in this equation (Lloyd & Besier, 2003) and a diagram may be seen in Figure 1.1:

$$F^{MT}(t) = F^{MAX}\left[f(l)f(v)a(t) + f_p(l)\right]\cos\left(\varphi(\mathrm{t})\right) \qquad \textbf{Equation 1-1}$$

Where F^{MT} is the muscle-tendon force at time t and is equal to the maximum force (F^{MAX}) multiplied by muscle activation, a(t), tension developed at length l [f(l)] and velocity v [f(v)] plus the passive elastic force at length l [f_p(l)], multiplied by the cosine of the angle between the muscle and tendon.

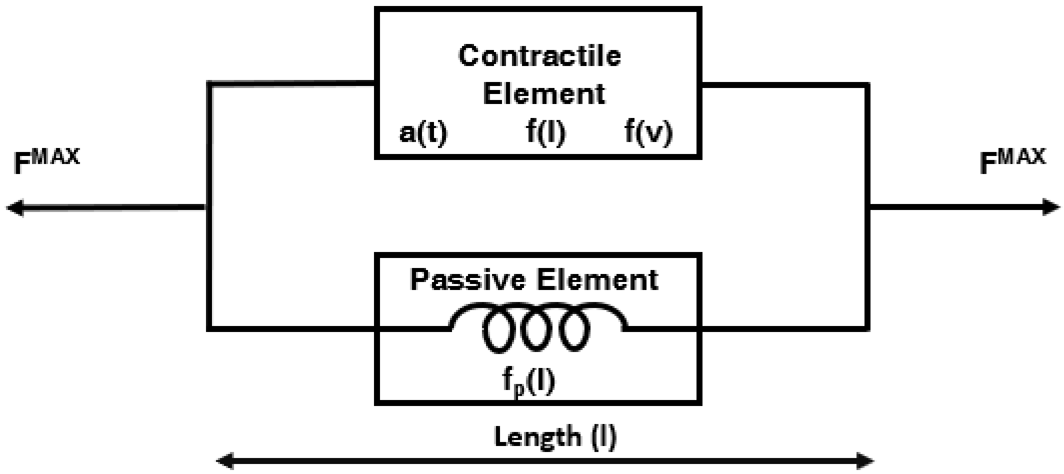

Figure 1.1 Hill-type muscle model diagram

The diagram provides a systems-level overview of the Hill-type muscle model. The passive element is a function of the passive force-length curve. The contractile, or active, element is a function of activation as well as the force-length and force-velocity properties.

The length-tension and force-velocity relationships represent phenomenon based on the sliding filament mechanism. The maximum tension that may be generated changes based on the overlap between the thick and thin filaments; as the muscle sarcomeres lengthen and shorten, the changing overlap between the filaments affects the tension that may be generated. Likewise, the state of a muscle in eccentric or concentric contraction further influences the tension that may be generated. The passive elastic muscle force, as the name suggests, is derived from the elastic properties of the muscle-tendon unit. As a muscle is lengthened, a tension is generated which follows an exponential curve. The tension generated by the passive forces can be negligible when a joint is in a neutral position, but follow an exponential curve when a muscle is stretched such as when a joint is moved near the limits of the range of motion (Lehman & Calhoun, 1990).

1.1.2 An Abridged Anatomy of the Hand

The anatomy and physiology of the hand is a complex topic that has had numerous books devoted to its details (Botte, 2003; Hirt, Seyhan, & Wagner, 2016; Jones & Lederman, 2007; Rayan & Akelman, 2012). In this section, I will briefly describe the characteristics of the muscles and structure of the hand relevant to this work. The hand is composed of 27 bones, which can be divided into three categories: the carpals, the metacarpals, and the phalanges (Taylor & Schwarz, 1955). The carpals are eight irregularly shaped bones which comprise the wrist. The palm of the hand is shaped by the five metacarpal bones, which lead to the four fingers and thumb. The remaining 14 bones are the phalanges: three bones for each finger, and two for the thumb. The phalanges closest to the metacarpal are known as the proximal phalanges, followed by the interphalanges and then the distal phalanges. The thumb is composed of only the proximal and distal phalanges.

The hand is composed of many joints; the digits alone have a total of 15 joints which have a total of 20 degrees of freedom (DOF) (Ingram, Körding, Howard, & Wolpert, 2008). The most proximal joint, commonly referred to as the wrist joint, is composed of two joints: the radiocarpal and midcarpal joints. These two joints permit flexion/extension and radial/ulnar deviation. Although the hand can be pronated and supinated, this movement occurs at the distal radioulnar joint in the forearm, not the wrist. The thumb is articulated by three joints: the carpometacarpal (CMC) joint at the base of the thumb and carpal bones, the metacarpal joint (MCP) between the metacarpal and proximal phalanges, and the interphalangeal (IP) joint located between the proximal and distal phalanges. The finger joints have a similar structure: the CMC joint are relatively fixed between the carpals and finger metacarpals. The MCP joints, which are commonly observed as the knuckles, are between the metacarpals and proximal phalanges. The next joint is the proximal interphalangeal (PIP) joint, followed by the distal interphalangeal joint (DIP).

The many joints of the hand make it capable of performing a wide number of movements, which are articulated by many muscles. The carpal muscles are located in the forearm and act on the wrist to perform flexion/extension and abduction/adduction movements through a combination of activations. These muscles are the extensor carpi radialis longus (ECRL) and brevis (ECRB), the extensor carpi ulnaris (ECU), flexor carpi radialis (FCR), and flexor carpi ulnaris (FCU). These muscles perform multiple actions; for example, FCU performs flexion and adduction (ulnar deviation) of the wrist. For a review of these muscles and their functions, see Jones & Lederman, 2007. Performing a single action such as flexion requires a careful balance of these muscles to counteract movement in abduction and adduction. The muscles which control the fingers can be divided into two groups based on the location of the muscle. The pronator and supinator muscles, which insert outside the wrist, perform pronation and supination movements of the wrist. The intrinsic finger muscles are small muscles located within the hand and are responsible for some thumb movements as well as abduction/adduction of the fingers. Intrinsic finger muscles also assist with flexion and extension movements of the digits in combination with the extrinsic finger muscles. The extrinsic hand muscles, which are central to this work, are located in the forearm and predominantly control the flexion/extension of the fingers and thumb.

The extrinsic finger muscles are connected from origins in the forearm to the fingers through long tendons which cross the wrist joint and insert at either the proximal phalanges or distal phalanges. The muscles included in this group are the extensor digitorum (ED), extensor indicis proprius (EIP), extensor digiti minimi (EDM), flexor digitorum profundus (FDP), and flexor digitorum superficialis (FDS). EIP and EDM insert on only the index finger (D2) and little finger (D5) respectively whereas ED, FDS, and FDP insert on the index, middle, ring, and little (D2-D5) fingers. Movements of the thumb are also controlled through extrinsic muscles, such as flexor pollicus longus, extensor pollicis longus, extensor pollicis brevis, and abductor pollicis longus, although these muscles are outside the scope of this work.

ED, FDS, and FDP control flexion/extension of the digits over the DIP and PIP joints through a combination of actions. ED and FDP insert at the distal phalanges while FDS inserts at the middle phalanges. The actions of ED and FDP fully extend/flex the digit, while activation of FDS flexes the finger at all joints except DIP. The concerted action of these muscles together permits a varied ability to manipulate the finger in different movements and postures (Chase & White, 1978). The ability of these three muscles to control more than eight joints is a complex topic which will be addressed in the following sections.

1.1.3 Mechanical Coupling of the Hand

ED, FDS, and FDP are considered to be individual muscles yet are the primary actuators of the fingers. The ability of these three muscles to control flexion and extension of the digits individually is only possible because those muscles are composed of smaller compartments which directly actuate the digits. While other muscles may have only a single tendon or two linking the muscle to the actuated joint, these muscles have multiple tendons which cross the wrists and insert on the phalanges (Malerich, Baird, McMaster, & Erickson, 1987; von Schroeder & Botte, 1995).

The tendons which spread to the digits are interconnected by the juncturae tendinum (Von Schroeder & Botte, 2001) and in some cases resemble spider webs (Leijnse, Carter, Gupta, & McCabe, 2008; von Schroeder & Botte, 1995). The organization and connections of these tendons can vary across subjects (Schenck, 1964; von Schroeder & Botte, 1995; Von Schroeder & Botte, 2001). This variation may be greater than a simple difference in connectivity; unusual anatomical connections such as FDP and a thumb flexor have been reported, with one study finding it present in at least one hand of 25% of cadavers (Linburg & Comstock, 1979) . These shared connections contribute to the mechanical distribution of force of the hand. As a muscle contracts, tension is generated on the tendon and its shared connections which insert on the other digits. If a single part of the muscle is only activated and generating tension for movement of one digit, digits which share tendinous connections may be affected. These effects are part of what is described as mechanical coupling – the mechanical characteristics of one part of the hand have an influence on another.

Further contributing to the mechanical coupling of the hand is the change in muscle lengths based on the hand posture. This is expected at a single joint: for example, a full extension of the elbow will result in a lengthening of the biceps. Similarly, a full extension of a finger will result in increase on the tension of the FDP tendon and a lengthening of the FDP muscle (Tanaka, Amadio, Zhao, Zobitz, & An, 2005). However, the extrinsic hand muscles span more than one joint and may be influenced by the state of those joints. The position of the wrist affects these muscle lengths and the tension of the muscle, thereby altering the force exerted by a finger (Kursa, Lattanza, Diao, & Rempel, 2006; Li, 2002; Tanaka et al., 2005).

The mechanical coupling in the hand is part of why it should be described as a system rather than a series of parts. The shared tendinous connections and influence by joint angles has an effect on the joints and muscles of the hand and shows that performing even simple movements is a challenge. However, the mechanical coupling is not the only aspect of the hand that makes it such a complex system.

1.1.4 Neural Coupling of the Hand

Beyond mechanical coupling, the hand is subject to neural coupling as well. In an experiment by Lang and Schieber, excursion angles of the fingers were tracked during single digit volitional (‘active’) movements and passive movements where the finger was moved by an outside force. When the excursions of the non-moved digits during active and passive movements were compared, it was found that the non-intended digits moved more during active than passive movements (Lang & Schieber, 2004). This simple experiment demonstrated neural coupling in the hand: active digit movements do not occur independently and cause movement of the neighboring digits.

1.1.4.1 Hand Synergies – Kinematics and Muscles

The neural coupling present in the hand may be a feature for a limb that appears to be specialized for grasping. The use of the hand has been divided into two categories: movements requiring the simultaneous use of multiple digits for grasp, or for the individuated movement of a digit. Grasp and grasping movements are the most common uses of the hand (Schieber & Santello, 2004), yet the use of the hand for grasping is a late evolutionary development and the human capability to create a variety of grasps is unmatched. Even the chimpanzee, our closest relative and whose hand morphology resembles that of humans, are unable to create a precision or power grip (Napier, 1960).

Grasping requires the coordinated movement of multiple digits in order to shape the hands around an object. When an individual reaches for an object, the fingers begin to assume the shape to grasp an object as the arm travels along its trajectory (Mason, Gomez, & Ebner, 2001) and show consistent covariation across the finger joints simultaneously (Santello, Flanders, & Soechting, 2002). Control over the many DOFs of the hand can be described by a small number of coordination patterns known as synergies. Principal component analysis (PCA) during grasping has shown that two components can account for more than 80% of the variance (Santello, Flanders, & Soechting, 1998).

The kinematic synergies across the joints of the hand are driven by the extrinsic hand muscles which receive diverging inputs from motor neurons (Butler et al., 2005; Keen & Fuglevand, 2004a; Reilly & Schieber, 2003; Yu, van Duinen, & Gandevia, 2010). The diverging inputs terminate in the subcompartments of ED, FDS, and FDP, which have ”highly selective core regions” that act specifically on each finger, and specifically for the movement of each digit and less selective regions at the periphery which are active for movements of the neighboring digit (Reilly & Schieber, 2003). EMG studies of these muscles have supported the synergies observed in the kinematic domain and provided a foundation on which the force synergies may be understood. Motor unit synchronies in muscles provide evidence of common synaptic input to motoneurons and functionally coordinate muscle synergies. Motor unit synchrony has been observed in the compartments of ED during hand opening movements (Keen & Fuglevand, 2004a). Work by Winges *et al.* has consistently shown motor unit synchrony between the thumb and finger flexors, as well as between the compartments of the finger flexors (Winges & Santello, 2004). This synchrony was shown to be particularly strong between the thumb and D2 flexor muscles (Winges, Johnston, & Santello, 2006) and may play a role in precision grip. Motor unit synchronization is also present in the intrinsic hand muscles, but to a much lesser extent than the extrinsic hand muscles (Huesler, Maier, & Hepp-Reymond, 2000). Motor unit synchrony is not a specialization for a single synergy, as work has found that motor units may participate in multiple synergies and that organization of synergies is distributed (Weiss & Flanders, 2004). Muscle synergies have also been observed between the extrinsic and intrinsic hand muscles: Johnston *et al.* demonstrated simultaneous and uniform scaling of EMG activity across these muscles during a precision grasp as wrist angle was altered (Johnston, Bobich, & Santello, 2010).

1.1.4.2 Neural Basis of Synergies

Identifying the origin of the neural coupling within the hand is a challenging endeavor. In the motor cortex, the fingers have a somatotopic representation in the motor cortex (Beisteiner et al., 2001; Dechent & Frahm, 2003). Neural recordings from these areas have been used to decode and reconstruct individual finger movements (Acharya et al., 2008; Aggarwal et al., 2008; Aggarwal, Tenore, Acharya, Schieber, & Thakor, 2009). However, the somatotopy of these regions features significant overlap (Dechent & Frahm, 2003) and transcranial magnetic stimulation in humans has induced synergistic finger movements (Gentner & Classen, 2006). Intracortical microstimulation of the primary motor cortex has induced synergistic muscle activity similar to volitional movements in nonhuman primates (Graziano, Cooke, Taylor, & Moore, 2004; Overduin, d'Avella, Carmena, & Bizzi, 2014; Overduin, D'Avella, Roh, & Bizzi, 2008). In an fMRI study of hand shaping and posture, Leo *et al.*showed that activity in motor regions could be described as a function of a small number of motor primitives that grouped together multiple joints (Leo et al., 2016).

At the spinal cord level, it has been demonstrated that spinal interneurons facilitate the divergence of motor commands to the hand muscles. In nonhuman primates, spike-triggered averaging of EMG activity of hand muscles has identified the role of spinal interneurons in postspike facilitation and postspike suppression in facilitating grip (Takei & Seki, 2010). Further examination of this phenomenon has identified that the link between premotor interneurons and muscle synergies, leading Takei *et al.* to claim that these interneurons underlie the observed coordination of hand movements (Takei, Confais, Tomatsu, Oya, & Seki, 2017). Given all these findings, it appears likely that muscle synergies are organized at both a spinal and supraspinal level.

1.2 Electromyography

The volitional contraction of skeletal muscle tissue occurs when spinal motor neurons generate action potentials that propagate along their axons and eventually depolarize at the synapse between the motor neuron axon and the skeletal muscle fiber, known as the neuromuscular junction. The depolarization generates a muscle action potential through a series of events, beginning with the release of acetylcholine at the neuromuscular junction. Acetylcholine diffuses across the synapse and binds to receptors on the myocyte at the motor end plate, triggering a muscle action potential. The muscle action potential travels along a channel known as the transverse tubule, opening the calcium channels along the way which release calcium ions into the intracellular space and enable the thick filaments to walk along the length of the thin filaments, thereby shortening and causing a muscle contraction.

Electromyography (EMG) is a technique which measures muscle activity by recording the electrical activity of the muscle action potential. EMG activity may be recorded non-invasively with surface electrodes or through the placement of intramuscular electrodes directly within the muscle belly (Figure 1.2). Both methods have their advantages and disadvantages. Surface EMG recordings are the summation of motor unit action potentials within an area and provide a global view of muscle activity (De Luca, Adam, Wotiz, Gilmore, & Nawab, 2006). In areas with small, densely-packed muscles such as the forearm, surface EMG recordings contain the activity of multiple muscles and it is difficult to disentangle the behavior of any one muscle due to crosstalk (Lynn, Bettles, Hughes, & Johnson, 1978). Intramuscular electrodes provide a finer focal resolution than surface recording and are capable of recording individual motor unit action potentials (Reilly, Nordstrom, & Schieber, 2004). Intramuscular electrodes are also less susceptible to crosstalk (Basmajian & De Luca, 1985). These characteristics make intramuscular electrodes an apt choice for recording from the extrinsic hand muscles. Multiple electrodes may be placed in ED, FDS, and FDP to record from the compartments which actuate the digits (Birdwell et al., 2013; Birdwell, Hargrove, Weir, & Kuiken, 2015; Cipriani, Segil, Birdwell, & Weir, 2014). Recording from deeper muscles such as FCU is also possible, whereas surface electrodes would likely be unable to accurately capture these signals due to spatial filtering.

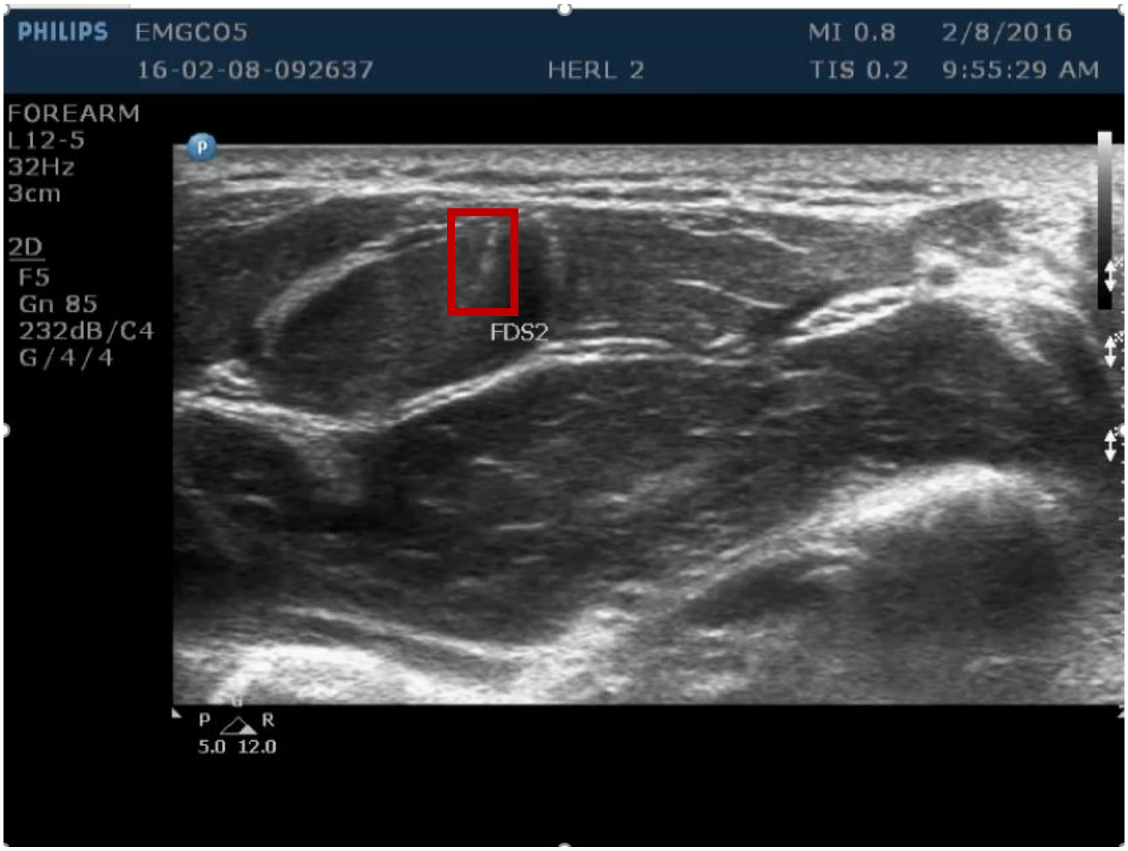

Figure 1.2 Insertion of an intramuscular electrode into a muscle

An intramuscular electrode, highlighted by the red box, is shown during insertion into FDS2 under ultrasound guidance.

Intramuscular electromyography has also seen renewed interest due to innovations in technology and applications towards prosthetic control devices. Presently, placement of intramuscular electrodes uses a needle to percutaneously implant the electrode in muscle tissue. Due to this, intramuscular electrodes can only be used for short-term (less than 24 hour) recordings and are susceptible to movement artifacts. Recent designs have demonstrated the capability for intramuscular electrodes to be permanently implanted in muscle tissue and wirelessly transmit information (Pasquina et al., 2014). The implantation of intramuscular electrodes offers benefits over surface electrodes for prosthetic control beyond the previously mentioned improved recording capability. Surface electrodes are susceptible to changing impedances due to sweat and air temperature which can threaten the stability of EMG recordings (Bell, 1993). Surface electrodes must be changed out daily, and the variation in the placement can also affect the signal quality or control algorithm (Hargrove, Englehart, & Hudgins, 2006). The chronic stability of intramuscular electrodes combined with the capability of recording small and previous unrecordable sites therefore makes this an appealing approach. A variety of implantable EMG recording devices are currently being developed (McDonnall, Hiatt, Smith, & Guillory, 2012; Merrill, Lockhart, Troyk, Weir, & Hankin, 2011; Pasquina et al., 2014), which may make a clinical take home device available in the near future.

1.2.1 EMG Signal Processing

The raw EMG activity collected directly from the muscle must undergo signal processing in order to be used for analysis or prosthetic control. For prosthetic control and use in Hill-type muscle models, EMG activity is often converted to a form of activation as described in Equation

1-1. EMG-to-Activation processing methods vary among researchers but have some common elements. The signal processing for intramuscular and surface EMG also varies due to the differences in the power spectrum (Christensen, Søgaard, Jensen, Finsen, & Sjøgaard, 1995). As much of this work is focused on intramuscular EMG, we will focus on the processing methods used for this signal.

A typical EMG-to-activation protocol begins with bandpass filtering EMG activity between 100 Hz to 4000 Hz, although significant variation in the specific frequencies are often used (Burgar, Valero-Cuevas, & Hentz, 1997; Johnston, Winges, & Santello, 2005; Kamavuako, Farina, Yoshida, & Jensen, 2009; Reilly & Schieber, 2003). The bandpass filter serves to remove high frequency noise and signal drift as well as movement artifacts which are caused by the physical movements of the recorded subject and reduce high frequency interference. The filtered signal is then typically rectified to obtain a positive waveform, as activation is considered a positive number. The next step in the processing chain often varies but typically has the same result of low pass filtering the signal. Many researchers then calculate the root mean square or moving average value of the signal over a 50-200ms time window or use a traditional low-pass filter the data at 10 Hz or lower (Cipriani et al., 2014; Smith, Kuiken, & Hargrove, 2016). These approaches arguably reach the same outcome, and work which has sought to compare the various approaches has found minor difference in force prediction accuracy (Mathiesen et al., 2010). Nonetheless, the resultant signal is then typically normalized to the maximal activity which has been recorded. The maximal activity is typically obtained through a maximum voluntary contraction (MVC), in which the subject attempts to generate as much isometric force as voluntarily possible. Other alternative methods of EMG-to-Activation have been proposed such as non-linear activation dynamics (Buchanan, Lloyd, Manal, & Besier, 2004), but the methods described above are standard. An example of such a process may be seen in Figure 1.3, which is replicated in Chapter 5 as Figure 5.3.

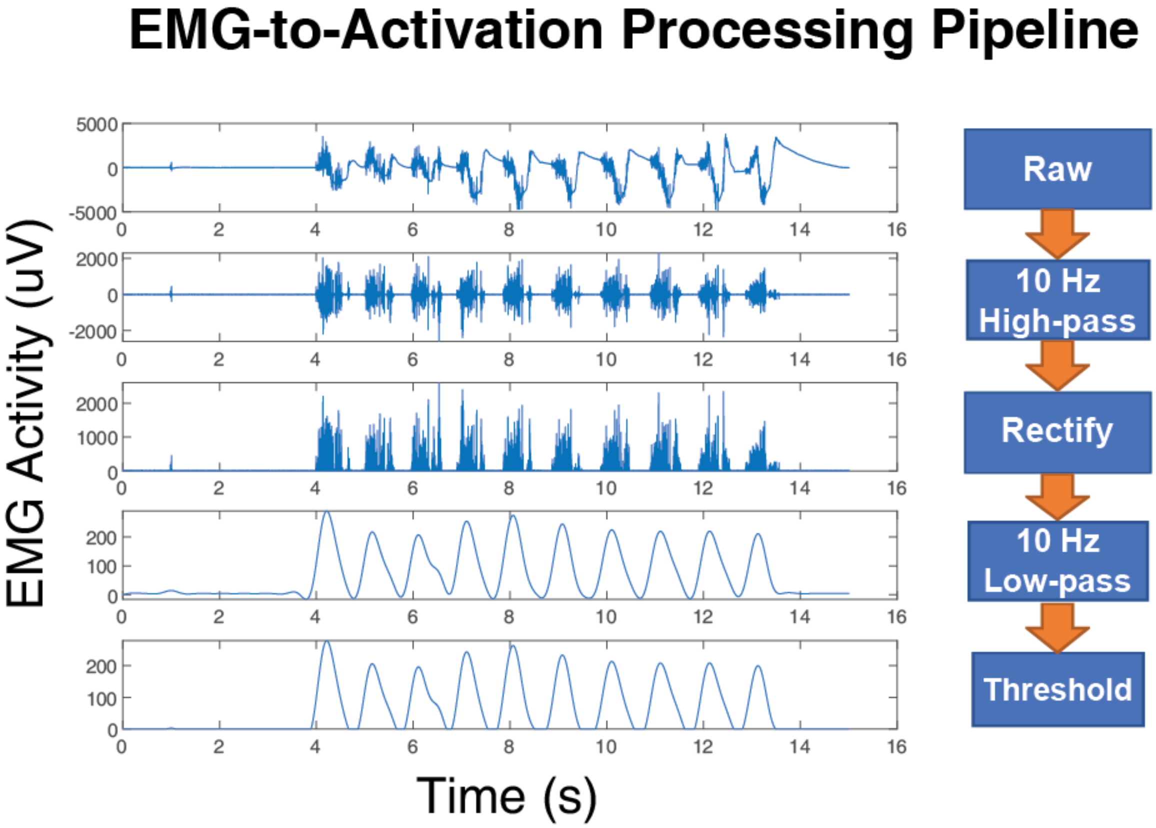

Figure 1.3 Sample EMG-to-activation process

Raw EMG activity is high-pass filtered before undergoing rectification, low-pass filtering, and a thresholding. This processing removes noise and drift from the signal and converts the EMG activity to activation. After thresholding, the signal is normalized to an arbitrary threshold and the optimizer searches to find the appropriate gains to scale the signal. Figure and caption are replicated from Figure 5.3.

EMG activity is not always used as an analogue for activation for prosthetic control. Prosthetic control designers may only be interested in certain features of the EMG signal and maximizing the information content received. Arguably the most common features used for prosthesis control are the time domain features popularized by Hudgins *et al* (Hudgins, Parker, & Scott, 1993). Briefly summarized, the Hudgins time domain features measure signal properties during a window of time. These properties are the mean absolute value, mean absolute value slope, rate of zero crossings, rate of slope sign changes, and the temporal length of the waveform (Hudgins et al., 1993). Other common time-domain features used are variance (Huang & Chen, 1999) and root mean square of the signal (Mathiesen et al., 2010). Willison amplitude (sometimes incorrectly referred to as ‘Wilson amplitude’) is a less commonly used feature that tallies the number of times the difference between sequential EMG samples is above a threshold during a moving window (Huang & Chen, 1999). Originally developed to identify muscle disease (Willison, 1964), the technique has shown a strong relationship to isometric force (Mathiesen et al., 2010).

The feature extraction methods listed are nowhere close to exhaustive as there are at least 50 different types (Phinyomark et al., 2013). There have been some efforts to compare the effectiveness of feature extraction on either prosthetic control tasks (Phinyomark et al., 2013; Scheme & Englehart, 2014) or predicting isometric force (Mathiesen et al., 2010). Of these three studies, Hudgins time domain features and Willison amplitude show some of the best performance. It should be noted that these studies are in no way exhaustive – the implementation of these features extractions has flexibility, e.g. the mean absolute value may be implemented in a fixed or sliding window and the timing of the window is open for debate, and the authors did not base their implementation on the optimal performance.

1.2.2 Myoelectric Prosthetic Control

Upper limb loss affects more than 540,000 Americans and is typically caused by either congenital birth effects or traumatic injury (Ziegler-Graham et al., 2008). Myoelectric prosthetic limbs are commonly prescribed to restore lost functionality (see section 1.0 for more information). EMG activity and its relation to muscle force has been well-studied due to its application as a command signal for a prosthetic device. The explosion of robotics technology has seen the development of motorized prosthetic hands that feature up to 6 controllable powered joints, such as the DEKA LUKE hand (Resnik, Klinger, & Etter, 2014). It can be argued that the limiting factor in myoelectric prosthetics is not the prosthesis, but the inability of control algorithms to take advantage of the degrees of freedom and restore dexterous movements to the user. A study by the Department of Veterans Affairs found that 33% of veterans who received an upper limb prosthesis rejected the device, with a significant number citing ‘not functional’ as the reason (McFarland et al., 2010). A wider review of upper limb amputee needs has shown that many patients desire increased independent control of the fingers so that they may perform activities of daily living such as tying their shoes or buttoning a shirt (Cordella et al., 2016).

Myoelectric control algorithms that seek to restore and replicate hand function must have several characteristics: it must support simultaneous movement of multiple DOF, allow for arbitrary movements and positions of the joints, and perform reliably enough that users are not concerned about erroneous movements or failures. These features are similar to those outlined by Dario Farina in describing the ideal characteristics of an upper-limb prosthesis: simultaneous and proportional control, insensitive to day-to-day changes in electrode impedance, adaptive to user fatigue, feature a minimal number of electrodes, require little training and minimal retraining, and produce movements with a delay below 200 ms (Farina et al., 2014). Efforts have been made to develop control schemes to address these priorities, but to date none have met these criteria.

1.2.2.1 Direct Control

Direct control is a control algorithm which maps the EMG activity of a muscle to a velocity signal for at least one DOF. Typically, a limited number of muscle sites are recorded and only a single DOF is controlled at a time. If a user requires the movement of multiple degrees of freedom, they must toggle through the modes (sequential control). Modes may be toggled through co-contractions or a manual toggle such as a foot switch (Williams, Meier, & Atkins, 2004). Mode switching may be beneficial to users, as a single pair of electrodes may be used to control a number of DOFs by cycling through a number of DOF and manually manipulating one at a time.

The implementation of direct control schemes can vary, but differential control is commonly used. In differential control, the difference in EMG activity between two EMG recording sites is measured, and if the difference is above a threshold then the joint moves in the desired direction (Smith, Kuiken, & Hargrove, 2014) at either a fixed (on-off control) or scaled (proportional control) velocity (Fougner, Stavdahl, Kyberd, Losier, & Parker, 2012). On-off control methods were traditionally offered in the past, but emerging proportional control systems have begun to replace them. There has been sparse literature which has sought to compare the effectiveness of on-off versus proportional control, and of the studies that have been performed there has been no definitive answer (Fougner, Stavdahl, & Kyberd, 2014; Sears & Shaperman, 1991). Direct control has also been implemented where a single EMG channel controls a joint. The default state of the DOF is at one extreme, and EMG activity is mapped to move the joint into the opposite state. When EMG activity is not present or below a set threshold, the joint returns to the original state (Cipriani et al., 2014).

Direct control has been attempted to control multiple DOF simultaneously with moderate success (Cipriani et al., 2014; Smith et al., 2014). A follow-up study by one of these groups compared simultaneous differential control to a method that used the weighted terms of every recorded muscle to control each DOF, and found that this method had improved performance (Smith et al., 2016). These findings suggest that additional information on movements may be captured from muscles not directly associated with the action. It can further be argued that these findings indirectly support the view of the hand as a system, and that muscles which are not directly controlling a joint may provide some synergistic support.

1.2.2.2 Pattern Recognition

Pattern recognition is a method of prosthetic control that classifies extracted EMG features into a preset movement or posture using recordings from muscle sites (Scheme & Englehart, 2011). Pattern recognition algorithms can vary; for example, a single EMG channel may sequentially control a single DOF at a time (Figure 1.4b) or multiple EMG channels may simultaneously control multiple DOF in parallel (Young, Smith, Rouse, & Hargrove, 2013). The chief advantage of pattern recognition is that it may allow for complex grips or hand configurations with a single command. Clinically available devices such as the i-Limb by Touch Bionics presently allow for the user to associate many predetermined grips and hand states with the EMG activity such as a co-contraction of muscles or 1-3 bursts of activity (*touch bionics Product Catalog*, 2015). Other pattern recognition approaches require a training data set based on intended movements. For example, the user can train to the hand open/close functionality of a classifier by attempting to replicate those movements while following a video prompt. Recent work has suggested that the use of the prosthesis itself, rather than a video, may improve this training (Simon, Lock, Stubblefield, & Hargrove, 2011).

The method of classification used for pattern recognition can widely vary. Classification schemes have used linear discriminant analysis (Leone et al., 2019; Zhang, Zhao, Han, & Zhao, 2014), artificial neural networks (Nazemi & Maleki, 2014; Tenore et al., 2007), or support vector machines (Noce et al., 2019). Linear discriminant analysis is typically favored at it is computationally efficient and accurate (Hakonen, Piitulainen, & Visala, 2015; Scheme & Englehart, 2011). The classification scheme is only part of the equation: developers have a wide array of EMG features to use as input for a classifier. The selection of a classifier and the features extracted must be carefully thought through. Work by Scheme and Englehart showed differences in classification error of up to 30% within the same classifier depending on the EMG feature used (Scheme & Englehart, 2014). This matter is further complicated as there was no clear EMG feature that consistently outperformed all others. Time domain features had the lowest error for linear discriminant analysis classifiers, but the most error compared to other features for support vector machines.

In contrast to direct control, pattern recognition removes the arbitrary freedom and movement of a joint in favor of fluid transitions between complex grips and postures. Task-based comparisons between pattern recognition and direct control methods have been mixed – take-home trials and in-lab experiments have claimed that pattern recognition outperforms conventional control (Hargrove, Lock, & Simon, 2013; Hargrove, Miller, Turner, & Kuiken, 2017; White et al., 2017) although in-lab testing by one of these groups has claimed increased efficiency using simultaneous direct control (Smith et al., 2014). There has been some effort to study user preference for these control methods. In one take-home study, users preferred direct control and performed better on tasks that forced users to use a prosthesis while under a high cognitive load (Resnik et al., 2018). In contrast, a pair of studies using able-bodied subjects in a lab environment found a lower cognitive load and improved performance with direct control (Deeny, Chicoine, Hargrove, Parrish, & Jayaraman, 2014; White et al., 2017).

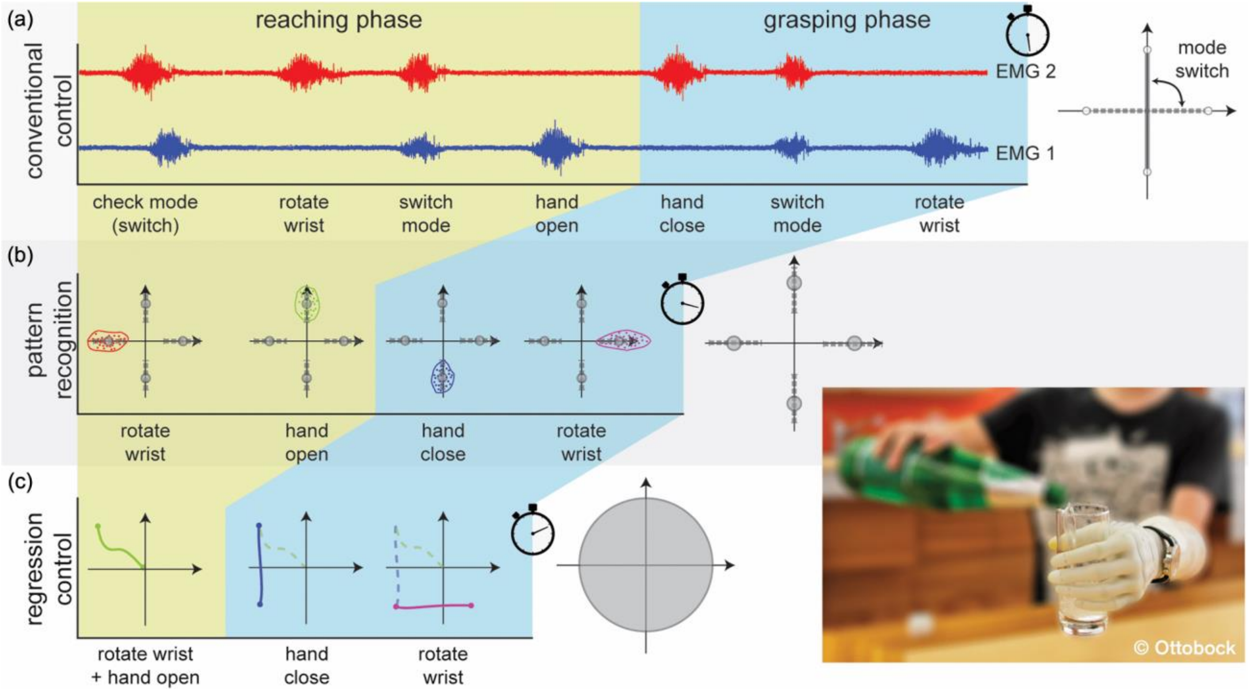

Figure 1.4 Comparison of myoelectric control methods

Illustration of three myoelectric control methods during a reach and grasp task a) conventional control, also known as direct control, controls a single DOF sequentially. The user switches between DOF by cocontracting the recorded muscles. b) An applied pattern recognition scheme for the same task. The feature space of the EMG signal is represented on a two-dimensional axis with four classes corresponding to the two DOFs. c) A direct control method that allows for simutlaneous proportional control over two DOFs, represented as two axes. The user is able to simultaneously rotate the wrist and open the hand, or perform both tasks individually. Figure adapted from (Farina et al., 2014) © 2014 IEEE

1.2.2.3 Model-based Controllers

Model-based controllers are an emerging technology that use controllers based on biomimetic models to offer naturalistic control over a prosthetic limb. The naturalistic control of a model-based controller is appealing as pattern recognition and direct control algorithms have a significant cognitive load associated with higher DOF control (Deeny et al., 2014). The development of a system based on biomimetic models has also been proposed to be more robust than a traditional prosthetic control algorithm. Pattern recognition and direct control rely on mapping EMG activity from specific muscles to limb kinematics, but do not account for the changes in EMG activity in response to orientation of the limb in space; ignoring these factors can lead to erratic and deteriorated performance (Jiang, Muceli, Graimann, & Farina, 2013). Model-based controllers may take these factors into account when predicting movements (Sartori, Durandau, Došen, & Farina, 2018). Pan *et al.* directly compared the performance of a musculoskeletal model versus linear regression and artificial neural network control over a virtual hand when the arm was placed in 9 different positions in space. In comparison to linear regression and artificial neural networks, the model-based controller had higher overall correlation coefficient, a lower normalized RMS error, and less variation across trials (Pan, Crouch, & Huang, 2019). These findings suggest that not only can a model-based controller outperform other methods, but that the performance will be consistent across positions of the hand and arm which are commonly encountered during activities of daily living.

Approaches to model-based control have varied amongst researchers. Sartori *et al.* developed a 3-DOF (2 DOF at wrist, 1 hand open/close) system using a subject-scaled model from OpenSim (Sartori et al., 2018). Crouch and Huang found that a lumped-parameter model was able to be quickly trained and used to trace a path with a virtual hand across 2 DOF (Crouch & Huang, 2017). A 23 DOF faster-than-real time model has also been developed (Blana, Chadwick, van den Bogert, & Murray, 2017), but published work on matching model to subject kinematic cs has only tested a few DOF (Blana et al., 2020).

While model-based controllers have the possibility of scaling up to higher DOF, they have not reached a level higher than 3 independent DOF. Part of this may be that it has only been recently that model-based controllers have become a viable and efficient alternative. Previously, hardware limitations in the past could not support simultaneously recording and processing EMG activity while also simulating the forward dynamics of a musculoskeletal model. Recent work in the field has contributed to easing this computational load by simplifying the calculation process for the biomechanics of forward simulations (Sobinov et al., 2019).

1.3 Summary of Work

The previous sections of this work have described the anatomy and physiology of the hand. The muscles, tendons, and bone tissues that construct the hand are well understood. The path of a neural signal to move the hand may be traced from the inception in cortical tissue down the spinal cord to the muscles that they innervate. The synergistic activations of the hand have been documented through principal component analysis. Through this knowledge, it is understood that mechanical and neural coupling is ever present. However, there is a gap in understanding these phenomena through the lens of electromyography. This is arguably one of the most necessary viewpoints that is needed, as it directly relates towards the clinical design and development of myoelectric prosthetic controllers. Technological development of robotic hands and EMG recording technology has surpassed prosthetic control algorithms, which have been limited in part due to our lack of understanding in the effects of coupling on EMG activity of the extrinsic hand muscles. The work contained in this dissertation is aimed at closing this gap.

First, the effects of mechanical coupling on EMG activity of the extrinsic finger muscles will be outlined and studied (Chapter 3). The changes in EMG activity in response to changes in wrist posture will be described, as well as how the extrinsic finger muscles assist in wrist movements. In the next chapter, neural coupling of the extrinsic finger muscles will be described in the context of EMG activity (Chapter 4). Neural coupling will be uncovered by describing the EMG activity across the extrinsic finger muscles during the agonist and antagonist movements of neighboring digits. The knowledge gained regarding EMG activity will be applied towards controlling a 17 degree-of-freedom model via forward simulation, and the development of a testing environment for prosthetic control (Chapter 5). Overall, the principal aim of this thesis is to develop fundamental knowledge related to EMG control of complex hand movements, with a focus on individual joint movements of the fingers and wrist, and apply to this knowledge to develop advanced prostheses for upper limb amputees.

2.0 General Methods

2.1 Experimental Summary

11 healthy, able-bodied subjects (7 males, 4 females) were included in this study. Subject ages ranged from 25-32 with an average age of 28.2±2.7 years. All subjects provided informed consent prior to any experimental procedure and all procedures were approved by the University of Pittsburgh and Army Research Labs Institutional Review Boards. All methods were performed in accordance with the relevant guidelines and regulations. Sixteen percutaneous EMG electrodes were implanted in extrinsic muscles of the hand (Table 2.1). Subjects wore a glove fitted with electromagnetic trackers to capture hand kinematics (Figure 2.1). Subjects then performed an extensive series of single joint movements with varying finger and wrist postures while EMG and kinematics were recorded.

2.2 Percutaneous EMG Recording

Percutaneous bipolar fine-wire electrodes (Motion Lab Systems, Inc., Baton Rouge, LA) were placed in sixteen forearm muscles. Each electrode pair consisted of two 0.051 mm diameter insulated stainless steel wires. Each wire was passed through a 27 gauge (30 mm long, for superficial muscles) or 25 gauge (50 mm long, for deep muscles) hypodermic needle and the ends of each wire were bent to form a hook. On each wire, 2 mm of insulation was removed from the end to form the active recording area of the electrode, and the two electrodes were offset from each other so that the deinsulated portions did not touch. Each bipolar pair was placed into the target muscle with a single needle insertion. Muscle locations were identified using palpation and ultrasonographic visualization techniques during instructed movements to guide electrode insertion (Henzel et al., 2010). Electrodes were placed by an experienced physician and subjects were asked to make many different movements during the ultrasound procedure and during electrode insertion itself to localize the electrode to the correct muscle or muscle compartment. After the electrode tips were visualized to be in the correct location using ultrasound, the needle was removed, leaving the wires in place as a result of the hooked ends. Care was taken to prevent the wires from becoming dislodged. The subject was asked to exercise the hand and wrist so that the wires were embedded in the muscle tissue and then a small adhesive bandage was placed at the wire exit site to prevent the wires from being snagged and dislodged. After all electrodes were placed, the arm was wrapped in a bandage to protect all the electrodes, lead wires and cabling on the arm for the duration of the experiment.

As this was part of a larger study, some of the 16 implanted electrodes targeted wrist muscles while others targeted the extrinsic finger muscles. A complete list of muscles implanted for each subject is listed in **Table 2.1.** Intramuscular EMG recordings were digitized with a multichannel neural recording system (Grapevine Neural Interface System with Surf S2 headstage, Ripple, Inc) at 30 kHz.

Table 2.1 List of muscles and electrodes implanted in each subject

	Subject										
Muscle	1	2	3	4	5	6	7	8	9	10	11
EIP	x	x	x	x		x	x	x	x		x
ED2	x	x	x	x		x		x		x	x
ED4	x	x	x	x	x	x	x	x	x	x	x
EDM					x		x	x		x	
FDS2	x			x							x
FDS3		x	x	x		x		x	x		x
FDS4	x	x		x	x	x	x	x	x	x	
FDS5											
FDP2	x	x		x							
FDP3			x			x	x		x	x	x
FDP4				x	x			x			x
FDP5		x	x		x			x			x
ECU	x	x		x	x	x	x	x	x	x	x
ECRL	x	x	x	x	x		x	x	x	x	x
FCU	x		x	x	x	x	x	x	x	x	x
FCR	x	x	x		x	x	x	x	x	x	x
SUP	x		x	x	x	x	x		x	x	
PRO	x		x	x	x	x	x		x	x	
APL	x		x	x	x	x	x	x	x	x	x
FPL	x	x	x	x	x	x	x	x	x	x	x
EPL	x	x	x	x	x	x	x	x	x	x	x
EPB		x									

2.3 Kinematic Motion Tracking

Hand and arm kinematics were recorded using an electromagnetic tracking system (trakStar, Ascension Technology, Inc.) integrated into the MotionMonitor (Innovative Sports Training Inc., http://www.TheMotionMonitor.com) recording software. This motion tracking system provides the ability to track the location of a series of wired sensors in six-dimensional space by creating a pulsed electromagnetic field in the workspace. The primary advantage of this system is that it enables sensors to be tracked even when obscured, which is particularly valuable for monitoring motion of the digits. The tracking sensors were attached to a glove, and located over the proximal, intermediate, and distal phalanges of the index finger; the proximal and distal phalanges of the middle, ring, and little finger; the metacarpal and phalanges of the thumb; and the dorsal center of metacarpals (Figure 2.1a). Tracking sensors were also placed over the distal portion of the radius and lateral aspect of the biceps to track the position of the arm. Subject-specific arm and hand segments were then created using the digitization process in the MotionMonitor software. The OpenSim v3.3 Inverse Kinematics tool (Delp et al., 2007) was then used to extract the joint angles from the .trc files using a scaled musculoskeletal model (Gritsenko, Hardesty, Boots, & Yakovenko, 2016).

2.4 Experimental Tasks

Subjects were asked to follow the movements of a virtual hand displayed on a computer screen. Subjects were seated, with their hand and arm held in front of them above the table (Figure 2.1b**)**. Each movement exercised a single DOF of the fingers or wrist for ten repetitions at 1 Hz. A list of all 42 trial types is provided in Appendix Table 1. For D2-D5 movements, subjects were asked to produce coupled motions of the metacarpal phalangeal joint along with the proximal and distal interphalangeal joints, with a focus on moving the metacarpal phalangeal joint through 90 degrees. All fingers motions were repeated while the subject maintained the wrist in a neutral posture (hand aligned with the forearm and thumb pointing up), or with the wrist in a flexed, extended, pronated, or supinated position at the limit of the wrist range of motion. During wrist movements, the fingers were held in either flexed or extended positions and the exercises were performed while the wrist was held neutral, pronated, or supinated. Pronation/supination movements were only performed during neutral wrist postures. The initial posture for D2-D5 movements was with all fingers extended and the wrist in one of five positions. For wrist movements, the initial starting pose was with the wrist held neutral and the fingers either flexed or extended, depending on the trial.

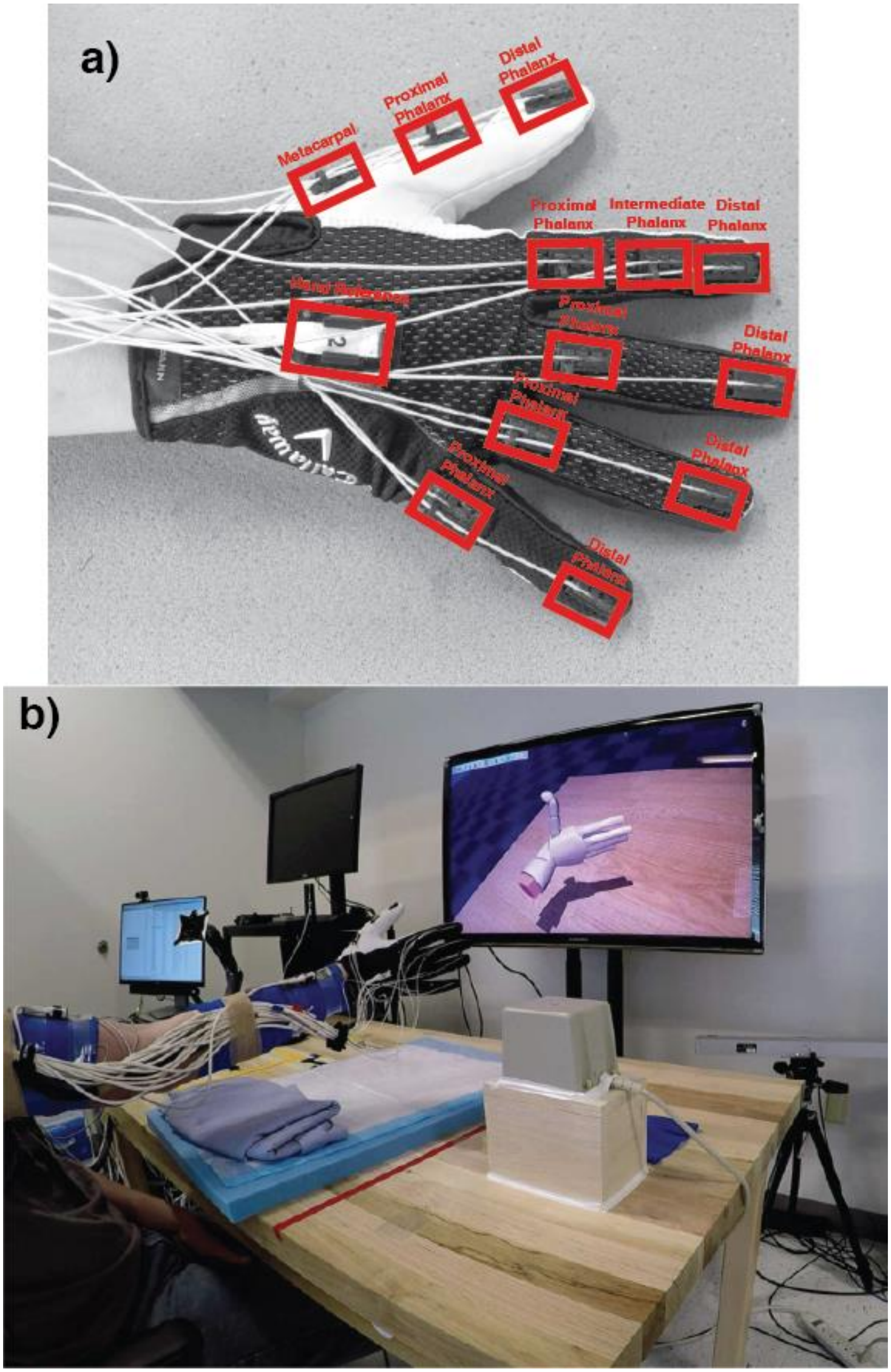

Figure 2.1 Overview of the experimental set-up

a) Electromagnetic tracking glove that subjects wore during the experiments. The red rectangles show placement of electromagnetic sensors in relation to the joints of the fingers. b) Subjects viewed and followed a video which demonstrated the hand posture, movement, and timing.

3.0 Effects of Wrist Posture on Finger EMG Activity

The majority of the work in this chapter has been published in Scientific Reports with the exception of the work in classification.

Wrist posture impacts the muscle lengths and moment arms of the extrinsic finger muscles that cross the wrist. As a result, the electromyographic (EMG) activity associated with digit movement at different wrist postures may also change. Therefore, we sought to quantify the posture-dependence of extrinsic finger muscle activity. Fine-wire bipolar electrodes were inserted in the extrinsic finger muscles of able-bodied subjects to record EMG activity during wrist and finger movements in various postures. EMG activity of all the recorded finger muscles were significantly different ($p<.05$, ANOVA) when performing the same movement in five different wrist postures. EMG activity varied by up to 70%, with the highest levels of activity observed in finger extensors when the wrist was extended. Similarly, finger flexors were most active when the wrist was flexed. For the finger flexors, EMG variations with wrist posture were most prominent for index finger muscles, while the EMG activity of all finger extensor muscles were similarly modulated. The extrinsic finger muscles also showed significant EMG activity during wrist movements with the digits held still regardless of finger posture. These results may impact the design of biomimetic control algorithms for myoelectric prosthetic hands, but further work in trans-radial amputees is necessary to determine whether this phenomenon persists after amputation.

3.1 Introduction

The human hand is a complex biomechanical system and both active and passive forces generated from muscles in the forearm are used to maintain postures and perform movements. The movement of a single finger alone generates torque at the wrist (An, Hui, Morrey, Linscheid, & Chao, 2017) that must be counteracted to maintain wrist posture. Similarly, single digit motion also generates torque in the joints of neighboring digits (Li, Latash, & Zatsiorsky, 1998; Zatsiorsky, Li, & Latash, 2000), a phenomenon known as force enslavement, which must in turn be counteracted by other finger muscles. This force enslavement effect has been suggested to be a combination of passive mechanical coupling driven by tendinous connections between digits as well as active coupling from higher order motor commands (Li et al., 1998; Schieber, Gardinier, & Liu, 2001). While there has been significant efforts to characterize the resulting electromyography (EMG) activity in the forearm muscles in these scenarios, prior work has primarily used surface EMG recordings and/or examined only a single muscle at a time (Butler et al., 2005; Kilbreath & Gandevia, 1994; Leijnse, Campbell-Kyureghyan, et al., 2008; Roman-Liu & Bartuzi, 2013), leaving an incomplete understanding of how the many extrinsic finger muscles are coordinated to produce single and multiple digit movements. Intramuscular EMG is an alternative method of recording EMG signals by placing fine-wire electrodes through the skin directly into muscles. Intramuscular recordings have been used for over 50 years to characterize muscle activity (Clamann, 1969; Harrison & Mortensen, 1962; Willison, 1964) and provides focal recording from a single target muscle that is difficult or impossible to achieve with standard surface EMG. Fine-wire electrodes can also record distinct signals from deep muscles and the different compartments of the multicompartment finger flexor and extensor muscles (Bickerton, Agur, &

Ashby, 1997; Henzel et al., 2010; Kilbreath, Gorman, Raymond, & Gandevia, 2002; Reilly & Schieber, 2003).

Extensive work has demonstrated that coupling between the digits is composed of mechanical (Keen & Fuglevand, 2003; Leijnse, Walbeehm, Sonneveld, Hovius, & Kauer, 1997) and neural components (Keen & Fuglevand, 2004a; Kilbreath et al., 2002; Lang & Schieber, 2004; Li et al., 1998; Reilly & Schieber, 2003), although the influence of inter-digit coupling on the coordination of single and multiple degrees of freedom (DOF) movements is not well understood. Experiments in humans have shown that electrical stimulation induces more focal and independent finger forces compared to volitional movement, suggesting that neural coupling does in fact result from cortical motor control strategies (Kilbreath et al., 2002). The influence of coupling is also visible during EMG recordings; an example may be seen in the work by Leijnse *et al.* (Leijnse, Campbell-Kyureghyan, et al., 2008), which shows phasic EMG activity in the extensor digiti minimi during a thumb tapping task. However, EMG activity of other muscles which appear to be functionally unrelated to the actuation of a joint may contain unique information that is relevant for prosthetic control. Improved EMG decoder performance was observed by Smith *et al.* (Smith et al., 2016) when all recorded extrinsic finger muscles were included in the decoder regression equations for each DOF. Conversely, prosthetic control schemes that rely on muscles crossing just a single joint, such as parallel dual-site control (Smith et al., 2014), could lead to inappropriate movements resulting from inter-digit coupling.

Similarly, wrist posture is known to have mechanical effects on the fingers, the most direct being motion of the relaxed fingers while the wrist is flexed and extended. For example, when the wrist is extended the fingers naturally curl into a tenodesis grasp (Mateo et al., 2013). This occurs because the extrinsic finger flexor muscles span the wrist and are subject to lengthening based on wrist angle, which in turn causes an increase in passive tension in the flexor muscles (Keir, Wells, & Ranney, 1996; Tanaka et al., 2005). The resulting increase in force has also been shown to affect the EMG activity necessary to maintain the static pose of a digit (Johnston et al., 2010). These posture-dependent changes in extrinsic finger flexor EMG have been well-studied in the context of grip force (Ambike, Paclet, Latash, & Zatsiorsky, 2013; Johansson, Backlin, & Burstedt, 1999; Johnston et al., 2010; Li, 2002; Morse, Jung, Bashford, & Hallbeck, 2006; Werremeyer & Cole, 1997) and lead to changes in EMG activity (Duque, Masset, & Malchaire, 1995; Mogk & Keir, 2003; Werremeyer & Cole, 1997). Duque *et al.* quantified this relationship between grip force and EMG as a series of nonlinear models for flexed, extended, and neutral wrist postures, demonstrating that these posture changes alter the relationship between grip force generation and EMG (Duque et al., 1995). However, most of these studies have focused on monitoring EMG activity at different wrist postures during tasks where the digits had to exert external loads, such as grasping tasks.

A further motivation to study the relationship between extrinsic finger muscle EMG activity and wrist posture is the potential impact on the design of control systems for prosthetic hands. Dexterous prosthetic hands exist, but a significant barrier to adoption is a lack of control algorithms which take advantage of the high degree-of-freedom movements that are offered in the prostheses (Cordella et al., 2016). Biomimetically-inspired control algorithms could possibly improve control (Crouch, Pan, Filer, Stallings, & Huang, 2018; Sartori et al., 2018), thus we sought to improve the understanding of the relationship between extrinsic finger muscle EMG activity and wrist posture.

In this study we used intramuscular EMG electrodes to target the compartments of the flexor digitorum profundus (FDP), flexor digitorum superficialis (FDS) and extensor digitorum

(ED), as well as the extensor digiti minimi (EDM) and the extensor indicis proprius (EIP) muscle, and sought to characterize the effect of changing wrist joint angles on EMG activity of the extrinsic finger muscles during structured hand movements. We also examined how the extrinsic finger muscles may contribute to wrist movements themselves.

3.2 Methods

Subject implantation, EMG recording, motion tracking, and experimental tasks for this study are described in Chapter 2.

3.2.1 Data Processing

Kinematic and EMG signals were processed offline using Matlab (The Mathworks, version 2016b). Kinematic data were smoothed with a 4th order low-pass Butterworth filter at 10 Hz to remove noise from the motion tracking system. The single-ended intramuscular EMG recordings were first differenced and the resulting signals were then high-pass filtered with a 4th order high-pass Butterworth filter at 10 Hz in order to remove low-frequency drift in the signal. Next, each signal underwent a process to remove electromagnetic noise generated by the kinematic motion tracking system (Figure 3.1a). The electromagnetic field was captured by the EMG recording system as a series of 100 µs pulses occurring at the pulse frequency of 100 Hz. We removed these narrow pulses from recordings offline by generating a template pulse train, and then subtracting it from the data. An example of the EMG signal before and after electromagnetic noise removal is shown in Figure 3.1a. After electromagnetic noise was removed, EMG signals were bandpass filtered with a 4th order Butterworth for 100 to 4000 Hz to remove movement artifacts, line noise, and high frequency noise. Similar bandpass filter settings are commonly used in intramuscular EMG recordings (Burgar et al., 1997; Kamavuako & Rosenvang, 2012; Valero-Cuevas, 2000).

Potential extrinsic finger muscle recordings were excluded during the data analysis phase if the EMG activity from an electrode was not modulated by single digit movement (Kamavuako et al., 2013; van Duinen et al., 2009), or if the electrode recordings were significantly contaminated by artifacts which occurred occasionally with the fine-wire electrodes. Artifacts were identified based on signal amplitude and shape. Events with peak voltages much greater than those occurring during a maximal voluntary contraction, or events with large instantaneous changes in amplitude or that did not resemble typical EMG activity or motor unit action potentials were considered artifacts. If multiple electrodes were in the same muscle or muscle compartment for a subject, we included only a single electrode with the highest signal-to-noise ratio. Electrode placement was verified after experiments by reviewing EMG activity from D1-D5 flexion/extension movements in neutral, flexed, extended, supinated, and pronated postures as well as from 14 trials of wrist movements.

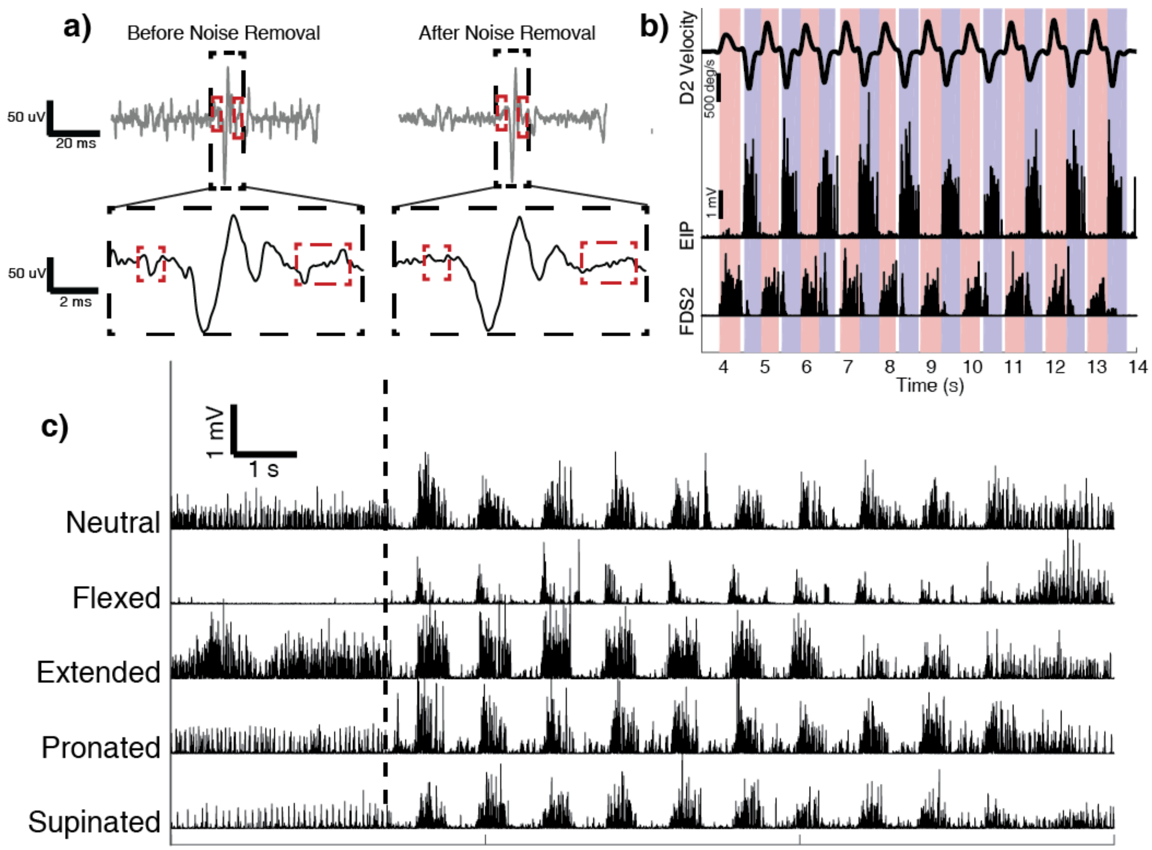

Figure 3.1 Overview of data processing and effects of wrist posture on EMG activity.

a) Comparison of EMG activity during rest before (left) and after (right) electromagnetic noise removal. Blocked in red are examples of electromagnetic artifacts introduced by the kinematic tracking system and the same signal after electromagnetic artifact removal. Left: EMG activity after high-pass filtering to remove DC offset and motion artifacts. The electromagnetic artifacts can be observed boxed in red. Right: The same EMG activity after electromagnetic noise removal. b) D2 metacarpal-phalangeal joint velocity and EMG activity of EIP and FDS2 during repeated flexion (red) and extension (blue) movements. The unshaded region between movements represents brief holding periods that were not included in calculations of EMG activity. c) Rectified and processed EMG activity of ED4 during repetitions of D4 flexion and extension in neutral, flexed, extended, pronated, and supinated postures. The dashed vertical line shows the task start cue. The hand was held in these static postures for approximately 4 seconds before performing 10 movement repetitions. Note the substantial change in EMG activity for the same finger movement in different wrist postures.

3.2.2 Data Analysis and Statistics

We divided the EMG data for every trial into flexion and extension phases using the kinematic recordings (Figure 3.1b). The angular velocities were low-pass filtered with a zero-phase digital filter at 10 Hz. We detected the movement phases by first identifying the positive and negative peak velocities. Movement onset was then detected based on the first zero velocity point preceding each peak, while the end of a movement was the first zero velocity point after a peak. The filtered EMG data were integrated over the relevant movement windows and divided by the duration of the movement to quantify the average EMG activity over the period. For example, the flexor digitorum superficialis was integrated during flexion movements and the extensor digitorum was integrated during extension movements.

3.2.3 EMG Normalization

Average EMG activity was normalized separately for finger and wrist movement analyses. As the primary objective of these analyses was to compare the way that EMG activity changed across different postures, we choose to normalize activity across the trials themselves, rather than to a maximal voluntary contraction. For finger analyses, mean EMG activity was calculated for each muscle and subject during digit movements in all wrist postures (e.g. Figure 3.1c). The EMG activity for each muscle was then normalized to the mean value from the wrist posture that evoked the largest EMG activity. For example, in Figure 3.1c, the average EMG activity of ED4 was highest when the wrist was extended. Therefore, all ED4 EMG activity for this subject was normalized to the mean value that occurred while the wrist was extended. Similarly, for wrist analyses, the mean EMG activity for each finger muscle was calculated for the four combinations of finger postures and wrist movements: fingers extended (‘flat’) during wrist flexion and extension and fingers flexed (‘fist’) during wrist flexion and extension. For the four movements, the EMG activity of each muscle and subject was normalized to the mean peak activity during the task.

3.2.4 Finger Movements

The normalized EMG activity of each muscle and compartment were tested for significant differences using a two-way ANOVA with subject and wrist posture (neutral, flexed, extended, pronated, and supinated) as factors. Post-hoc pairwise testing to identify differences in EMG activity for movements in the postures assessed was performed using Tukey’s honest significant differences (HSD) test for multiple comparisons.

3.2.5 Wrist Movements

The normalized EMG activity of ED, EDM and EIP muscles were combined into a single ‘extensors’ group, while FDS and FDP were combined into a ‘flexors’ group. Since the data were not normally distributed ($p<.05$, Kolmogorov-Smirnov test,) a Kruskal-Wallis test was conducted on the EMG activity of the extrinsic finger flexors and extensors to detect whether EMG activity of finger flexors and extensors differed based on finger position. Post-hoc pairwise testing was performed using Dunn’s test with a Bonferroni correction.

3.2.6 Classifying Wrist Posture from Extrinsic Finger Muscle EMG Activity

To investigate whether extrinsic finger muscle EMG signals might contain information about wrist posture, we developed a classifier to examine the capability of predicting wrist posture based on finger EMG activity alone. We trained two linear discriminant analysis classifiers, one for the extrinsic finger extensors and the other for the flexors, to predict if the movement of a digit was performed when the wrist was held in a flexed, neutral, or extended wrist posture. Each classifier was cross-validated using k-folds, with k = 5.

3.3 Results

3.3.1 Finger Movements at Different Wrist Postures

3.3.1.1 Finger Extensors

For all the finger extensor muscles, both posture and subject had a significant main effect on EMG activity (p<.0001, ANOVA). Further, the EMG activity of every finger extensor muscle was highest when the wrist was held in an extended posture. This activity was significantly higher than all other postures assessed (p<.001, Tukey's HSD, Figure 3.2**)**. In contrast, when the wrist was flexed, the finger extensors generated the lowest level of EMG activity during the extension phase of the motion, ranging from mean levels of 30 ± 13% to 53 ± 30% of their maximum activity level with the wrist was extended. These significant changes in EMG activity in response to wrist posture were consistent across all of the extensor muscles with the highest levels of EMG activity occurring when the wrist was extended and the lowest levels occurring when the wrist was flexed. EMG activity for the finger extensors with the wrist in the neutral, pronated, and supinated postures was at an intermediate level and varied depending on the muscle. When the wrist was held neutral during digit extension movements, average EMG activity ranged from 47 ± 22% to 61 ± 35% of its maximum value with the lowest activity occurring in the D2 extensors (ED2, EIP) and progressively increasing for ED4 and EDM. Average EMG activity when the wrist was pronated ranged from 50 ± 28% to 67 ± 21%. Notably, the two index finger extensor muscles were differentially modulated when the wrist was pronated. While ED2 and EIP activity were similar when the wrist was in the neutral, extended or supinated postures, the average EMG activity for ED2 and EIP was 50 ± 28% and 61 ± 26%, respectively when the wrist was pronated. This effect may be driven by the differing origin and insertion points of the ED and EIP muscles, which are accentuated during wrist pronation. With the wrist supinated, EMG activity across all the finger extensors varied the least, with all muscles having average activity levels between 49 ± 33% and 59 ± 31% of their maximum.

Of the extensor muscles assessed, ED4 showed the greatest difference in activity based on wrist posture. Of the ten possible pairwise comparisons (e.g. neutral vs. flexed, neutral vs. extended), all but neutral vs. supinated postures showed significant differences ($p<.01$, Tukey's HSD). ED2 and EDM were affected the least by changing wrist posture; only pairwise comparisons testing extension against the other postures showed statistical significance (Figure 3.2e).

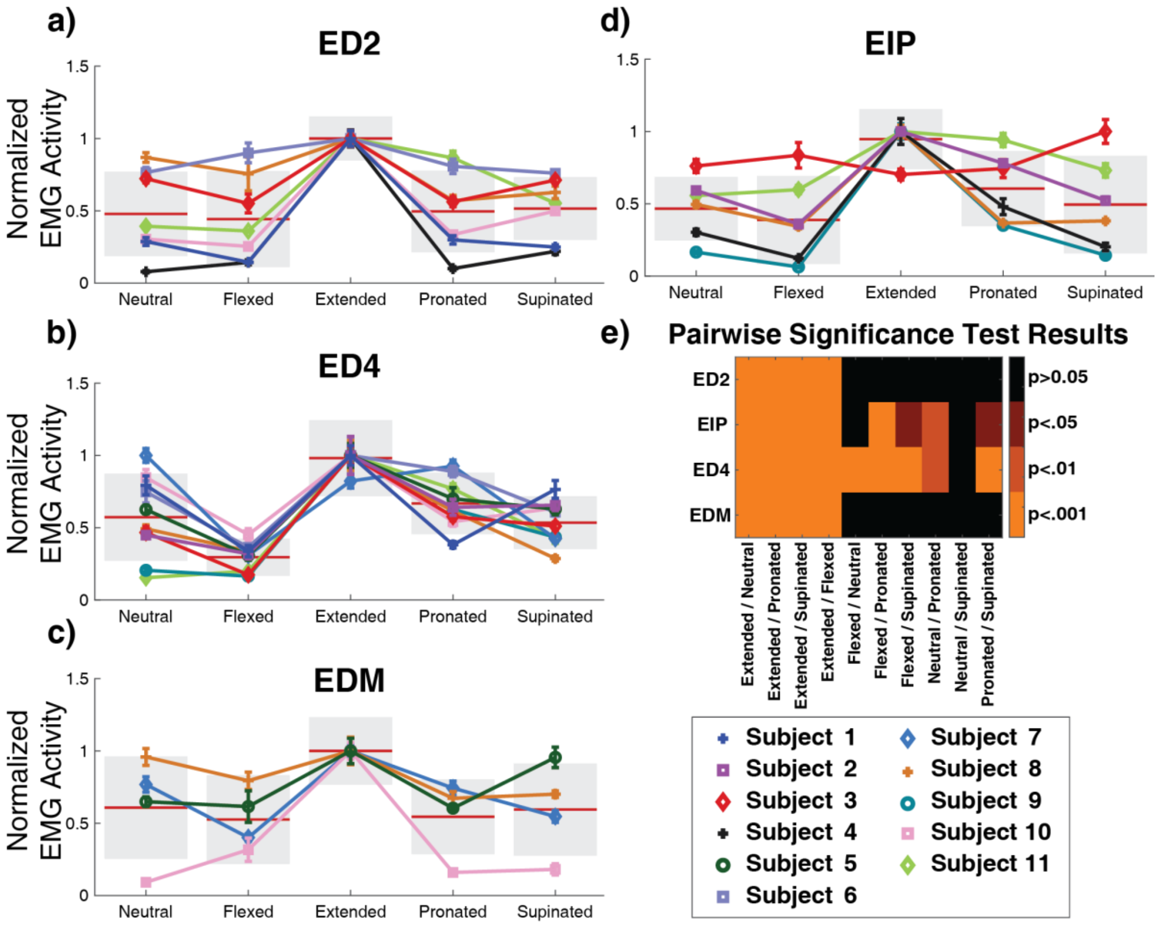

Figure 3.2 Finger extensor EMG activity in different wrist postures

(a-d) Overall mean normalized EMG activity for each subject for the extrinsic finger extensors during extension motions with the wrist in neutral, flexed, extended, pronated, and supinated postures. All finger extensors had their maximum EMG activity during extension movements when the wrist was held extended. Individual data points represent the subject mean and error bars are standard error of the mean. Data are color and marker coded for each subject. The horizontal red bars at each wrist posture show normalized group means and the standard deviation across subjects is shown as a gray box. Pairwise comparisons of EMG activity between the wrist extended and all other postures showed significant differences ($p<.001$, Tukey's HSD). e) Heat map of pairwise significant differences for EMG activity of the extrinsic finger extensor muscle for all combinations of wrist postures.

3.3.1.2 Finger Flexors

Similar to the finger extensors, wrist posture had a significant effect on the EMG activity of all of the finger flexor muscles (p<.001 for all muscles except FDS4, p<.05, ANOVA with Tukey’s HSD). The finger flexor muscles were most active when the wrist was held in the flexed posture, with the exception of FDS4 and FDP4. FPD4 was most active in a neutral posture with an average normalized EMG activity of 95 ± 26%, although the low number of muscle recordings could have an effect on this result. FDS4 was also most active in the neutral wrist posture with an average normalized EMG activity of 87 ± 25%, although this was not statistically higher than other wrist postures. With the wrist in the neutral posture, the other flexor muscles had average activity levels that were much lower and ranged between 54 ± 18% to 73 ± 22% (Figure 3.3). When the wrist was extended, the EMG activity of the flexor muscles to produce the same finger flexion motion ranged from just 31 ± 12% (FDS2) to 76 ± 21% (FDP3) of that required when the wrist was flexed. In contrast to the finger extensors, the individual finger flexor muscles showed little difference between extended, pronated, and supinated postures. Interestingly, the overall effect of wrist posture on EMG activity was most prevalent for D2 and D3 than D4 and D5 (Figure 3.3), whereas all finger extensors were affected similarly by changes in wrist posture (Figure 3.2).

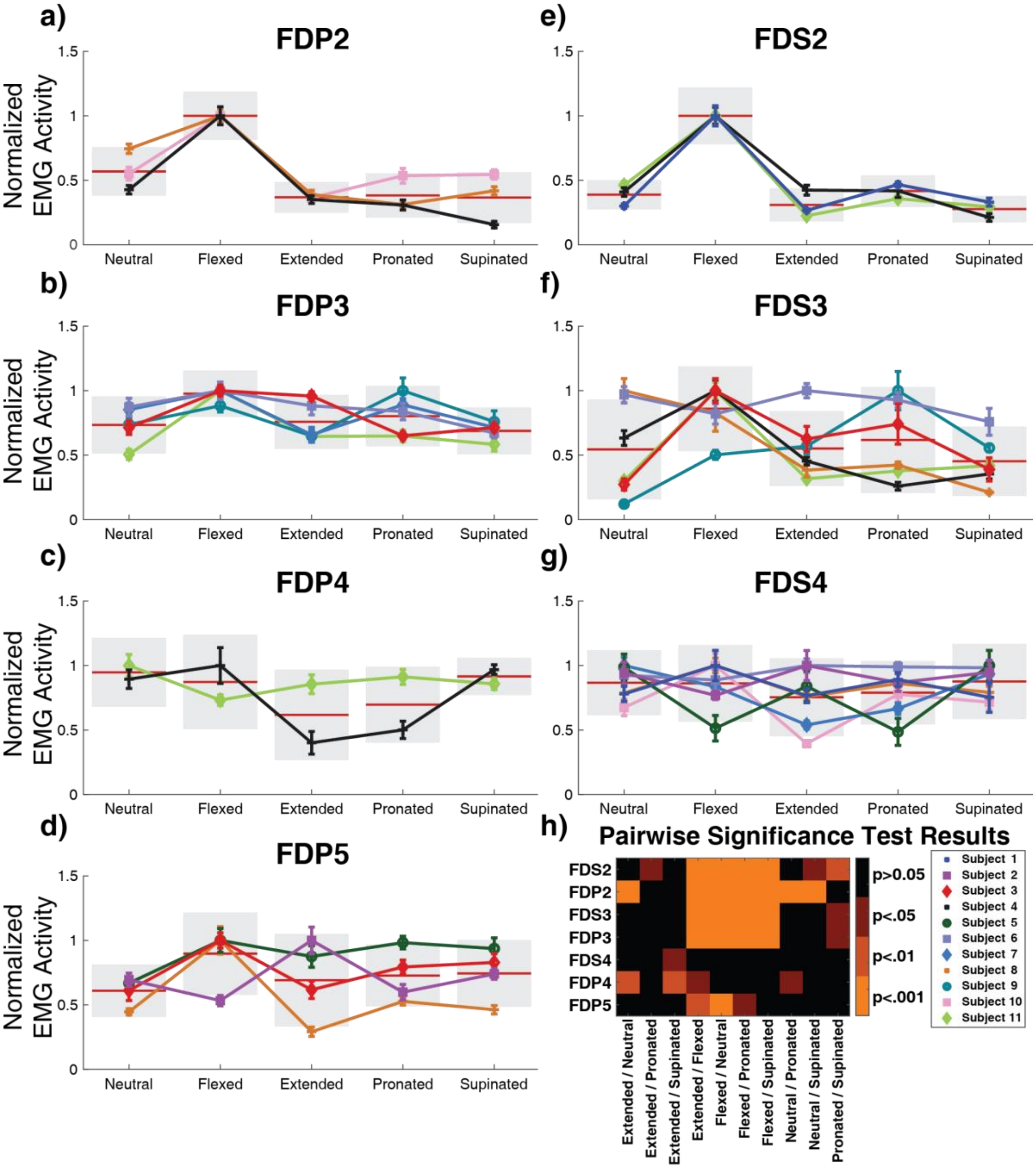

Figure 3.3 Finger flexor EMG activity during different wrist postures

(a-g) Overall mean normalized EMG activity for each subject for the extrinsic finger flexors during flexion motions with the wrist in neutral, flexed, extended, pronated, and supinated postures. The D2, D3, and D5 finger flexors showed significantly elevated EMG activity when the wrist was flexed. Individual data points represent the subject mean and standard error of the mean. Data are color and marker coded for each subject. The horizontal red bars show normalized group means and the standard deviation is shown as a gray box.. h) Heat map of pairwise significant differences (Tukey's HSD) of EMG activity between postures for the extrinsic finger flexors.

3.3.2 Inter-Subject Variance

For all muscles that were assessed, excluding FDS2, the individual subject had a significant effect on how wrist posture effected extrinsic finger muscle EMG activity ($p<.05$, Tukey's HSD). This main effect response was primarily driven by high responders, which were subjects that had particularly high levels of finger EMG activity when the wrist posture matched the action of the finger muscle (e.g. wrist extension for finger extensors). ED2 in Subjects 1 and 4 (Figure 3.2a), EDM in Subject 10 (Figure 3.2c), EIP in Subjects 4 and 9 (Figure 3.2d) and FDP5 in Subject 8 (Figure 3.3d) are all examples of this. Overall this effect was less pronounced in the finger flexor muscles. There were a few other notable instances of inter-subject variance that we observed in these data. For example, the FDP5 EMG activity in Subject 2 (Figure 3.3d) was maximized when the wrist was extended, rather than flexed, as was the case for all other subjects. In this case, the EMG activity clearly showed that this electrode was in the FDP5 muscle as it highly active only during flexion of the 5th digit. In this subject, motion of the 5th digit was atypical in that most of the flexion and extension occurred at the proximal interphalangeal joint when the wrist was extended, rather than the metacarpal-phalangeal joint. This highlights the other primary reason for inter-subject variability that we observed.

3.3.3 Extrinsic Muscle Finger EMG Activity During Wrist Movements

The extrinsic finger extensor muscles were highly active during wrist extension regardless of the finger posture. In fact, finger extensor EMG activity was significantly higher when the fingers were fully flexed and the wrist was being extended than when the fingers were extended and the wrist was being flexed ($p<.001$, Dunn's, Figure 3.4a). In the four combinations assessed (wrist extension/flexion with fingers extended/flexed), the extrinsic finger extensor EMG showed a wide range of activity levels. The highest EMG activity occurred during wrist extension when the fingers were held extended where the median normalized EMG activity from the finger extensors was 98% (IQR 85%-111%). When the wrist was extending and the fingers were held flexed, the median normalized EMG for the finger extensors declined to 52% (IQR 35%-77%). During wrist flexion movements, finger extensor EMG activity was 28% (IQR 16%-44%) when the fingers were held extended and was even smaller at 18% (IQR 9%-33%) when the fingers were held flexed. All pairwise comparisons of EMG activity for the different movement and posture combinations were significantly different ($p<.001$, Kruskal-Wallis test with Dunn's post-hoc test). Overall, we found that the finger extensor EMG activity changed by more than a factor of three when the fingers were held extended based on whether the wrist was moving in extension or flexion.

The EMG activation patterns of the finger flexor muscles showed a similar pattern to that observed in the finger extensors, with finger flexors significantly more active during wrist flexion movements than wrist extension movements, even when wrist extension was performed with the fingers in a fist (Figure 3.4b). The highest EMG activity of the movements and postures assessed occurred during wrist flexion when the fingers were fully flexed at a median normalized EMG activity of 96% (IQR 82%-111%). The next highest level of EMG activity was during wrist flexion with the fingers extended with a median normalized value of 49% (IQR 21%-72%), nearly half of the highest value. Even when the fingers were being actively held in extension, finger flexor muscles were active during wrist flexion movements. EMG activity for the finger flexors was lowest during wrist extension movements; during extension movements with the fingers flexed, the median normalized EMG activity was 29% (IQR 15%-47%). When the wrist was extended and the fingers were extended, median normalized EMG activity was the lowest at 15% (IQR 7%-27%). The difference in activity levels were all significant (p<.001, Kruskal-Wallis test with Dunn's post-hoc test) and varied by more than threefold depending on whether the wrist was flexing or extending when the fingers were fully flexed.

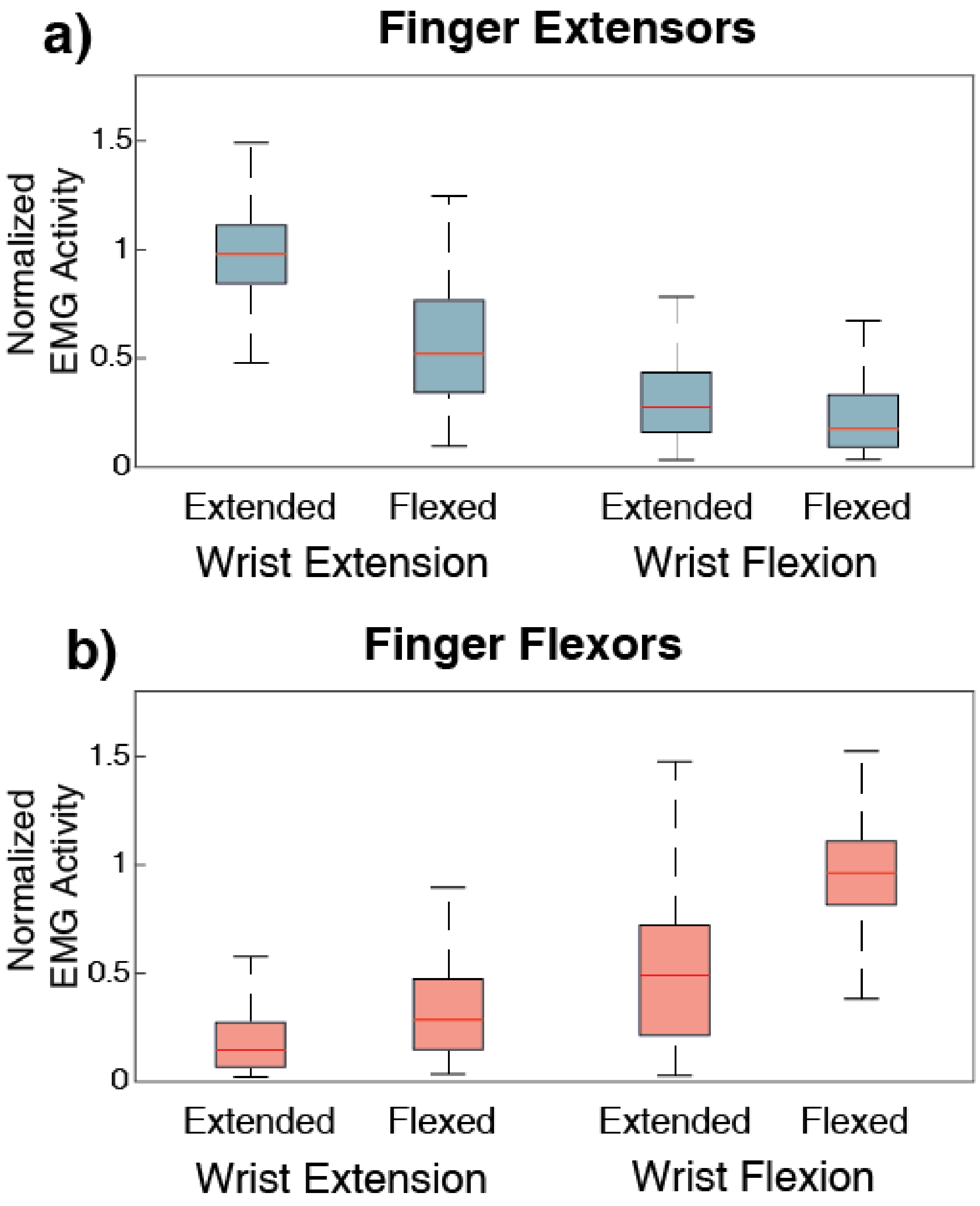

Figure 3.4 Effect of finger posture and wrist movement on finger muscle EMG

Normalized mean EMG activity for a) finger extensors (N=22 muscles) and b) finger flexors (N=28 muscles) during wrist extension and flexion movements in flat and fist postures. For each of the 11 subjects, 10 repetitions were performed for movements in each posture. The red line shows the median, and the outer boxes are the first and third quartile. Error bars represent the 5-95% confidence interval. All posture and movement combination showed significant differences (p<.005, Kruskal-Wallis with Dunn post-hoc testing).

3.4 Classifying Wrist Posture from Extrinsic Finger Muscle EMG Activity

Since we found that that extrinsic finger muscle EMG activity was often highly modulated by wrist posture, we asked whether wrist posture itself could be classified simply from the flexor or extensor finger muscle EMG activity. Overall, using just finger extensor muscles, the classifier accuracy was 63.5% ± 4.0% (99% confidence interval) and using just finger flexor muscles, the classifier accuracy was 47.4% ± 4.3% (99% confidence interval), both which were significantly above the chance level of 33%. True class prediction accuracy varied depending on the posture but followed the same pattern for both classifiers (Figure 3.5). The most accurate true class predictions occurred when the wrist was held in the same posture as the finger action: wrist extended for the finger extensors (86.9%) and wrist flexed for the finger flexors (66.4%). When the wrist was in a neutral posture, true class accuracies were lowest for both classifiers at 32.7% for the finger extensors and 22.5% for the finger flexors. The confusion matrices and true class accuracy for both classifiers are shown in Figure 3.5, and additional information on precision and recall is provided in Table 3.1.

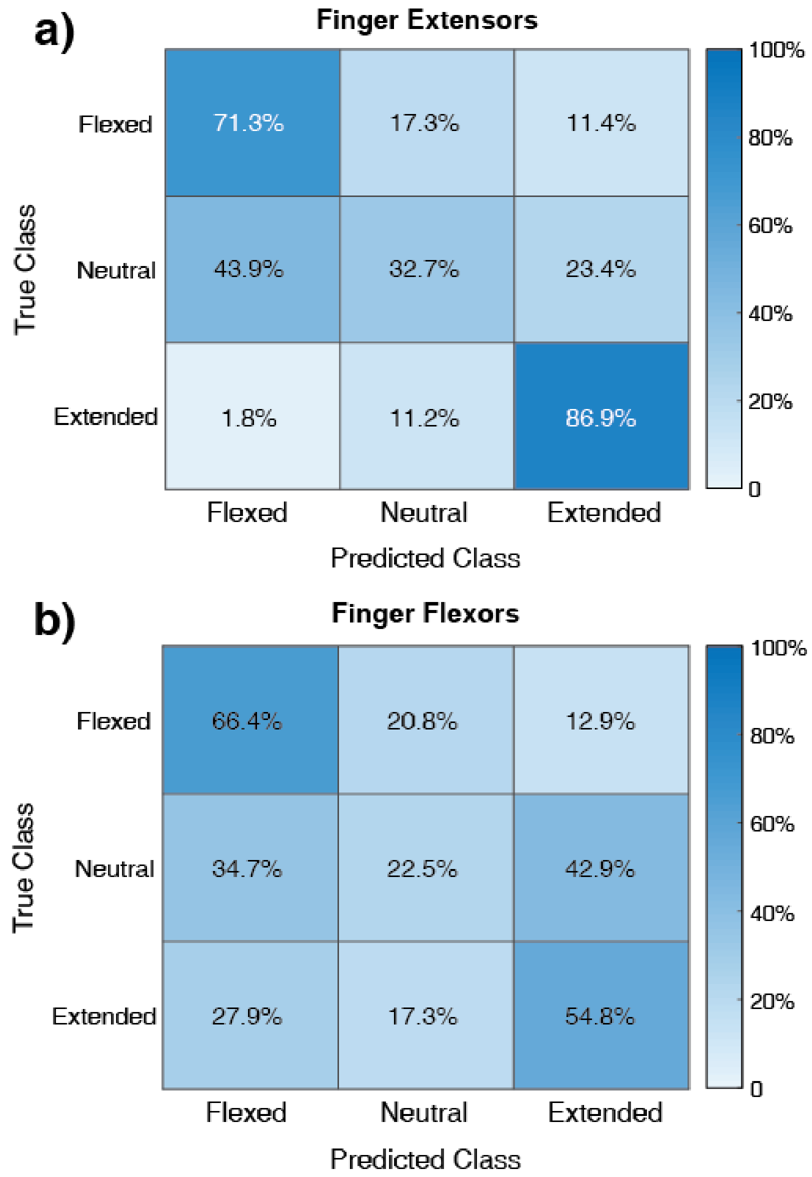

a) Finger Extensors

True Class \ Predicted Class	Flexed	Neutral	Extended
Flexed	71.3%	17.3%	11.4%
Neutral	43.9%	32.7%	23.4%
Extended	1.8%	11.2%	86.9%

b) Finger Flexors

True Class \ Predicted Class	Flexed	Neutral	Extended
Flexed	66.4%	20.8%	12.9%
Neutral	34.7%	22.5%	42.9%
Extended	27.9%	17.3%	54.8%

Figure 3.5 Classification of wrist posture from finger EMG activity

Confusion matrices and true class accuracy for the linear discriminant classifiers for the a) finger extensors and b) finger flexors. The diagonal of the matrices shows the percent of correct predictions (true positive rate); the other percentages in each row are the incorrect predictions of other hand postures (false positives). a) The finger extensors show the highest accuracy (86.9%) for detection of the extended wrist posture, and the lowest accuracy (32.7%) for neutral posture. The most common misclassification for the neutral posture was for the wrist flexed posture. For the finger extensors, the differences in EMG activity for flexed and neutral postures were minor and only significant for ED4, which may be the driving cause of this error. b) The finger flexors show similar results as the extensors, but with lower overall accuracy. Prediction of the flexed posture was the highest at 66.4%, followed by extended posture at 54.8%. Neutral posture classification had the lowest accuracy at 22.5%.

Table 3.1 Precision and recall for posture classification

Extensors			Flexors		
Wrist Posture	**Precision**	**Recall**	**Wrist Posture**	**Precision**	**Recall**
Extended	0.869	0.712	Extended	0.548	0.493
Neutral	0.327	0.533	Neutral	0.225	0.378
Flexed	0.713	0.612	Flexed	0.663	0.378

3.5 Discussion

In this study, we found that there were wrist posture-dependent effects on extrinsic finger muscle EMG activity, which is consistent with previous reports (Duque et al., 1995; Johanson et al., 1990; Mogk & Keir, 2003; Roman-Liu & Bartuzi, 2013)’. We also expanded on this work by investigating EMG activity from the individual muscle compartments of the FDS, FDP and ED muscles, specifically while using completely unloaded finger movements like would occur during hand pre-shaping in reach-to-grasp actions (Fligge, Urbanek, & Van der Smagt, 2013; Janssen & Scherberger, 2015) . An important issue is that using intramuscular electrodes instead of surface electrodes increased the likelihood that the recorded signals were indeed from the same muscle in all postures. With surface EMG, there can be significant motion of the muscles under the skin, making it difficult to ensure that recordings at all wrist postures would be from the same muscle (Duque et al., 1995; Roman-Liu & Bartuzi, 2013).

In these experiments, we found that during single digit motions, both the finger flexors and extensors exhibited significant changes in their EMG activity based on the posture of the wrist, and in some cases varied by as much as 70% of their normalized value. We have also shown evidence that the extrinsic finger muscles have higher levels of activity during wrist movements that are performed in the same direction of action regardless of finger posture, which suggests that these muscles assist with unloaded wrist movements. These muscles may therefore also play a role in maintaining static wrist postures, which is consistent with other studies (Werremeyer & Cole, 1997).

There are multiple causes for EMG activity to change based on wrist posture. Previous work has shown that grip and fingertip forces decrease as wrist posture moves further into a flexed posture (Ambike et al., 2013; Li, 2002). It has been suggested that this may be in part due to the diminished force production capacity of the flexors as they shorten (Li, 2002). If the required force output or tasks remains the same and force production ability diminishes, an increase in EMG activity is required to increase force generation (Aratow et al., 1993; Solomonow, Baratta, & D'Ambrosia, 1991).

Posture dependent activation levels may also be attributed to the altered tension of the antagonist extrinsic finger muscles caused by lengthening of muscles and tendons during different wrist postures, which change the force necessary to make such movements (Loren et al., 1996). The increased passive force of the extrinsic finger muscles when the is wrist extended and flexed has been previously documented (Gonzalez, Buchanan, & Delp, 1997; Keir et al., 1996; Li, 2002). For example, when the wrist is extended, the FDS and FDP muscles are lengthened, which generates an increased flexion torque on the digits (Li, Zatsiorsky, & Latash, 2000; Savage, 1988). The extensor digitorum and other assisting muscles must therefore generate more force, and thus EMG activity, to counteract the increased tensions of the flexor muscles both to maintain finger position and to perform extension movements. During finger flexion movements while the wrist is still held extended, the lengthened finger flexor muscles generate substantial passive forces that assist in flexion movements and therefore require less EMG activity to make a flexion movement. This may also explain why the flexor compartments of the radial digits (FDS2, FDS3, FDP3) had the lowest activation in the supinated posture, while the flexor compartments of the ulnar digits (FDS4, FDP4, FDP5) were substantially more active in the same posture. Despite the muscle compartments showing consistent patterns of responses, such as elevated EMG activity of the finger extensors when the wrist was extended and lower activity when the wrist was flexed (Figure 3.2), there were differences in the magnitude of those responses across fingers. This may be explained in part by the differences in passive forces generated by the individual compartments at different wrist postures. The study by Keir *et al.* showed that passive muscle force differences of up to 200% may occur between compartments of the same muscle, such as in the case of FDS2 and FDS4 (Keir et al., 1996). The moment contributions of FDS and FDP also vary across the digits (Li et al., 2000). It is therefore plausible that the extrinsic finger muscle compartments exhibit some differences in response magnitude based on wrist posture, but that the overall pattern of responses is maintained.

EMG activity was subject-dependent and the effect of the subject was found to be significant for nearly all muscles. This is due in part to instances where a muscle was primarily active in a single wrist posture, and much less active, in some cases just 10-30% of the normalized activity, in other wrist postures (e.g. Figure 3.2a,d). Interestingly, the EMG activity patterns of these high responders appeared to be limited to a single muscle. For example, EDM of subject 10 showed high EMG activity during the extended posture but low activity during the other postures (Figure 3.2c). In the other muscles and movements of subject 10, the EMG activity showed a range of responses similar to other subjects (Figure 3.2a-b, Figure 3.3a,f). Although high responders had less pairwise differences in EMG activity due to posture, their performance still demonstrates that EMG activity for movements is affected by wrist posture. It is unsurprising that differences between subjects were observed. Control over the hand and fingers has been shown to vary substantially across subjects (Hager-Ross & Schieber, 2000; Salonikidis et al., 2009) and the number of muscles within the hand lends itself to redundant control where different muscle activity combinations could be used to achieve similar kinematic outputs (Latash, Scholz, & Schöner, 2002).

The accuracy of the classifiers used to determine wrist posture based on the integrated finger EMG activity were significantly above chance, demonstrating that information regarding wrist posture can be obtained from the extrinsic finger muscles. The high level of classifier accuracy for wrist postures in the agonist direction (wrist extended for the finger extensors, flexed for the finger flexors) suggests that information on wrist state can be gathered from the extrinsic finger muscles. However, information is limited to this preferred direction, due to the poor performance in predicting neutral posture. The performance of the classifiers is a reflection of the results reported in Figure 3.3 and Figure 4.4; all muscles assessed showed at least some overlap between EMG activity in the neutral posture and the posture in the opposite direction of the action (flexed for the finger extensors, extended for the finger flexors), which caused difficulty in differentiating between these postures. Of the 11 muscles assessed, only 3 showed significant differences between EMG activity occurring in the neutral and antagonist postures, making it difficult to effectively distinguish between those postures when all muscles are taken into consideration. We chose to use separate classifiers rather than a single classifier to highlight the strengths of the flexors and extensors for predicting wrist posture in the flexed and extended postures respectively.

A core limitation of our work was that we were unable to determine how much or the change in extrinsic finger EMG activity based on posture was due to the necessity of overcoming mechanical coupling effects, such as the changing passive forces of antagonist muscles lengthening, as opposed to a motor control strategy in which the fingers assist in maintaining wrist posture. We are therefore unable to directly ascribe whether this phenomenon is a reaction to passive forces or a method of control that uses multiple muscles for force generation. Electrode placement was also a challenge in certain cases. For example, we didn't have electrodes in ED3 due in part to the location of the posterior antebrachial cutaneous nerve. Electrode placement in FDS4 and FDP4 also proved challenging. Four electrodes that were targeted to FDP4 penetrated too deeply and were believed to be located in the flexor carpi ulnaris muscle in post hoc experiment data analysis, as the electrodes showed no response to finger movement but were active during wrist flexion and adduction. We were unable to determine whether this was due to the small size of these muscles or electrode migration that may have occurred immediately after placement while subjects first moved their hands. Another limitation on our work was the testing of pronation and supination postures. While we did test finger movements in these wrist postures, we did not explore activity during pronation and supination movements as thoroughly as Mogk *et al.* and it was difficult to draw meaningful conclusions on these postures, as there did not seem to be a consistent behavior across the muscles examined (Mogk & Keir, 2003). Biomechanical models of the arm and hand may assist in understanding these postures, as the EMG activity of the extrinsic finger muscles may be impacted by the changing muscle lengths and moment arms which can be modeled in simulation software.

In this study we demonstrated that wrist posture significantly influences the necessary action of finger muscles as demonstrated by the large changes in EMG activity of the extrinsic finger muscles in able-bodied subjects. Indeed, in certain cases, a three-fold change in finger muscle activity was required to produce the same finger kinematics when the wrist was held in different postures. For the finger flexors, these effects were most pronounced for muscles controlling the index finger. Future work could investigate whether the effects of wrist posture on finger muscle activity are still present in traumatic transradial amputees where these mechanical influences are removed. This could help clarify whether these interactions represent a learned feed-forward control strategy driven by the cortex or might be predominantly driven by real-time sensory-driven feedback.

4.0 Coactivation and Stabilization of the Extrinsic Finger Muscles

The volitional movement of a finger involuntarily generates force in a neighboring digit. This phenomenon is partially due to the neural and mechanical coupling present in the extrinsic hand muscles. Previous work has shown muscle activation of the extrinsic finger muscle compartments when neighboring digits have performed the same and opposite type of movement, known as coactivation and stabilization respectively, but the underlying muscle activations have not been well-studied. In order to understand how the extrinsic hand muscles coordinate to control the fingers, we inserted fine-wire intramuscular electrodes to record electromyographic (EMG) activity during single digit flexion and extension tasks. The normalized integrated EMG activity of the muscles during non-associated movements was compared to activity during a static pose. All of the 11 extrinsic hand muscles and compartments tested showed significantly higher EMG activity compared to static pose during at least one non-associated movement ($p<.01$, Bonferroni t-test). The finger extensors showed EMG activity across a broad range of digits, while the flexors were typically only active for movements of neighboring digits. Subjects showed variability in the ability to perform individuated movements, which we quantified using an individuation index. We further developed a set of generalized models to describe the EMG activity of an extensor or flexor muscle during movements of the same or opposite action based on distance from the digits. These results provide an overview of the EMG activity across 11 muscles and shows the coordination across the muscles during single digit movement.

4.1 Introduction

Movements of the fingers are complex tasks that require the coordination of multiple muscles and tendons that span across up to four joints. Flexion and extension movements of the index, middle, ring, and pinky fingers (D2-D5) are primarily actuated by three muscles: the flexor digitorum superficialis (FDS) and flexor digitorum profundus (FDP) for flexion, and the extensor digitorum communis (ED) for extension. These three muscles can control four fingers due to finger-specific subcompartments which exert force on the tendons that actuate digits (Butler et al., 2005; Keen & Fuglevand, 2004a; Reilly & Schieber, 2003; van Duinen et al., 2009). It has been well-established that the fingers are subject to enslaving effects: the involuntary production of force by non-intended fingers during a digit movement (Kilbreath & Gandevia, 1994; Li et al., 1998; Schieber & Santello, 2004; Zatsiorsky et al., 2000). Enslaving effects have been attributed to a combined influence of factors (Zatsiorsky et al., 2000): mechanical coupling of the muscles and tendons (Keen & Fuglevand, 2003), a shared common input to motor neurons across the compartments (Keen & Fuglevand, 2004a, 2004b; Kilbreath et al., 2002; Reilly et al., 2004), and diverging motor commands (Schieber, 1991, 1995, 1996; Schieber & Hibbard, 1993; Schieber & Santello, 2004).

Given the neural-related causes of enslaving effects, it is unsurprising that the extrinsic finger muscles show significant coactivation for non-actuated digits during similar actions. This phenomenon can be prominently seen through electromyographic (EMG) analysis, and has been documented in the ED (Birdwell et al., 2013; Leijnse, Campbell-Kyureghyan, et al., 2008; van Duinen et al., 2009), FDS (Butler et al., 2005), and FDP (Birdwell et al., 2013; Kilbreath & Gandevia, 1994; Reilly & Schieber, 2003). Efforts have been made towards quantifying the levels of independence and coactivation of the extrinsic finger muscles in humans through force (Yu et al., 2010; Zatsiorsky et al., 2000) and EMG activity (Birdwell et al., 2013; Kilbreath & Gandevia, 1994; Leijnse, Campbell-Kyureghyan, et al., 2008; Reilly & Schieber, 2003; van Beek, Stegeman, van den Noort, Veeger, & Maas, 2018). However, these works are limited in at least one of several ways. They neglect to compare EMG coactivation to a baseline level of activity such as during a static pose, do not test across a broad range of movements, and/or examine a limited number of muscle compartments.

While it is well-established that the extrinsic finger muscles show EMG activity during similar movements by neighboring digits, less is known about EMG activity of these muscles during opposite movements. Previous work has shown EMG activity of FDS3 and FDP2-3 during a low force isometric contraction of ED2 (Birdwell et al., 2013), and EMG activity of ED during hand closing movements (Johanson et al., 1990). These activations by muscles in response to the opposite movement has been suggested to be a motor control pattern for stabilization (Birdwell et al., 2013; Reilly & Schieber, 2003). Collecting data on how these muscles react to antagonist and other digit movements is vital towards understanding motor control over the hand.

Beyond motor control, understanding how the extrinsic finger muscles behave holds direct relevance towards upper-limb myoelectric prosthetic control. The muscle bellies of ED, FDS, and FDP are located in the forearm and may still be present after transradial amputation, allowing for collection of EMG signals that can be used for myoelectric control after limb loss (Cipriani et al., 2011; Pasquina et al., 2014; Segil, Huddle, & Weir, 2017). Mapping EMG activity from these residual muscles for direct or model-based control over prosthetic finger movements has been proposed for myoelectric prosthetic hands (Birdwell et al., 2015; Cipriani et al., 2014; Sartori et al., 2018). These methods often require setting a baseline threshold for EMG activity to prevent unwanted movement. Setting a threshold can require significant time and effort for each EMG channel, as setting a threshold too low may not prevent unwanted movements and setting it too high can cause substantial effort to be needed to cause movement. It is therefore imperative that a dataset which catalogues the EMG activity of the extrinsic finger muscles across a range of single digit movements be established in order to inform prosthetic control designers.

4.2 Methods

Subject implantation, EMG recording, motion tracking, and experimental tasks for this study are described in Chapter 2. Data processing is described in Chapter 3.2.1.

4.2.1 Data Analysis and Statistics

EMG data were divided into flexion and extension phases based on the angular velocity of the moved digit. Angular velocities were low-pass filtered with a zero-phase digital filter at 10 Hz. Movement timing was detected by finding the peak positive and negative velocities within a trial. The onset of a movement was then recorded as the first zero velocity point preceding a peak, and the end of movement was the first zero velocity point after a peak (see Section 3.2.2 and Figure 3.1b). Filtered EMG were then integrated over the movement window and divided by the duration of the movement. EMG activity for static pose was collected from the same trials as D2-D5 movements during the first 4 seconds of trials when the hand was held in a neutral position with the fingers extended and thumb pointed upwards. EMG activity was integrated over a random length of time between 0.5-0.7 seconds 3 times per trial, then divided by the duration of time.

4.2.1.1 Trial Rejection

Analysis of digit kinematics after experiments showed that some subjects demonstrated variability in the time to complete movements across the digits. This variability was not consistent across subjects and could have possibly influenced the results of analyses. In order to reduce this, the average time to complete flexion or extension of the digits was calculated across D1-D5 movements for each subject. Trials that were 100 ms faster or slower than the average (~500 ms) for that movement were excluded from analysis. If six or more trials (60% of the repetitions) for any movement was excluded by this criterion, the subject was not included in analysis for movements of that type. We tested a range of time buffers to determine the effect of this on subjects excluded and determined that 100 ms balanced consistency in trial repetitions and subject exclusion (Figure 4.1). Subjects 3, 4, and 7 were excluded from analysis of flexion movements, and subjects 2 and 9 from extension movements.

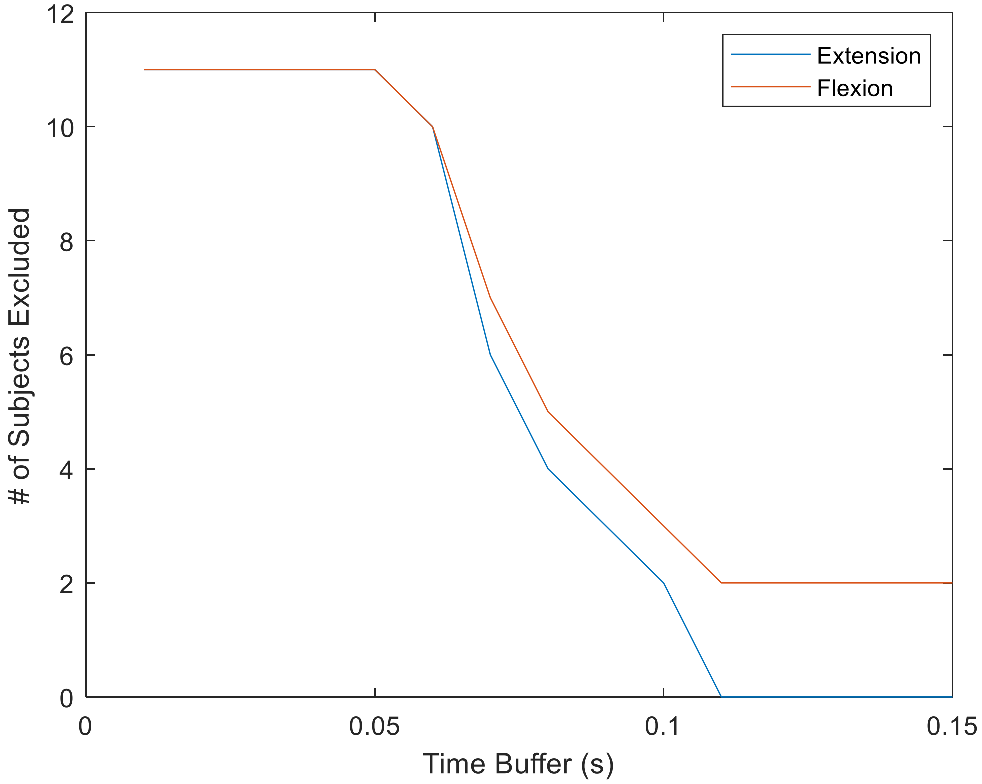

Figure 4.1 Effect of time buffer on subject exclusion

Subjects were excluded if six or more repetitions of a movement (flexion or extension) for a digit were outside of the subject's average movement time +/- the time buffer. Subjects were tested twice and only excluded from analysis of the movement they failed. For example, a subject may have been excluded from analysis using flexion movements, and thus removed from coactivation analysis of flexors and stabilization of extensors, but still included in coactivation analysis of the extensors and stabilization of the flexors.

4.2.2 Coactivation and Stabilization

Integrated EMG activity across all movements was normalized to the mean EMG activity of the action associated with the muscle for each subject to capture the range of activity for the movements being studied. For example, EMG activity of ED2 was normalized to the average EMG activity of the muscle during D2 extension movements. Coactivation was measured as the EMG activity during D1-D5 movements that performed the same action as the muscle measured, e.g. for

ED2, this was during extension movements of the fingers. Stabilization was measured as the EMG activity during D1-D5 movements during the opposite action as the muscle measured; using ED2 again was an example, this was EMG activity of that muscle which occurred during flexion movements. EMG activity for these movements was normalized to the same measurement used in coactivation: the EMG activity during the associated movement and digit (e.g. for ED2, D2 extension).

Statistical analysis was performed with a type III sum of squares general linear model for each muscle, using the normalized integrated EMG as the dependent factor. Subject and movement type (static pose, D1-D5 flexion or extension depending on muscle and analysis) were included in the model as fixed factors. Two models were built for each muscle to evaluate EMG activity during coactivation (agonist movements) and stabilization (antagonist movements). The normalized integrated EMG activity was the dependent variable. Subject and movement (static pose, D1-D5 flexion or extension) were included in the models as the fixed factors. Follow-up analysis was performed with pairwise comparisons on the estimated marginal means to compare EMG activity across movements and static pose. A Bonferroni correction was included to account for multiple comparisons.

The coactivity of the extrinsic finger muscles was scored using an individuation index, where 0 is equal EMG activity across all movements and 1 is no EMG activity above static pose levels during non-actuated movements. The individuation index (II) is described in Equation 4-1:

$$II = 1 - \frac{\overline{EMG}_{noninstructed} - EMG_{Static}}{\overline{EMG}_{instructed} - EMG_{Static}} \qquad \textbf{Equation 4-1}$$

Where $\overline{EMG}_{noninstructed}$ is the weighted average of the normalized integrated EMG activity of the muscle during non-actuated movements (e.g. for ED2, D1 and D3-D5 extension),

$\overline{EMG}_{instructed}$ is the average normalized integrated EMG activity during the associated movement, and EMG_{Static} is the normalized EMG activity during the static pose.

4.2.3 Generalized Models

We developed a series of generalized models for the extensors and flexors to describe the coactivation and stabilization behaviors. Each model is comprised of the group of muscles which perform the same movement; the extensor model is composed of EIP, ED, and EDM while the flexor model is a combination of the FDS and FDP compartments. In order to combine the muscles, the data that was used in the general linear models described previously was recoded. The primary movement associated with a digit was coded as ‘D’. The neighboring radial and ulnar digits were labeled ‘D-1’ and ‘D+1’ respectively; digits further away continued with this naming scheme. Models were constructed as a type III sum of squares general linear model, with normalized integrated EMG as the dependent factor and movement type as a fixed factor.

4.3 Results

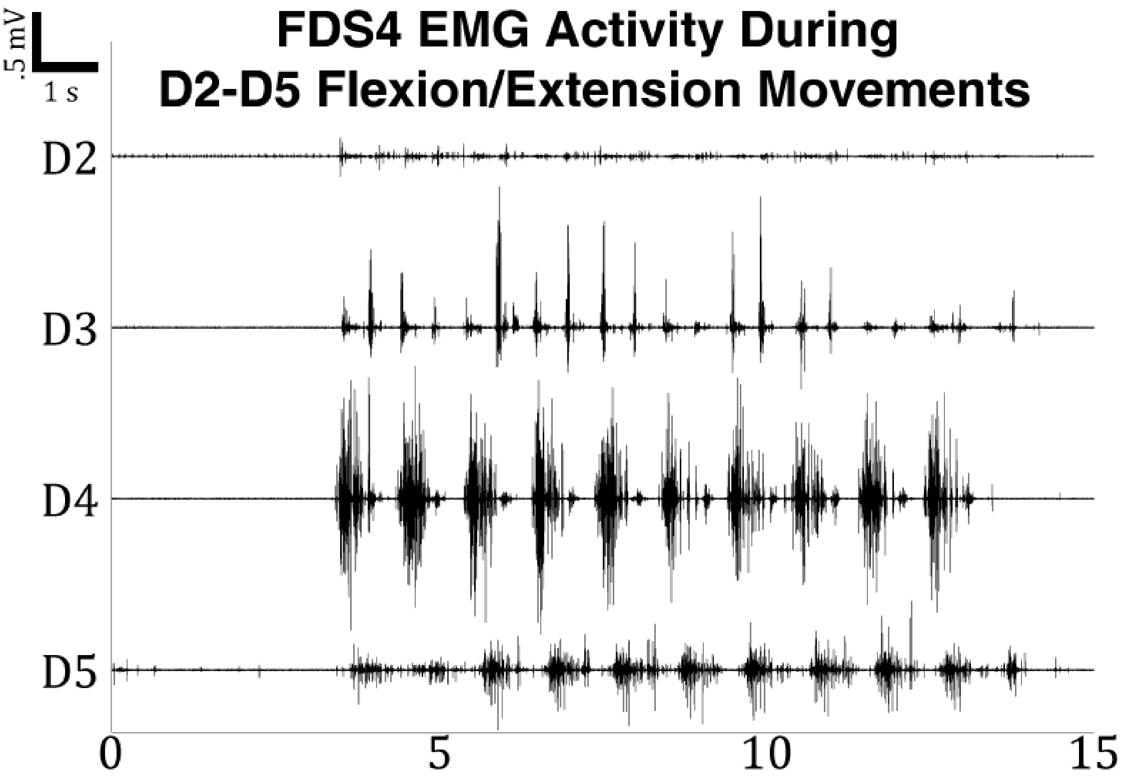

Figure 4.2 EMG activity of FDS4 during D2-D5 movements

EMG activity from FDS4 from four trials consisting of 10 repetitions of finger flexion and extension. EMG activity was high-pass filtered at 100 Hz and underwent noise removal. Despite FDS4's association with D4 flexion, it shows clear modulation during movements of the neighboring digits as well as D2. EMG activity was high-pass filtered at 100 Hz.

4.3.1 Coactivation

All extrinsic finger muscles assessed, with exception of FDS2, showed significant EMG activity above static pose EMG activity levels during non-actuated movements using pairwise comparisons. EMG activity during these movements was the highest for movements of neighboring digits and tapered off for movements further away. An example of the EMG activity observed is shown in Figure 4.2. The finger flexor muscles showed less EMG activity for non-actuated movements than the finger extensors. For the flexors, EMG activity was only sometimes above static pose levels for neighboring digit movements, whereas the extensors muscles were consistently active for adjacent digit movements and those further away. EMG activity during static pose for the flexors was below 10% of the normalized integrated EMG activity, except for FDS2 at 19%. In contrast, the extensor muscles showed EMG activity between 20-30% during static pose.

4.3.2 Finger Flexors

For the flexor muscles assessed, movement and subject were significant factors ($p<.05$) for all models, and all models showed a significant interaction effect ($p<.001$) except for FDP4 (Figure 4.3e). The flexors muscle compartments showed a selective response for digit movements, and typically only showed a small amount of EMG activity for the movement of a neighboring digits. None of the flexor muscle compartments had EMG activity above static pose activity for movements that were more than one digit away.

This result is further emphasized by the low levels of EMG activity during static pose, which was tested against the EMG activity observed during movements. For FDS2-4, EMG activity during the static pose was between 7-19% of the normalized EMG activity (Figure 4.3b,d,f). FDP2-5 static pose EMG activity was lower and between 2-6% (Figure 4.3a,c,e,g). Out of all the muscles assessed FDS2 was the most selective, showing significant EMG activity only during D2 flexion. All other flexors assessed showed significant EMG activity for at least one other movement, although the pattern of coactivation varied based on the digit. FDS3 was significantly active during D4 flexion (67% of normalized EMG activity, $p<.001$), but not for D2 flexion (15%, ns). EMG activity of FDS4 was significantly active during D2-D5 flexion, at 16%-20% of the normalized EMG activity when performing non-D4 flexion movements.

FDP2 showed an unusual pattern of EMG activity, as the highest EMG activity occurred during D3 flexion (170%, p<.001), and no significant EMG activity for D4 and D5. Unlike the other muscles, only data from one subject for FDP2 was available. FDP3 showed significant levels of EMG activity during D2-D4 flexion with 20% normalized EMG activity during D2 flexion and 55% for D4 flexion (p<.001). The coactivity shown is similar to FDS3, which was also strongly modulated for D4 flexion. FDP4 was less active than FDS4 during the movement of neighboring digits; significant EMG activity only occurred during D3 flexion (20%, p<.005). Besides D5 flexion, EMG activity of FDP5 was only significantly present during D4 flexion (39%, p<.001).

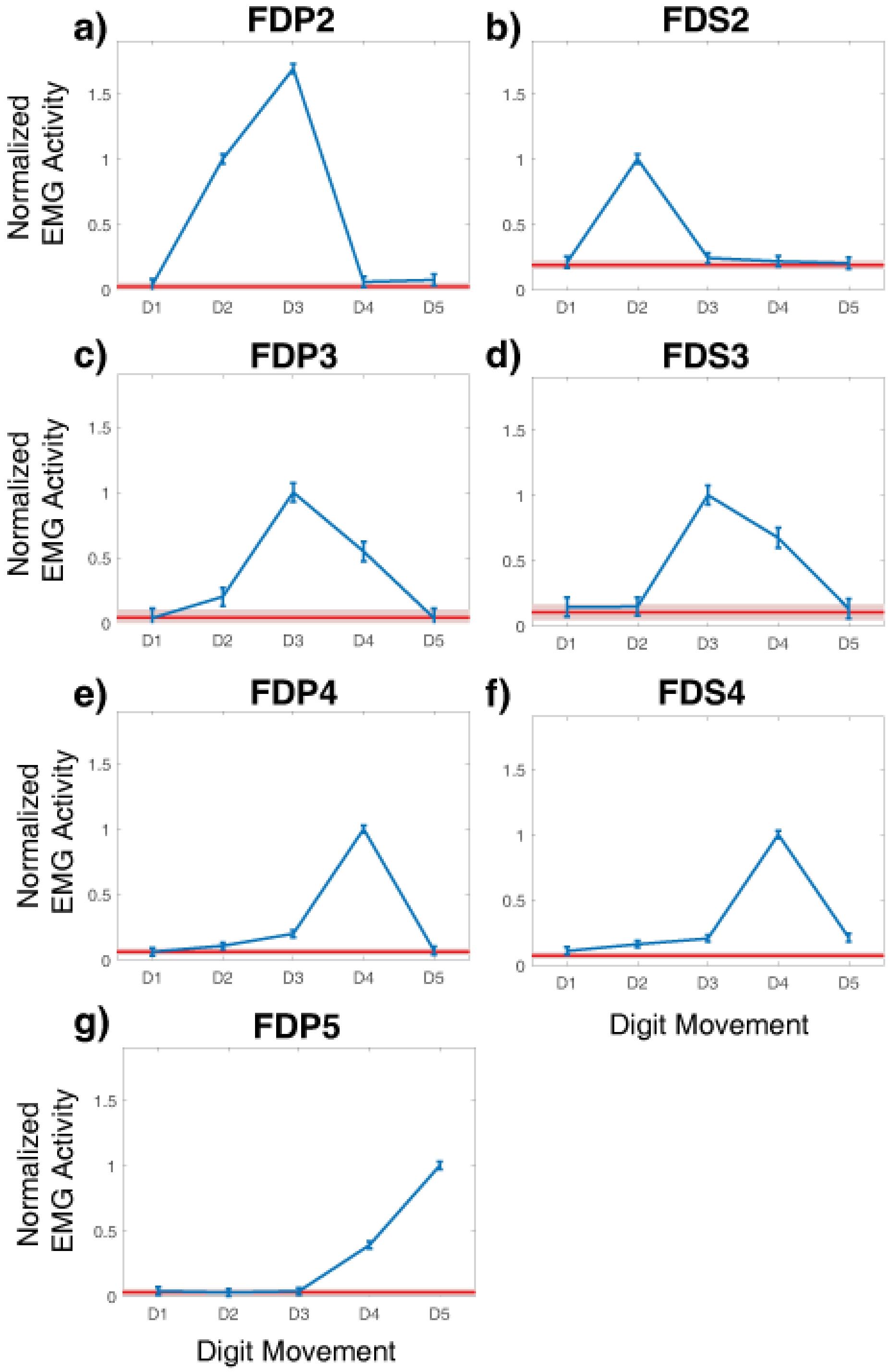

Figure 4.3 Coactivation across the extrinsic finger flexor muscles

The subplots show the generalized models developed for the extrinsic finger flexors. Each point represents the estimated marginal mean and error bars show the 95% confidence intervals of EMG activity during flexion movements. The horizontal red bar and shaded area represent the estimated marginal mean of EMG activity during static pose and the 95% confidence intervals.

4.3.3 Finger Extensors

In contrast to the flexor muscles, the extensors showed high levels of EMG activity across many movements of the digits. ED2, EIP, and ED4 models showed EMG activity significantly above static pose during all movements. EDM was the most selective extensor muscle but still had EMG activity significantly above static pose during D3-D5 movements. The EMG activity of the extensor muscles decreased for movements that were further away from the actuated digit. For all extensor muscle models, subject and movement were found to be a significant factor ($p<.001$) and showed a significant interaction effect ($p<.001$).

ED2 and EIP showed the highest levels of coactivity during D1 extension movements at 85% and 89% of the normalized EMG respectively (Figure 4.4a-b). EMG activity of these two muscles was lower for extension movements of digits further away from D2, down to 50% and 40% for ED2 and EIP during D5 extension. For ED4, the highest levels of coactivity were during D3 and D5 extension movements at 58%. EMG activity of ED4 continued to decrease for movements further away, with the lowest level of EMG activity occurring at 38% during D1 extension (Figure 4.4c). Out of the extensor muscles assessed, EDM was the most selective but still showed coactivation for D4 (73%) and D3 (50%) extension movements (Figure 4.4d).

The EMG activity of the static pose of the extensors ranged from 21-29% of the normalized value. This level, which was much higher than those of the flexors, was due to the static pose in which subjects held their fingers extended. Compared to the flexor muscles, the higher level of EMG activity during static pose meant that detecting differences from static pose would only occur if higher levels of EMG activity were recorded during digit movements. Given this, the coactivation that was observed from the extensor muscles is further highlighted.

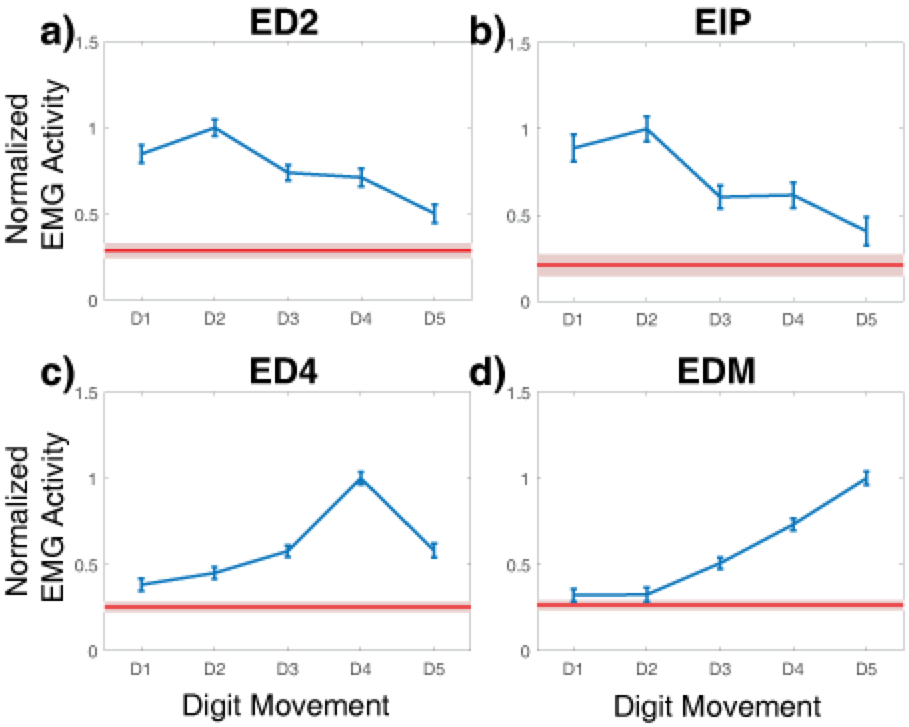

Figure 4.4 Coactivation across the extrinsic finger extensor muscles

The subplots show the generalized models developed for the extrinsic finger extensors. Each point represents the estimated marginal mean and error bars show the 95% confidence intervals of EMG activity during extension movements. The horizontal red bar and shaded area represent the estimated marginal mean of EMG activity during static pose and the 95% confidence intervals.

4.3.4 Individuation Indices

We characterized the ratio of EMG activity during non-associated digit movements to associated movements using the individuation index (II) described in Equation 4-1. The individuation indices reinforce the coactivity findings while exploring differences in subjects for each muscle. For the flexor muscles, the trend of selectivity was still seen as most subjects were above 0.8. The lowest index (least selective) was found to be FDP2 at .55; however, this was from a single subject who showed an anomalous level of activity. In contrast, FDS2 was the most selective flexor muscle with an average index of 0.9. Beyond the D2 flexors, FDS and FDP were largely in agreement: FDP3 and FDS3 had a lower index on average than FDP4 and FDS4 respectively (Figure 4.5a). Flexor subjects had similar levels of individuation indices, with only a couple of notable outliers. The individuation indices of the extensor muscles exhibit nearly the opposite behavior. ED2 and EIP showed much lower individuation indices than ED4 and EDM (Figure 4.5b) and are the lowest observed of any muscle, whereas ED4 and EDM had approximately equivalent indices overall. The extensor muscles showed a strong variance of responses in individuation indices across subjects, with ED2 having a range of 0.55.

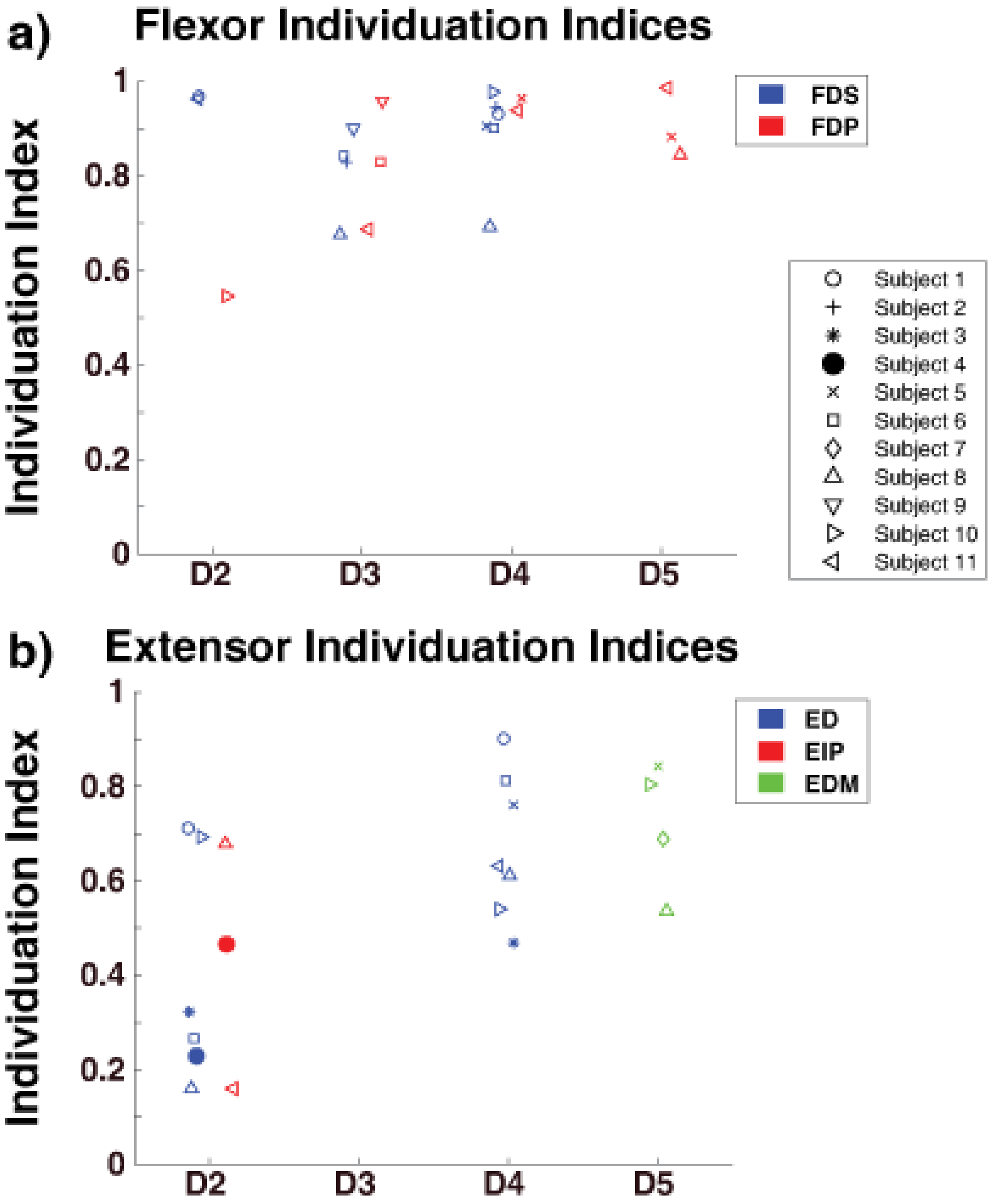

Figure 4.5 Individuation indices of finger flexors and extensors

Subjects are coded by shape, and muscles are coded by color. The horizontal axis represents the associated finger. For the multicompartment muscles such as FDS, FDP, and ED, the horizontal axis corresponds with the associated compartment. An individuation index of 1 represents a muscle that shows no significant activity during the same action of other fingers, whereas an individuation index of 0 represents equivalent EMG activity across all movements.

4.4 Stabilization

The flexor and extensor muscles showed different behaviors during antagonist movements. For the flexor muscles, EMG activity was always above static pose level and typically the highest when the associated digit was extending. For the extensor muscles, EMG activity was typically low when the associated digit made flexion movements. Similar to the behavior observed during coactivation, the flexors showed low levels of EMG activity with all movements below 30% of normalized EMG activity, whereas the extensors were much more active and generally between 40-80% of normalized EMG activity for many flexion movements.

Across all models, movement, subject, and the interaction effects were found to be significant ($p<.001$ except for FDP4 movement, $p<.05$). Pairwise comparisons were performed on a per muscle/model basis by comparing the estimated marginal means with a Bonferroni correction.

4.4.1 Flexors

The flexor muscles showed some EMG activity significantly above static pose during extension movements, but this was generally only for one or two movements. The highest EMG activity occurred in FDS2 during D2 extension at 30%. FDS2 was also significantly active during D1 and D3 extension at approximately equal levels of 16-17% respectively ($p<.001$). FDP2 was also significantly active during D1-D3 extension ($p<.005$), as well as D4 extension ($p<.05$) with EMG activity ranging between 14-22%. FDP3 was found to be more selective than FDS3. FDP3 was active only during D3 extension (17%, $p<.001$) whereas FDS3 was active for D3-D5 movements ($p<.001$), with the highest activity during D4 extension (22%) and low activity for D3 and D5 (14% and 11%). FDS4 and FDP4 overall showed very low levels of EMG activity during extension movements, with EMG activity of FDS4 for D1-D5 movements between 8-13% and FDP4 6-15%. Nonetheless, FDS4 EMG activity was still significantly above static posture activity for all D1-D5 extension ($p<.001$) whereas FDP4 was only significantly active for D4 extension (15%, $p<.05$). FDP5 also showed low EMG activity during extension movements and had EMG activity slightly above static pose levels for D5 extension (10%, $p<.001$) and D1 extension (7%, $p<.001$).

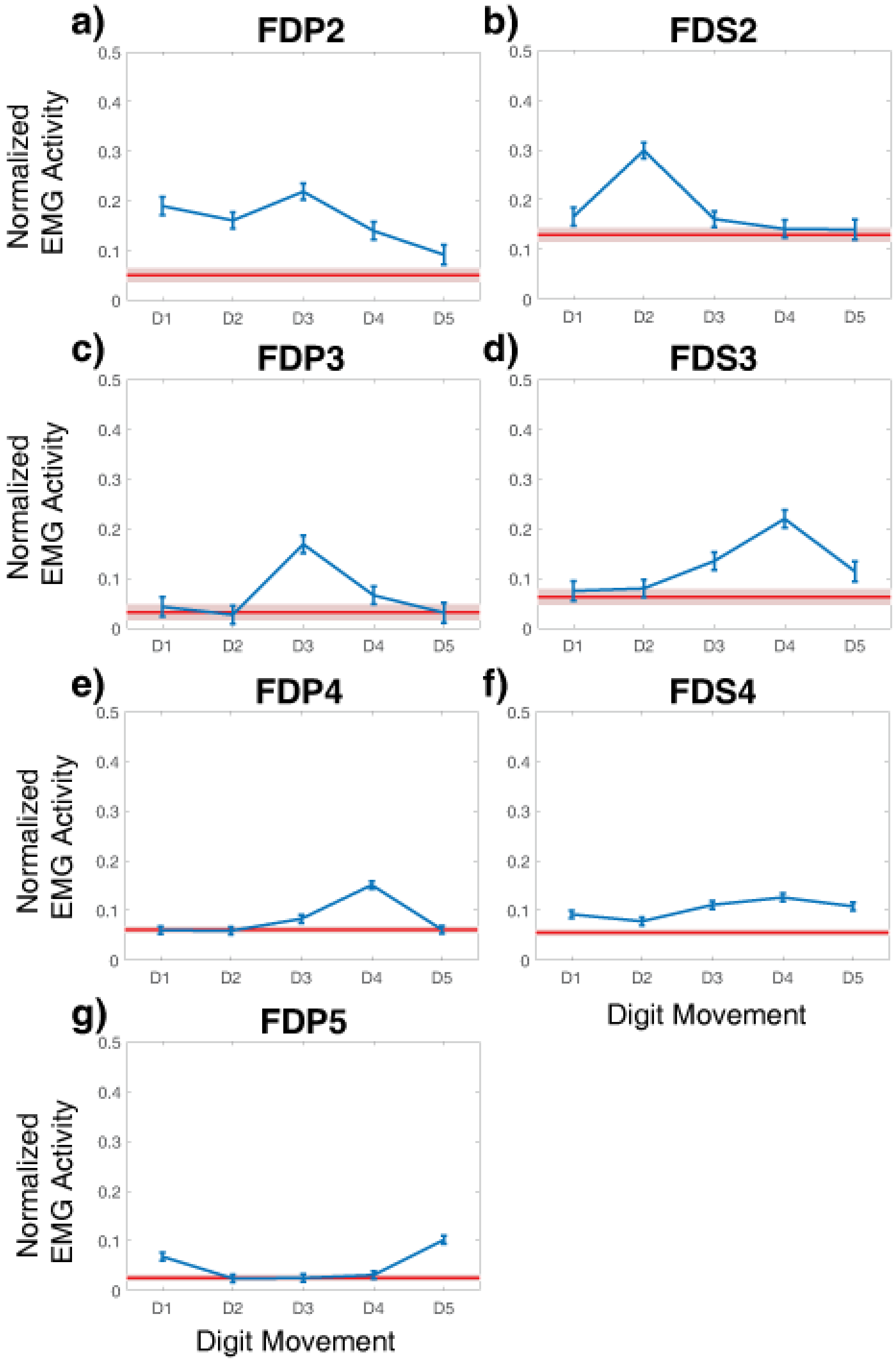

Figure 4.6 Stabilization of the extrinsic finger flexor muscles

General linear models for the extrinsic finger flexor muscles, representing the normalized EMG activity during extension movements. Each point represents the estimated marginal mean and error bars show the 95% confidence intervals of normalized EMG activity during extension movements. The horizontal red bar and shaded area represent the estimated marginal mean of EMG activity during static pose and the 95% confidence intervals.

4.4.2 Extensors

The extensor muscles showed a high level of EMG activity during flexion movements and shared some common patterns of EMG activity. No extensor muscles (ED2, EIP, ED4, and EDM) showed significant EMG activity above baseline rest during D2 flexion, but all extensor muscles were significantly active during D3 flexion. For ED2, EIP, and ED4, EMG activity during D3 flexion was the highest observed for coactivation, ranging from 59-76% of normalized EMG activity levels (p<.001). For EDM, the most EMG activity during flexion was observed during D4 movement at 85% of the normalized value (p<.001). ED2 and EIP showed common responses to flexion movements of the digits. Both muscles showed significant EMG activity approximately 50% of normalized EMG activity and during D4 flexion (ED2: 55% EIP:36%, p<.001). ED4 and EDM also showed similar patterns of EMG activity, with significant EMG activity occurring during D3-D5 flexion (p<.001). EDM was also significantly active during D1 flexion (60% normalized EMG activity, p<.001) while ED4 was not.

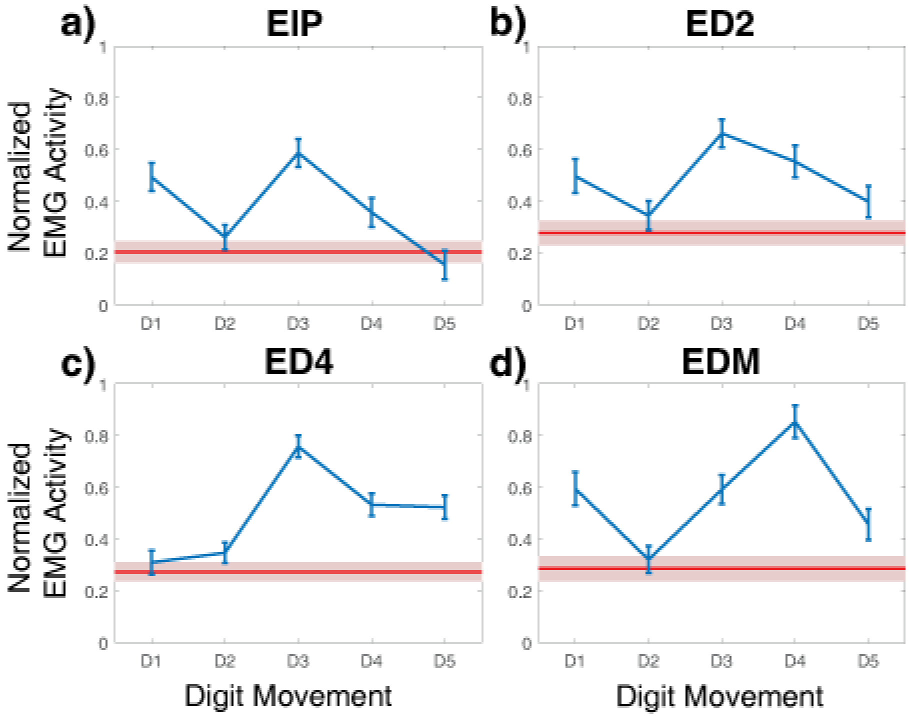

Figure 4.7 Stabilization of the extrinsic finger extensor muscles

General linear models for the extrinsic finger extensor muscles, representing the normalized EMG activity during flexion movements. Each point represents the estimated marginal mean and error bars show the 95% confidence intervals of normalized EMG activity during extension movements. The horizontal red bar and shaded area represent the estimated marginal mean of EMG activity during static pose and the 95% confidence intervals.

4.4.3 General Models of Coactivation and Stabilization

A set of generalized models for the extensors and flexors was developed to model coactivation and stabilization of the extrinsic hand muscles. Both the extensor and flexor muscles have the highest level activation during the associated movement, labeled ‘D’ (Figure 4.8a-b). As movements are performed by digits further away from the associated movement, EMG activity declines until it reaches the same level as static pose. EMG activity of the flexor muscles declines more drastically than that of the extensors. For the flexor muscles, EMG activity of D-1 and D+1 is 21% and 44% of the normalized EMG activity whereas the extensor EMG activity of D-1 and D+1 is between 65% and 74%. At D-2 and D+2, the EMG activity of the flexors is 11% and nearly indistinguishable from static pose (8%) whereas the extensor EMG activity at 47% and 68% is well-above static pose (26%).

The stabilization models show a stark contrast between the stabilizer muscles. For the extensor muscles, EMG activity was indistinguishable from static pose during flexion of the associated digit D, but higher for movement of the neighboring digits.

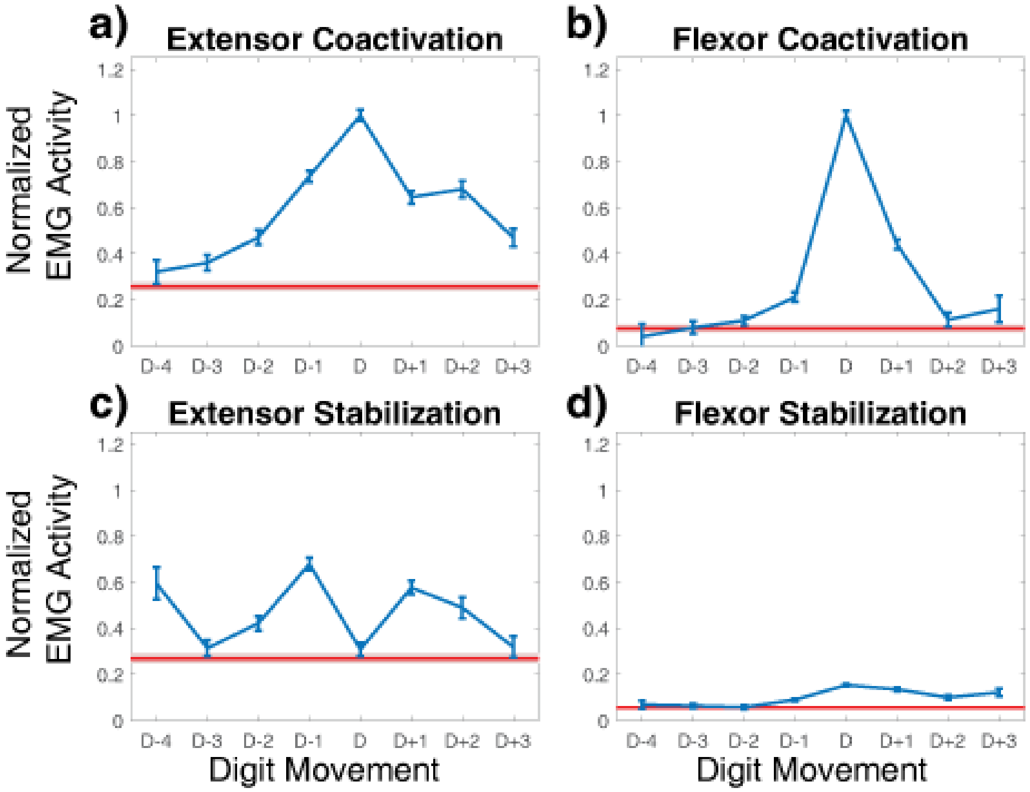

Figure 4.8 Generalized models of coactivation and stabilization

Generalized models of the extensors and flexors during agonist (coactivation) and antagonist (stabilization) movements. a-b) The highest EMG activity of the muscles occurs during the agonist movement of the associated digit, and decreases for movements further away. The extensors show a slower decline in EMG activity versus movement distance in comparison to the flexors, which do not show significant EMG activity occurring for finger movements more than one digit away.

4.5 Discussion

Coactivation, and to a much lesser extent stabilization, have been previously studied through the lens of electromyography and digit movement (Birdwell et al., 2013; Keen & Fuglevand, 2003, 2004b, 2004a; Kilbreath & Gandevia, 1994; Kilbreath et al., 2002; Leijnse, Campbell-Kyureghyan, et al., 2008; Li et al., 1998; Reilly et al., 2004; Schieber, 1995; van Beek et al., 2018; van Duinen et al., 2009; Zatsiorsky et al., 2000). These studies have still left a significant gap, which we addressed. Many studies only examined a single muscle during a unique task, making it difficult to compare responses of the muscle groups. The tasks used often involved large levels of force generation on the digits, and do not explore coactivation and/or stabilization during low force movements which are commonly performed during daily life. Over the course of this study, we addressed these gaps: we simultaneously examined EMG activity from ED, EIP, EDM, FDS, and FDP during low force movements during agonist and antagonist movements of D1-D5 using intramuscular EMG to target the individual muscle compartments.

We found that the finger extensors showed more coactivation than the flexors, and these results are further emphasized by the static pose position, which caused a higher EMG activity for comparison for the extensors than the flexors. These findings may be due to two reasons. The flexion movements involved use of the FDS and FDP muscles, therefore requiring less force generation from any single muscle which may have removed the need for activation of neighboring muscle to assist with the movement. It is also likely that humans are able to selectively activate the flexor compartments more than the extensors. The most common use of the hand involves grasping of the hand, an action largely performed by the finger flexor muscles. A review of hand function by Schieber and Santello explains that finger individuation during grasping allows for more complex grasps and complicated manipulations, such as tying a knot (Schieber & Santello, 2004). Extension of fingers can aid in manipulation, but the movements are largely driven by the flexor muscles.

Kilbreath and Gandevia showed coactivity of the FDP compartments when subjects lifted a weight on each finger which generated approximately 50% of a maximal voluntary contraction (MVC) for that digit (Kilbreath & Gandevia, 1994). Our results deviated from Kilbreath and Gandevia in that we found different patterns of coactivation present in some compartments of FDP. In particular, FDP3 for two of our subjects showed high levels of EMG activity during D4 movements, whereas Kilbreath and Gandevia found EMG activity below 10% MVC during the D4 task. Although we did not assess MVC levels, the movement tasks performed by subjects were likely well below the threshold Kilbreath and Gandevia used.

We presented EMG activity of the finger flexors and extensors during antagonist movements, dubbed stabilization, but found varied responses from the muscle compartments. For FDS and FDP, no consistent behavior was observed. For example, FDP2 was active during D1-D4 movements, with the most activity during D3 extension whereas FDP3-5 were most active for extension of the associated digits and showed little EMG activity for other movements. This pattern may have been influenced by the pose subjects held their hands, in which all fingers were extended. Because the non-moving digits were already extended, there was no clear mechanical need for the flexors to provide a stabilizing force to resist the extension of the neighboring digits.

Subjects often showed variance in our analysis, but this finding appears to be common across similar literature. Häger-Ross and Schieber’s study on the ability of the digits to perform individuated movements saw individuation indices of the middle and ring finger varying between 13% and 17% respectively (Hager-Ross & Schieber, 2000). In EMG research, Kilbreath and Gandevia’s subjects showed a difference of 40% MVC activity in FDP2 during the D4 task

(Kilbreath & Gandevia, 1994). Visual inspection of the raw EMG of subjects 5 & 6 presented by Leijnse, Campbell-Kyureghyan, Spektor, and Quesada show different responses to the same repeated tapping task. For example, EIP of subject 6 shows EMG activity during a D4 task at nearly the same level as during the D2 task while subject 5 does not (Leijnse, Campbell-Kyureghyan, et al., 2008). The group also discussed variance between subjects in EMG activity of ED2 and EIP in D2 tasks, suggesting that the redundancy of the muscles leads to these behaviors.

The individuation indices provide an overview of the variation by subjects to perform individual movements. The finger flexors showed little variance across the individuation indices; subjects generally had indices within .1 for each muscle with an occasional outlier. In contrast, the extensor muscles had much more variance. This was consistent across all four extensor muscles: ED2, EIP, ED4, and EDM. In some subjects, independence (or the lack thereof) was largely consistent across the muscles. Seven muscles from Subject 8 were included in the analysis. Of those seven muscles, five (ED2, ED4, EDM, FDS3, and FDS4) had among the lowest individuation indices per muscle. In comparison, Subject 1 had the highest individuation indices for three out of the four muscles assessed.

Electrode placement may have also played a role in the observed variation. Reilly and Schieber have suggested that there are four core regions of the FDP with motor units that act selectively for a digit and peripheral areas around these cores that feature overlapping motor units (Reilly & Schieber, 2003). Therefore, it is possible to see varying responses from the muscle compartment from the same subject. An example of this may be seen in Figure 4 of Reilly and Schieber's work: electrode B and C, placed in a compartment of FDP, both show preferential EMG activity for D3 flexion. During D2 and D4 extension, electrode C shows EMG activity while electrode B only shows minor activity for D4 extension. Due to this variability as well as variability in subject individuation, we felt it was most appropriate and informative to describe our results as generalized models to provide an overview of the patterns of EMG activity in the extrinsic hand muscles.

Our work was limited by having subjects hold the hand with the fingers extended. This position was used for static pose, which served as a baseline for EMG activity to compare to activity during movements, and as a position for the other fingers during movements. The posture had two effects: it influenced the EMG activity collected during static pose and set a higher level of EMG activity for comparison for the extensors, and a lower level for the finger flexors. We do not believe this impacted the results of the coactivation analysis, as the extensors demonstrated significant levels of EMG activity above static pose across most of the movements. Likewise, despite a lower level of EMG activity during static pose the flexors showed selective activation. However, the extended position of the non-moving fingers of the hand may have impacted the EMG activity flexor muscles during extension movement, as it was unnecessary for the flexor muscles to activate and stabilize the position of the associated digit during the movement of neighboring fingers.

We have performed one of the broadest EMG studies to date of the extrinsic finger muscles. We have collected and reported on data collected from 11 muscle sites in able-bodied subjects to model EMG activity during flexion and extension movements of D1-D5 for the purposes of understanding coactivation and stabilization. We found that the extensor muscles showed EMG activity during extension and flexion, even for movements more than one digit away, whereas the flexors were more selective and only active for the associated movement and a neighboring digit. This work may be useful towards understanding patterns of EMG activity of the extrinsic hand muscles for prosthetic control, but it is unknown whether the same patterns of coactivation and stabilization will remain or how they will change. Future work should focus on repeating this experiment in transradial amputee subjects.

5.0 Optimization of EMG Activation and Simulation of Forward Dynamics

Electromyographic (EMG) signals from extrinsic hand muscles that remain after amputation can be used to control prosthetic hands. Clinically available systems typically use one of two algorithms for control: pattern recognition, in which predetermined prosthetic movements or states are commanded based on recognizing patterns of activity across multiple EMG sensors, or direct control, in which EMG activity directly controls output for a given degree of freedom (DOF). Both approaches face challenges in taking full advantage of modern prosthetic hands that can control individual fingers. In order to address some of the challenges of existing control schemes, we have developed an optimization approach to determine the impact of different intramuscular EMG to muscle activation signal transformations to drive an alternative control scheme based on a biomimetically inspired, dynamic model of the hand with Hill-type muscle actuators. Using kinematics and EMG activity recorded from up to 16 muscles in three able-bodied subjects, we attempted to optimize the linear gains of a signal processing chain in order to drive the forward kinematics of a 17-DOF musculoskeletal model and recreate five different movements and postures of the hand. Using this incomplete set of data from the hand, we are able to reproduce movements of the wrist and fingers with normalized RMS positional error levels of down to 0.23±.08 of the normalized range of motion averaged across 17 joints.

5.1 Introduction

Research on upper-limb prosthetic control has exploded in recent years and struggled to keep pace with emerging myoelectric prosthetic devices. Present myoelectric prosthetic hands can offer six degrees-of-freedom of at the fingers and wrist, yet few control algorithms are able to take advantage of this to restore dexterous and simultaneous control over the joints. Previous efforts towards prosthetic control algorithms have typically attempted to restore hand function through either direct control, e.g. matching EMG activity to velocity (Cipriani et al., 2014; Smith et al., 2014), or by using pattern recognition to configure the hand in a predetermined shape (Hakonen et al., 2015; Leone et al., 2019; Scheme & Englehart, 2011). These algorithms are unable to fully restore dexterous hand functionality to the user as they suffer from one or more issues as algorithms are unable to scale beyond a few DOF for simultaneous control and users are unable to move the hand and fingers into arbitrary or spontaneous shapes. The ideal characteristics of an upper-limb prosthesis incorporates these factors, as well as minimal delay and little training (Farina et al., 2014).

Pattern recognition and direct control may never overcome these issues due to fundamental designs that prevent them from emulating the underlying control of the hand. For pattern recognition, it is self-explanatory: the classification of EMG activity into predetermined postures is incongruent with the ability to manipulate the hand into arbitrary methods. For direct control, it is the fallacious mapping of EMG activity to a kinematic property such as velocity. EMG activity is a representation of the neural drive to activate a muscle and generate force. Deriving velocity from such a metric requires factoring in the torque generated by the muscle about each joint which requires knowledge of the moment arm, muscle length, and contraction velocity as well as the net torque generated by agonist and antagonist muscles working at the joint.

Further confounding this issue is the complexities involved in the activation of multiple agonist and antagonist muscles in the hand muscles during even simple movements. Not surprisingly, whole-hand movements such as grasp require the synergistic activation of multiple muscles (Santello et al., 1998, 2002). However, even simple movements such as flexing a single finger requires the activation of multiple muscles to stabilize the non-moving digits (Reilly & Schieber, 2003). Model-based systems which have included this information have seen enhanced performance (Paclet & Quaine, 2012). These coordinated synergies are believed to be coordinated through the central nervous system (Overduin et al., 2014, 2008; Schieber & Santello, 2004; Takei et al., 2017; Takei & Seki, 2010), which suggests that muscle synergies may persist after trans-radial amputation even if there is no mechanical need.

Biomimetic model-based controllers have been proposed as an alternative control method. These controllers are particularly appealing as they may be more robust than traditional controllers (Sartori et al., 2018), offer arbitrary and dexterous control over a prosthesis, and require less training than traditional devices. Whereas a traditional device must be trained to associate EMG activity with a movement or map a joint to a kinematic output, the emergent properties of a biomimetic model can allow for generalizable EMG activity to accommodate a broad space of movement and posture combinations (Pan et al., 2019). Biomimetic controllers typically rely upon muscle activation as an input. The translation of EMG-to-activation is problem that has been approached in various ways. This has included decomposing EMG activity into motor unit action potentials (Kapelner et al., 2019), using non-linear models (Buchanan et al., 2004; Lloyd & Besier, 2003), artificial neural networks (Wang & Buchanan, 2002), or through the use of traditional feature extractions such as low-pass filtering, Willison Amplitude, zero-crossing, and so forth (Kamavuako et al., 2009). Very little effort has been put forth into testing and comparing EMG-to-activation methods, which has caused a lack of consensus amongst researchers for the optimal method. Further causing difficulty is the variables involved in these feature extraction methods. Feature extraction techniques such as mean absolute value have parameters which may be set, such as the window size for calculation, sliding vs. non-sliding window, and the update rate of the sliding window. When testing such differences in parameters, the amplitude of EMG activity used for normalization must also be recalculated which can cause further difficulty in comparing EMG processing methods. The effectiveness of an EMG-to-activation method cannot be definitively declared unless the parameter space is robustly explored.

In order to address this, we have developed an optimization environment in which EMG-to-activation methods may be robustly tested. Using previously recorded kinematics and EMG data, we are able to optimize the gains of an EMG-to-activation signal and simulate the forward dynamics of a 17 degree-of-freedom (DOF) musculoskeletal biomimetic model. In this study, we demonstrate as proof-of-concept the ability of the optimizer and model to accurately control movements of the fingers and wrist across a broad range of movements and postures.

5.2 Methods

5.2.1 Optimizer Overview

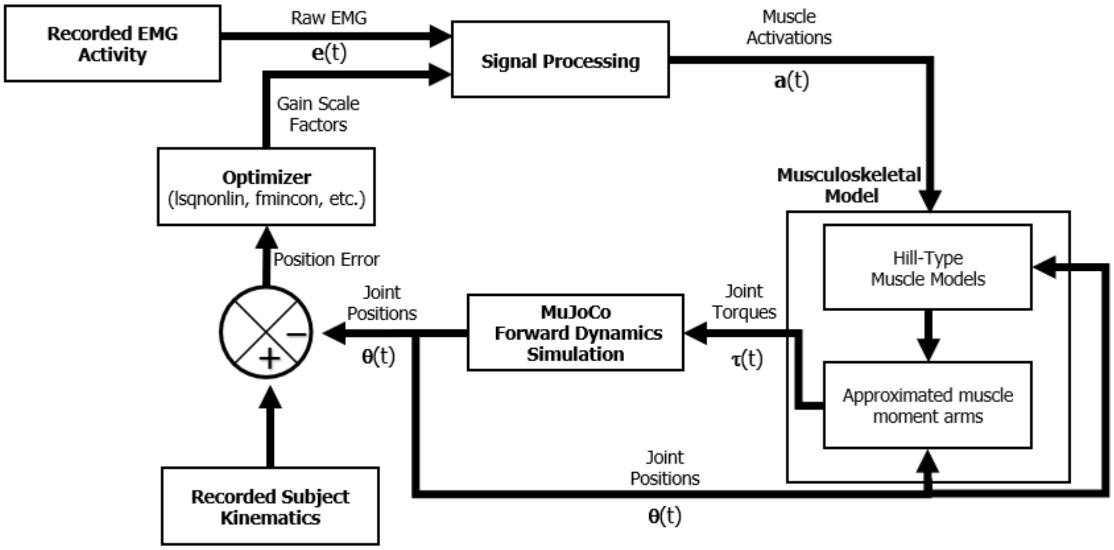

Figure 5.1 Block diagram of optimizer system

Offline recorded EMG activity e(t) undergoes signal processing to convert to muscle activation a(t). The muscle activation is input to the musculoskeletal model with joint positions θ(t) to calculate the output torques τ(t) across the joints. The torques are applied to the forward dynamics simulation in MujoCo and the timestep is advanced to receive the simulated joint positions. The simulated kinematics are compared to the subject kinematics to calculate the error, which is then used as a fitness measurement for the optimizer function to adjust the linear gains applied at the signal processing step.

The optimizer system is composed of several subsystems. The major components of this system are signal processing, the musculoskeletal model, forward simulation, and optimizer. Previously recorded EMG activity e(t) is input into the signal processing subsystem, where the signal is converted into activation a(t). Activation and the position of up to 18 degrees-of-freedom are then used as input to the musculoskeletal model. The muscle force is calculated using a Hill-type muscle model as well as the muscle moment arm for each of the muscles within the model. The resulting torques, both passive and active, τ(t) are then tallied for each joint and entered into the MuJoCo 2.0, where the forward dynamics are applied, the time step is advanced, and the model kinematics $\theta(t)$ are extracted to calculate the next series of muscle forces and moment arms. This loop repeats until the entire trial or series of trials is completed. The subject kinematics are then compared to the recorded subject kinematics. An error is calculated between these signals and used as the measure of fitness for the optimization subsystem which adjusts the scaled gains.

5.2.1.1 Signal Processing

The signal processing subsystem receives raw EMG activity as an input and outputs the muscle activation. In this subsystem, the EMG may be converted to activation using a chain of processing steps specified by the user in the config file. The order and properties of the processing steps can be varied, and processing methods may be repeated. For example, an acceptable processing step would be a low-pass filter at 1000 Hz, rectification, high-pass filter at 100 Hz, and then low-pass again at 10 Hz. The signal processing block is adaptable, and new processing methods may easily be added into it. Some examples of included programmed methods used in EMG-to-activation besides standard filtering methods include mean absolute value with configurable window size and sliding movement, the Willison Amplitude, and thresholding. The signal processing block interacts directly with the gain scaling factors; gain scaling is applied directly after the completion of signal processing.

5.2.1.2 Musculoskeletal Model

The musculoskeletal model receives neural activation and joint positions as input and produces torque for the joints. The musculoskeletal model can be separated into two components: the Hill-type muscle model, and moment arm calculation. The Hill-type muscle model uses activation and joint position to calculate muscle force. In the muscle model, joint position is used to determine the length of the muscle as part of the calculation for active and passive force, while activation is the volitional drive to create a movement. Muscle lengths are also used to calculate the moment arms as part of the force to torque calculation. The initial step of the musculoskeletal model uses the initial starting position of the recorded kinematics.

5.2.1.3 Forward Simulation

MuJoCo is a physics simulation environment which can simulate the movements of a model of the hand. The hand model uses user-defined parameters, such as joint stiffness and viscosity as well as specified masses of the hand and digit segments to calculate the kinematics when a torque is applied. The forward simulation applies the torques from the musculoskeletal model to the physics model in MuJoCo simulation. After the torques are applied to the joints, time is advanced a step and the new joint positions are passed back into the musculoskeletal model. At the initial time step, the joint positions are set to starting position of the recorded kinematics. The forward simulation of the system can run in faster than realtime; for a 16 second trial, forward simulation and musculoskeletal modeling calculations may be completed in 2 seconds on a consumer-grade PC.

5.2.1.4 Optimizer

The optimizer block adjusts the gain scale factors based on the error between the forward simulation and recorded subject kinematics. The error is calculated across each joint and normalized to the total range of motion for the joint. The error for each degree-of-freedom is calculated to the root mean square (RMS), and multiplied by a weighted term before being summed. The optimization function used may be interchanged. For this study, the least-squares non-linear optimizer function (lsqnonlin) was used. Lsqnonlin was selected as it allows for optimization of multiple variables, and the solution space may be constrained.

5.3 Experimental Procedures

Methods for EMG and kinematic data collection are described in Section 2.0.

5.3.1 Subject Selection

Of the 12 subjects implanted with electrodes, three were selected to demonstrate the optimization process. Subjects were selected based on having EMG activity from four wrist muscles (ECU, ECRL, FCU, FCR) and at least one agonist-antagonist pair (preferably more) for a digit. Subjects were also preferentially selected based on having a close to complete set of muscles which represented the extrinsic finger muscles. A list of subjects and corresponding signals to the optimizer as well as the digits included in movement trials are shown in Table 5.1.

Table 5.1 Signal list by subject for optimization

	Subject 4	Subject 8	Subject 10
Signal Label	ECRL	FPL	ECU
	ECU	APL	ECRL
	FCU	ED2	EPL
	FDP4	ED4	EDM
	EPL	EIP	APL
	ED4	EDM	FPL
	EIP	EPL	ED4
	ED2	PECM_M	SUP
	APL	FDS3	FDP3
	FPL	FDP2	PECM_M
	SUP	FDS4	FCU
	FDP2	FCR	FCR
	FDS2	ECU	PT
	FDS3	ECRL	ED4
	FCR	FDP5	ED2
	PT	FCU	FDS4
Digit	Index (D2)	Index (D2)	Ring (D4)

5.3.2 Optimization and Forward Simulation

Five trials were chosen from each of the subjects for analysis: digit flexion/extension when the wrist was held 1) neutral, 2) flexed, and 3) extended, and wrist flexion/extension when the fingers were 4) fully flexed and 5) fully extended. The digit trials selected varied between subjects. Because subjects did not have identical placement of electrodes, the digit trial was selected based on the electrode placement of at least one flexor and extensor muscle. Preference was given for digits which had EMG activity recorded from the most associated muscles.

Optimization of the trials was run two ways: batch and single trial optimization. In batch optimization, all 5 trials were optimized simultaneously to find a single set of gains that minimized the error across the trials. For single trial optimization, gains were optimized individually to each trial to minimize the error within each trial. In some instances, the optimization process became trapped in local minima. In order to overcome this, optimizations were run multiple times and the initial starting point of the gains was randomized. Batch optimizations were run 20 times, and single trial optimizations were run 5 times each for a total of 25 runs.

The objective of the optimizer functions was to reduce the weighed sum of the RMS position error. The position error was calculated at each of the 17 DOF of the model by measuring the difference between the subject and model kinematics. Position error was then normalized by range of motion for the joint, and the root mean square was calculated. The RMS error of each joint was multiplied by a subject-dependent set of weights. Across all subjects, 12 out of 17 joints were given a weight of 0; the joints which were weighed greater than 0 were the D2-D5 metacarpal (MCP) joints and wrist flexion/extension.

The RMS positional error was chosen as the fitness metric after considering using the correlation coefficient and identifying four types of outcomes with both metrics (Figure 5.2). The chief advantage of the RMS positional error is that it provides an accurate metric for the performance of a joint during both movements and static poses. Although having a high correlation coefficient is also ideal, there are instances in which a high correlation coefficient does not appropriately represent a movement (Figure 5.2b). Similarly, a low correlation coefficient does not necessarily mean poor performance. In Figure 5.c, the fingers are held in a static pose. The low correlation coefficient would initially suggest that there is a poor match between the simulated and subject kinematics, but observation of the joint position over time shows that the simulated joint accurately replicates the position of the subject.

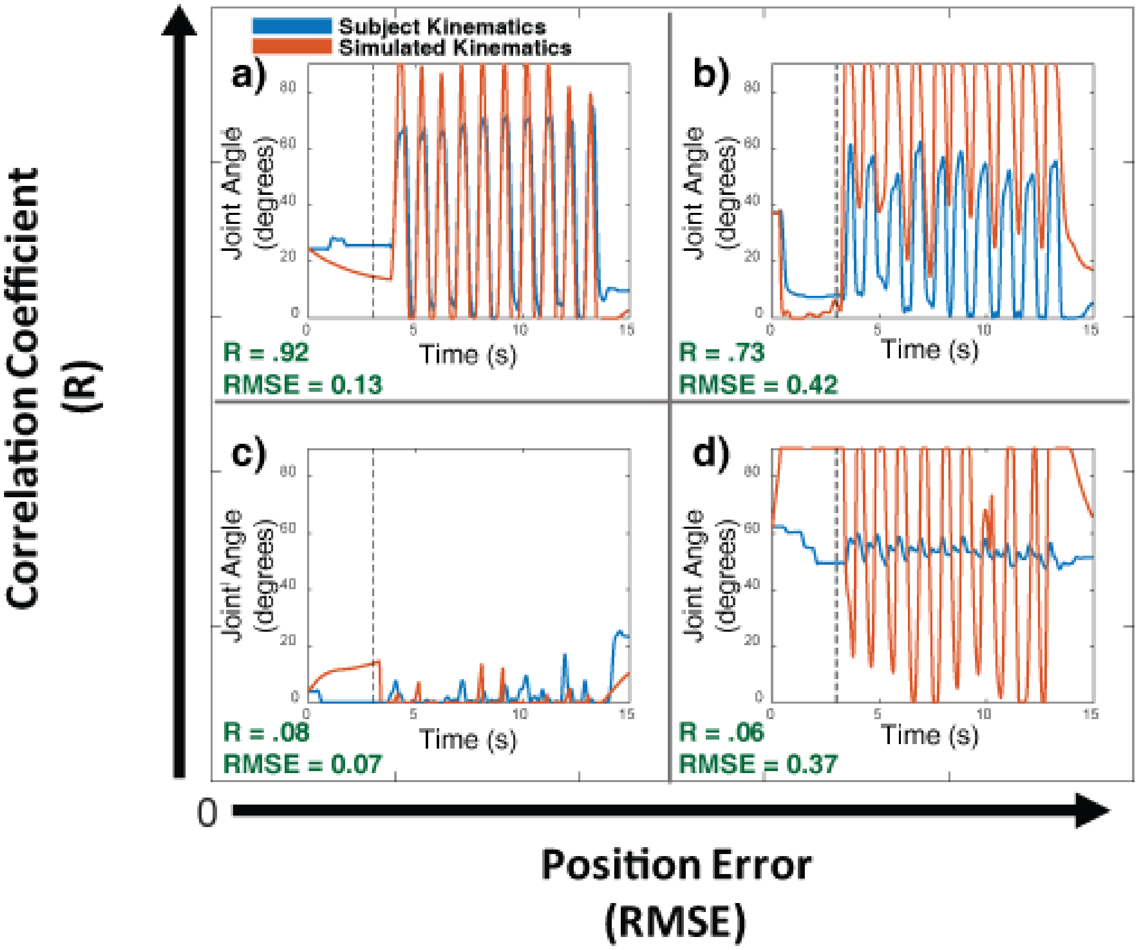

Figure 5.2 Visualization of R and RMS error values with joint kinematics

Subject (blue) and optimized simulated (red) kinematics are shown for static and dynamic states in the matrix above. The x and y axes represent increasing correlation coefficients and position errors respectively, and how kinematics which reflect these combinations of measurements, e.g. high RMS and low R, may appear. a) High R, Low RMSE: the desired outcome to match the subject kinematics. b) High R, High RMSE: the general trajectory of the movement is matched, but there is significant error between the position of the joint. c) Low R, low RMSE: kinematics in this quadrant are often from static poses. d) High R, High RMSE: a failure to optimize.

5.3.3 Signal Processing

EMG activity was high-pass filtered at 100 Hz with a 4th order butterworth filter, rectified, low-pass filtered at 2 Hz with a 4th order butterworth filter, and thresholded. Thresholds for the EMG activity were based on the mean EMG activity of each subject basis by activity when the subject had posed their hand with the fingers extended, wrist neutral, and self-supported above the table, and empirically adjusted. The filtered EMG activity was then normalized to 10,000. 10,000 was selected as it was a high enough level which EMG activity would be below, but low enough that the boundaries of the gains could still be scaled to maximize the activation as necessary. EMG activity was then downsampled from the originally recorded 30,000 Hz to 100 Hz to match the sampling rate of the subject kinematics. Figure 5.3 provides an overview of this process and how the shape of the signal changes with each of these steps.

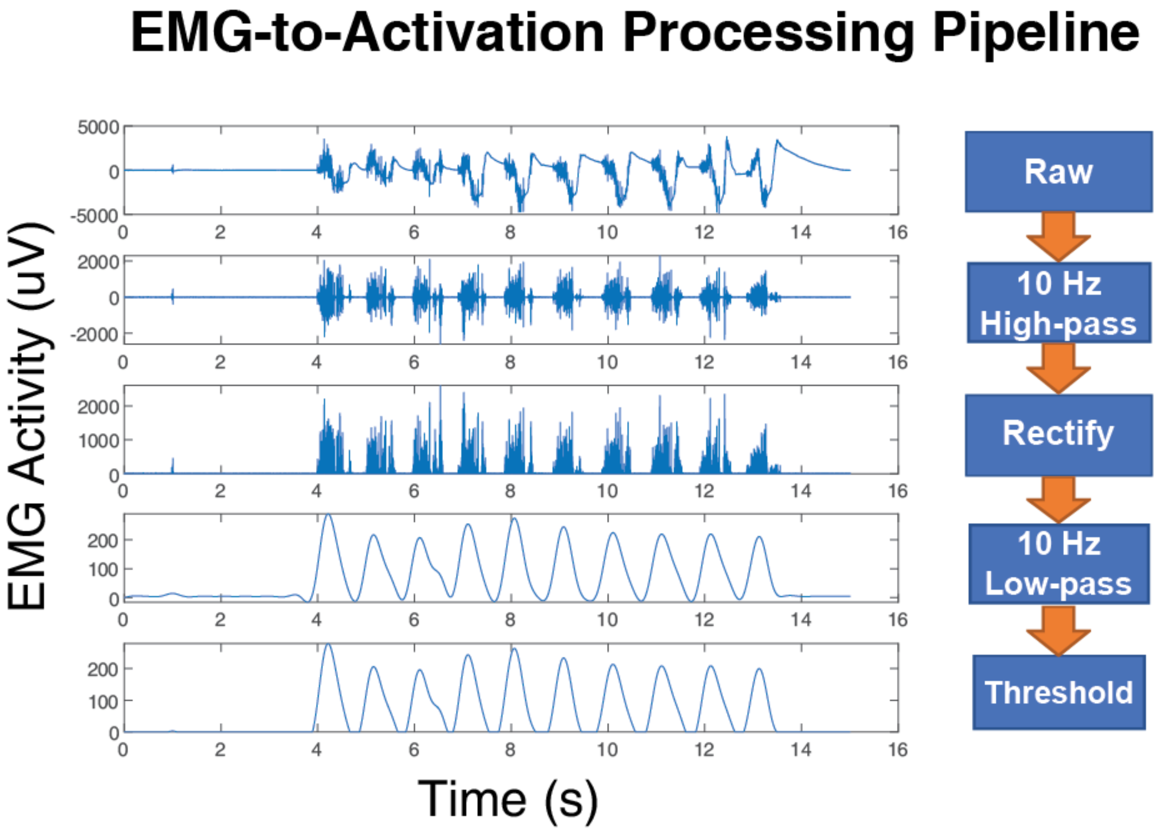

Figure 5.3 EMG-to-activation processing pipeline

Raw EMG activity is high-pass filtered before undergoing rectification, low-pass filtering, and a thresholding. This processing removes noise and drift from the signal and converts the EMG activity to activation. After thresholding, the signal is normalized to an arbitrary threshold and the optimizer searches to find the appropriate gains to scale the signal.

5.3.4 Statistical Analysis

After optimization runs were completed, trials with the lowest average RMS error for the wrist and digit MCP joint which was moved (D2 for Subjects 4 and 8, D4 for Subject 10) were included in final analysis. In addition to the wrist and digit MCP joints, the average normalized RMS error was calculated across all the joints. The correlation coefficients were calculated for all joints, and an overall average of all the coefficients for the joints was also calculated.

5.4 Results

Optimization was performed on subjects 4, 8, and 10 in two methods: optimization to a single trial, or to five trials to obtain a set of generalized gains. An example of the resulting kinematics for may be seen in Figure 5.4 for subject 8. The simulated results mimic the pacing of movements and posture of the subject. The common source of error from the trials shown in Figure 5.4 is from overshooting and undershooting the peak positions during flexion and extension movements. The results shown in Figure 5.4 represent the best and worst performances from the trials; the MCP joint during wrist flexion/extension with the fingers (Figure 5.4d) has the highest error for the tested MCP and wrist joint across all subjects and batch/single optimizations. In contrast, the wrist joint in Figure 5.4c has some of the lowest RMS error.

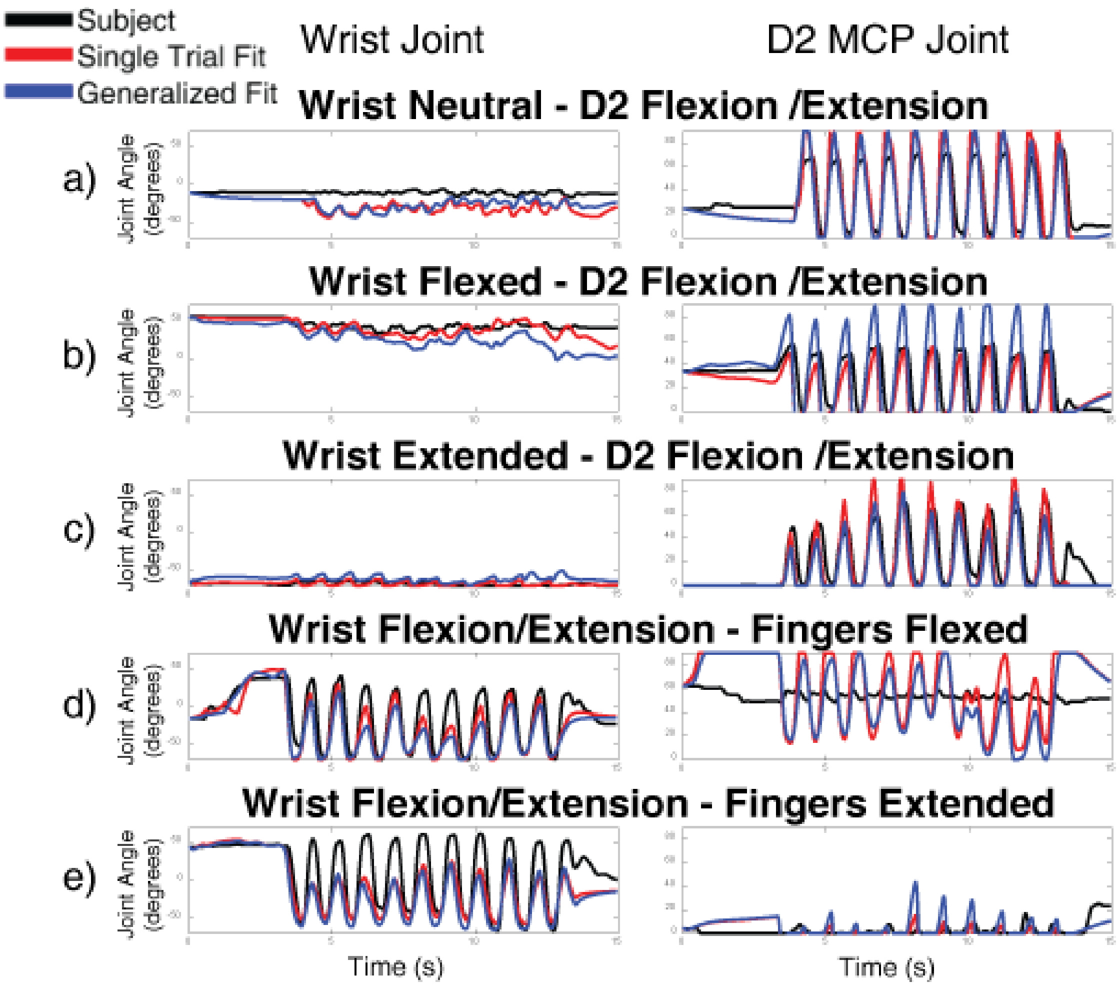

Figure 5.4 Comparison of subject kinematics to optimizer kinematics

Subject kinematics (black) and the resulting optimizer kinematics for single trial fit (red) and generalized fit (blue) for the wrist and D2 MCP joints for subject 8. The overfit single trial models predictably outperform the generalized batch results and closer match the subject kinematics.

Across all subjects, the overall lowest RMS error was at the wrist followed by the MCP joint of the tested finger. This is consistent with the weighting scheme used which was placed a higher importance on the wrist than the MCP joint. For subjects 4, 8, and 10, the average wrist error for generalized optimizations was 0.10±.04, 0.15±.07, and 0.19±.09 respectively whereas single trial optimizations for subjects 4, 8, and 10 were 0.09±.04, 0.12±.08, and 0.16±.07. For subjects 4, the RMS error at the MCP joint was the highest observed of the three subjects; the RMS error of the MCP joint was much higher at 0.44±.13 for the generalized fit but much lower at 0.22±.09 for single-trial fit (Figure 5.5a). Subjects 8 and 10 had lower average RMS errors of 0.13±.20 and 0.38±.09 for generalized fits, and 0.17±.10 and 0.32±.08 for single-trial fits (Figure 5.5c,e). Out of the three subjects, subject 8 had the best performance and least difference between generalized and single trial gains. The overall average RMS error for subject 8 was the same for general and single trial optimization runs: 0.24. Subjects 4 and 10 both had higher levels of RMS error; subject 4 had an overall average RMS error of 0.35±.07 and .26±.06 for general and single trial optimizations. Subject 10 had similar levels of error at 0.35±.07 and 0.27±.09 as well (Figure 5.5).

The correlation coefficients of the subjects showed a broad range of responses. In nearly all cases, the highest correlation coefficients were observed during single trial optimizations despite not being a factor in fitness optimizations. For subjects 4 and 8, the highest correlation coefficients were associated with the wrist joint. The wrist joint of subject 4 had a R value of 0.57±.43 for generalized optimization and 0.67±0.42 for the single trial optimization. The wrist joint of subject 8 had a correlation coefficient of 0.54±.35 and 0.572±.32 for the generalized and single trial. Subject 10 had a lower wrist performance with correlation coefficients of 0.38±0.4 and 0.49±.43 for generalized and single trials. The MCP joints had a lower correlation coefficient than the wrist for subjects 4 and 8. For subject 4, the D2 MCP joint had a correlation coefficient of 0.38±.23 and 0.39±.31 for generalized and single optimizations. Subject 8 showed better performance and equal performance, with an average R of 0.53±.47 and 0.53±.46 for generalized and single optimizations. The highest correlation coefficients were associated with Subject 10 D4 MCP joint at 0.69±.19 and 0.62±.25 for generalized and single optimizations. The correlation coefficients of the wrist and digit MCP joints were much higher than the average joint correlations.

For all subjects, the overall average of the joints was below 0.16 for both general and single trial optimizations (Figure 5.5b,d,f).

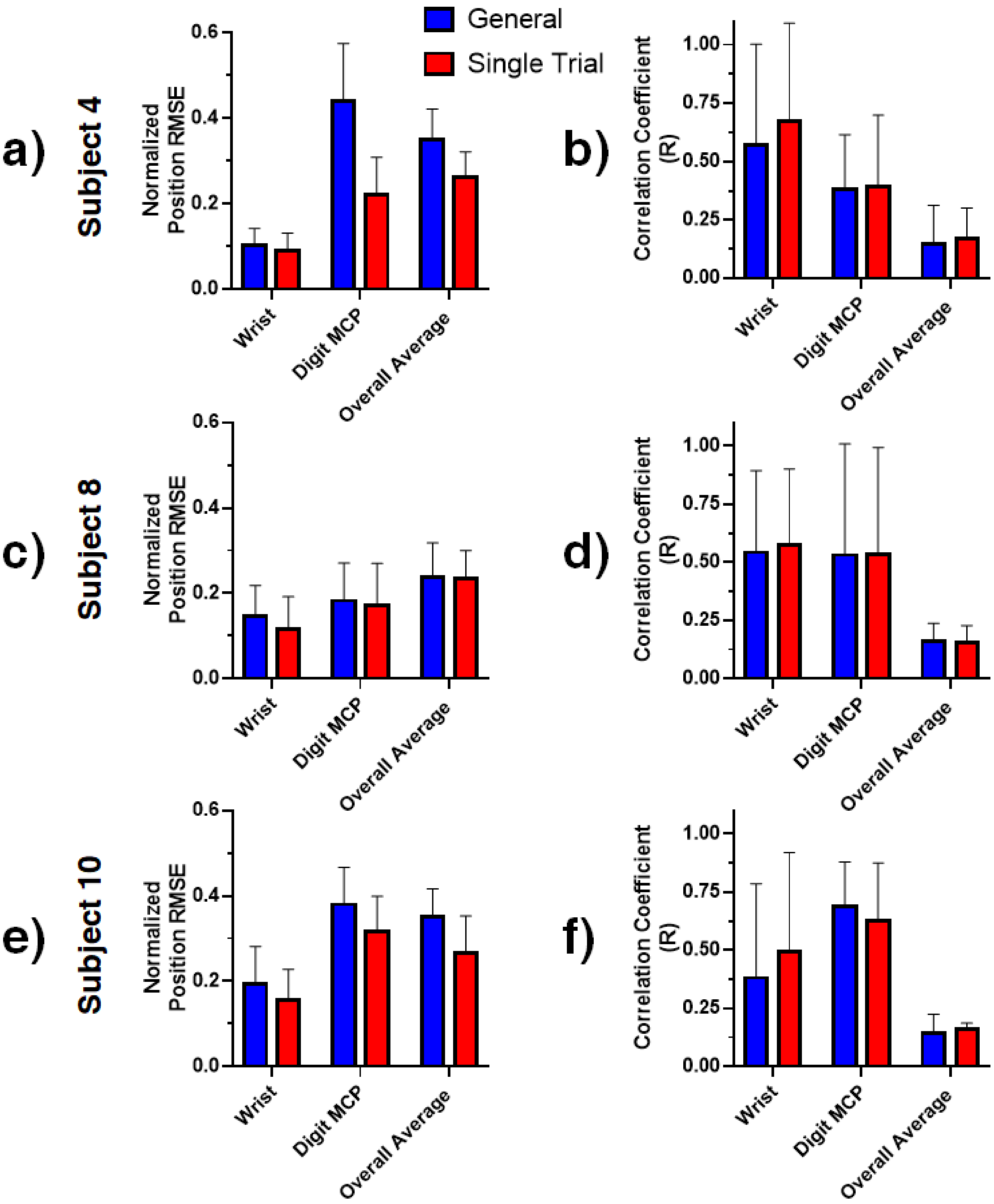

Figure 5.5 Error and correlation coefficients of optimization results

Mean and standard deviation of the normalized RMS error and correlation coefficients by subject for generalized (blue) and single-trial fit (red). Across all subjects and joints, the single trial optimizations consistently have lower RMS error. These difference in values range from being less than 2%, as seen in Subject 8, or much larger as shown in the MCP joint of Subject 4.

5.5 Discussion

In this study, we have demonstrated the ability of our optimization and modeling system to reproduce movements of the fingers and wrist in 17 degrees-of-freedom using a limited set of muscle EMG activity. The overall average RMS error for the generalized models was between 0.24-0.35, whereas the average RMS error for the single trial fits for subjects was 0.24-0.27. At the wrist joint, which was the most weighed in the fitness calculation, the average RMS error was between 0.1-0.2 for generalized fits and 0.09-0.16 for single trial fits. Our work shows that with a limited set of muscle targets, a generalized set of gains can be calculated to control a 17-DOF model to perform arbitrary movements in a variety of postures.

In these experiments, we demonstrated that a model may be trained on a broad set of movements and postures for generalizable applications and suffer less than an average RMS error of 0.1 compared to single trial optimizations. The difference in error of single and generalized fits varied between the subjects. For subjects 4 and 10, the average difference was approximately 0.9, whereas subject 8 had a difference in error of single and generalized fits as 0.03. A possible explanation for this discrepancy is that more attention was given to the selection of a threshold for subject 8; subject 8 had undergone robust testing in the optimization system for over a year prior to this experiment, and the optimal threshold level had been selected. In contrast, subjects 4 and 10 had not previously had their threshold levels tested in the optimizer and had been selected based on the mean EMG activity during a static hold position. While this was a fair initial starting point, more testing could be performed with the optimizer could feasibly attempt to vary the thresholds to identify a better threshold. The thought behind the development of the optimizer was meant for tasks such as this; because the optimizer will find the optimal gain setting for EMG-to-activation, different parameter spaces can be tested without having to re-examine the scaling of the signal.

The trials that the model was trained and evaluated on consisted of an initial period of static hold lasting three seconds followed by ten repetitions of a digit or the wrist while the other digits maintained a static pose. Although our overall error across the joints appeared to be high, it is important to keep this information in context when evaluating the effectiveness of the optimizer – during digit flexion and extension, the other fingers were not kept neutral but at a fully extended state.

In our results we showed RMS error and the correlation coefficients, although we did not use the correlation coefficient as a fitness measurement nor consider it in the selection of the final trials. We chose to include the correlation coefficients to demonstrate the dissonance which may be observed when reporting results of prosthetic control devices. Correlation coefficients have value in quantifying the form of a movement, but not whether that movement was accurately performed. Figure 5.2b demonstrates that a high correlation coefficient can deceptively implicate that all is well, when the actual movement is drastically different. Similarly, a low correlation coefficient does not implicate a poor level of control. As shown in Figure 5.2c, the position is maintained and has an RMS error of 0.07, yet the correlation coefficient would suggest a drastic mismatch between the states of the subject and simulation. For these reasons, we believe that RMS error is an effective metric. RMS error can provide an accurate measurement of when a joint is kept in a static posture (Figure 5.2c) as well as the accuracy of a joint during dynamic movements (Figure 5.2a).

A major limitation of this work is the EMG data set used and lack of representation of all the extrinsic hand muscles. The musculoskeletal model can simultaneously simulate 54 muscles of the arm, with 33 of those muscles related to the extrinsic hand muscles. A maximum of 16 electrodes were implanted in a single subject at a time, giving incomplete coverage of the hand. In many of the subjects, only one or two digits had an associated extensor or flexor muscle with them. Because the model receives no activation for muscles which were not recorded, no torque is generated within these digits. As shown in Chapter 2, the extrinsic finger muscles generate torque which assists in wrist movements. Missing digits therefore effect torques generated at the wrist, which must then be compensated by the remaining muscles in the dataset. This can also affect digit movements: besides the intrinsic muscles, flexion/extension of the finger is coordinated by at least three muscles: FDS, FDP, and ED. When there is only partial coverage of these muscles, the activation must be scaled higher than normal to compensate for the deficiency.

Our work with the optimization system was also limited as we used only a single physics model. The forward dynamics of the model were simulated on a physics model of the hand and fingers which feature independent joint stiffnesses, damping, and mass values, all of which may drastically change the kinematic output even when the same activation signal is used. These values were derived from observing simulations and adjusting the parameters based on the results. Future work with the musculoskeletal model can work on further adjusting the parameters of the physics model to also improve performance. This may be accomplished by incorporating the model parameters into the optimization (e.g. allowing the model parameters to be fit), or through running multiple optimizations using a model with varying parameters to identify which EMG-to-activation and model combination are capable of achieving the lowest error.

The calculation of our fitness metric played a large role in our results. For this study, we used the weighted sum of the normalized positional error from the joints as the fitness function. Previous work in optimizing EMG activity for musculoskeletal models have focused on using joint torques (Lehman & Calhoun, 1990; Lloyd & Buchanan, 1996) as part of the fitness function. Our optimization system can do this, but we chose to focus on using the kinematics for this work as the behavior of the model and outputs are more easily interpreted, predictable, and able to be balanced. When using torque as an error function, difficulties may emerge; torque cannot be normalized on a per joint basis, and the necessary torque to be generated can be altered depending on the properties of the physics model. This makes balancing the torque error and weighing it across joints, with varying masses, stiffnesses, and damping to be a difficult endeavor. Another issue that arises, and a primary reason for using kinematics instead of torque for fitness, is that a minor difference in torque may have major ramifications. For example, if the torque for a movement is .01 N*m, an error of ± .015 N*m will either increase the torque of the movement in the given direction or move the joint into the opposite direction. A fitness function that uses such a metric (e.g. RMS) would weigh these errors equally despite one being opposite of user intent. Beyond these issues, kinematics as a fitness function has also been promoted as being more pertinent for training models to be used with trans-radial amputees (Crouch & Huang, 2016).

Future work with the optimization system will attempt to compare the effectiveness of EMG-to-activation methods, such as by comparing the effect of filter cut-off on EMG-to-activation performance. We also hope to use this system with datasets that have been recently released, which may feature more extensive coverage of the extrinsic hand muscles. Ideally, testing this model with new datasets would include EMG activity recorded from the residual muscles of transradial amputees.

6.0 Conclusions and Future Work

6.1 Summary

Control over the hand is deceptively complex and requires the coordinated efforts of many muscles to maintain postural stability while moving a joint. These details are commonly overlooked in the development of upper-limb prosthetic control devices. This is not necessarily due to the hubris of prosthetic control designers, but due to the lack of published works which demonstrates how mechanical and neural coupling is manifested in the EMG activity of the extrinsic hand muscles. This work is some of the first of its kind to show intramuscular EMG activity from so many extrinsic finger muscles across a broad range of movements.

6.1.1 Mechanical Coupling

The extrinsic hand muscles may stretch across more than 6 joints and therefore generate torque at those joints during muscle contraction intended to manipulate only a single joint. In Chapter 3, we demonstrated how such mechanical coupling may influence EMG activity. For example, we showed how the extrinsic finger muscles participate in the generation of torque at the wrist; EMG activity of the extrinsic finger muscles was not only a function of finger posture but also wrist movement. Likewise, we demonstrated that EMG activity of the extrinsic finger muscles during finger movements is affected by wrist posture. This has been examined by other groups, but not with intramuscular electromyography nor with the posture and wrist combinations used (Duque et al., 1995; Mogk & Keir, 2003; Werremeyer & Cole, 1997).

Subject variance played a large role in the results of this work, particularly in the effects of wrist posture on finger EMG activity. For example, EMG activity of ED2 showed a broad range of responses across subjects – in some subjects, wrist posture strongly altered EMG activity during D2 movements, whereas other subjects showed little to no effect. There are three plausible causes, or a combination thereof, that caused subjects to show such difference in magnitude between responses. The first is that anatomy across subjects may vary in such a way that the effect of wrist posture becomes muted. Perhaps the force necessary to make the movements is less affected by the lengthening or shortening of tendons, or variation in the origin/insertion of the tendons that caused them to be more lengthened or shortened than others. Another possible cause is that the neighboring digit assisted with the generation of force, due to shared tendon connections via the juncturae tendinum – essentially suggested that the generation of force was distributed to the neighboring digit which assisted with the movement. This is plausible, as digit independence has been showed to vary significantly across subjects (Hager-Ross & Schieber, 2000). Unfortunately, the dataset collected is limited in that there is not complete coverage of the extrinsic finger muscles, so we are unable to attempt to correlate coactivation of the neighboring digit with the magnitude of the effect of wrist posture. The final cause is that the placement of electrodes varied in the muscles between subjects. Reilly and Schieber showed a variation in EMG responses from electrodes placed in the same compartment of the extrinsic hand muscles. They suggested that the compartments have a center-out gradient of coding, where the center of the compartment is strongly active for that digit and the peripheral edge is less specific and becomes more active for the neighboring digit (Reilly & Schieber, 2003). It is likely that all three of these factors play a role rather than any one specifically.

6.1.2 Neural Coupling

The coordinated movements of the hand are only capable of occurring due to the neural coupling present. The numerous degrees of freedom offer a large solution space that is reduced by a synergistic framework. Given that the most common usage of the hand is for grasping and shaping the hand into a limited set of postures (Schieber & Santello, 2004), it is unsurprising that humans are not optimized for independent control of the fingers. In Chapter 4, I presented how this neural coupling is manifested in electromyographic signals of the extrinsic hand muscles. I characterized coactivation, EMG activity present when a neighboring digit performed the same action, and stabilization, EMG activity when a neighboring digit performs the opposite action, of ED, FDS, and FDP and developed a set of general models of behavior for the extensors and flexors.

On its face, these results provide information on the EMG activity of the extrinsic finger muscles and offer an expected level of EMG activity during a series of movements. These results have value to prosthetic control designers but looking deeper into common patterns across the extrinsic finger muscles unlocks new perspectives on synergies in the hand. In these results, I showed that the extrinsic finger extensor muscles show significant levels of EMG activity during the extension movement of neighboring digits, even for digits on the opposite side of the hand. During flexion movements, the extrinsic finger extensors still show significant EMG activity for distant digits – for example, ED2 showed EMG activity significantly greater than resting baseline even during D5 flexion. High levels of EMG activity appear to be a defining characteristic of the extrinsic finger extensors. Yet for D2 flexion, none of the extrinsic finger extensors assessed (EIP, ED2, ED4, and EDM) showed any significant EMG activity (Figure 4.7) This unusual behavior may be the result of a synergy across the fingers related to a stereotypical pinch grip. Whereas most digit flexion movements would result in a diverging motor command that elicits flexion in the neighboring digits, which the subjects overcame by volitionally focusing on keeping their fingers extended, during D2 flexion a unique command descends that does not diverge to neighboring flexor compartments and cause flexion of these digits. This is further supported by the asymmetric pattern of FDP3 and FDS3 shown in Figure 4.3: EMG activity of these compartments is greater than 50% of the normalized EMG activity during D4 flexion, but nearly indiscernible for D2 flexion. Patterns of EMG activation such as this fall under the umbrella of neural coupling and are rarely taken into account by prosthetic control developers, yet vital to understanding the hand.

6.1.3 Musculoskeletal Modeling and Optimization

We developed a testing environment that sought to find the optimal gains for an EMG-to-activation algorithm in order to drive the forward dynamics of a 17 DOF model of the hand. The objective of this work was to recreate movements performed by users in an offline environment. We demonstrated that we are capable of accurately recreating movements using an incomplete set of muscles to drive a Hill-type musculoskeletal model of the hand (Figure 5.4). In single trial optimizations, we can achieve a normalized average RMS error of below 0.17 of the normalized range of motion across 17 DOF. When control over the model was broadened to using a set of generalized gains, the increase in error was modest at .01. It is expected that performance will degrade as a specialized model becomes tuned for generalized movements, and the increase in error is an acceptable level in this regard.

We also explored how the RMS error and correlation coefficient may provide an incomplete picture of performance. Correlation coefficient was a useful metric for measuring how well the model followed a movement but had no value in determining the accuracy of holding a static pose. We provided an example of this in Figure 5.4c, which showed a comparison of subject and model kinematics of a joint meant to be held in a static posture. Despite having a normalized RMS error of .08 and matching the position of the subject, the model had a low correlation coefficient of .07.

The EMG-to-activation signal processing that we used is common in prosthetic control algorithms but may not be a good representation of activation. EMG-to-activation may be accomplished through other methods. The work presented was meant as a demonstration to show how machine learning could be applied to EMG-to-activation to find the optimal solution for a set of parameters and grade it based on output kinematics. Our methods of EMG-to-activation have been proposed that have value in being explored which go beyond low-pass filtering. For example, Kapelner *et al.* used a decomposition algorithm to convert EMG activity into neural spike trains to control a 3 DOF musculoskeletal model (Kapelner, Sartori, Negro, & Farina, 2020) and non-linear dynamics have been proposed as well (Zajac, 1989).

6.2 Future Work

Technological innovation has outpaced the body of research available on the EMG activity of the hand in able-bodied and amputee subjects, so future works should be focused on continuing to explore development in these fields. There is still much more to explore in the field of mechanical coupling, neural coupling, and particularly in musculoskeletal modeling. The focus of this work was geared towards improving knowledge in the field of motor control of the hand and electromyography for prosthetic control applications. There are still large gaps present in these fields, and this work has not scratched the surface in examining how trans-radial amputees may control the extrinsic hand muscles.

6.2.1 Coupling of the Extrinsic Hand Muscles

Our work was not an all-inclusive analysis of mechanical coupling in the hand and how it can affect EMG activity. Future work could still continue in this direction by performing follow-up studies that examine more wrist postures, including intermediate angles, and mapping the change in EMG activity for the movements as a function of these angles. Further building off of this, the effect of wrist posture when the arm is placed in different positions in space should be examined. Although arm position is expected to change the EMG activity of the extrinsic hand muscles, and indeed has been shown in a study to affect prosthetics control (Pan et al., 2019), more work is needed to bring awareness to this phenomenon.

Further work in neural coupling could focus on characterizing EMG activity patterns of the extrinsic hand muscles during common synergies. The work in Chapter 4 only scratched the surface on characterization of these extrinsic hand muscles by exploring coactivation and stabilization. We recorded and presented data that was observed but failed to present a strong theory on why each muscle had that response. As noted in the previous section, the idiosyncrasies present in some of the EMG data may be possibly explained by motor primitives and synergies across the extrinsic hand muscles. Perhaps the mistake was by characterizing the muscles, rather than the movement and how it related to stereotypical patterns of movement in the hand and neglecting to treat the hand has a system.

A major area of interest for us is exploring how coupling in the extrinsic hand muscles persists after traumatic limb loss in trans-radial amputees. The effects of wrist posture on finger muscle EMG activity is caused by the lengthening and shortening of muscles, which alters the level of activation necessary for the generation of equivalent force as well as the force requirements themselves. It is presently unknown whether this pattern of activity will remain after the loss of the limb, or whether it will dissipate due as there is no longer a change in the muscle lengths or force requirements. We are also interested in exploring coactivation in the extrinsic finger muscles in trans-radial amputees. The question arises of whether the synergies that are present across the extrinsic hand muscles persist after the loss of the limb or instead dissipate due to disuse. Further coactivation may also be present as the ability to independently move the fingers could possibly diminish.

One challenging area in this work was ensuring that subjects had performed the full range of motion for the movements. We only realized well after experimentation how much variability subjects showed in performing (or not) the assigned movements. In part this is because performing the movements while having sixteen wires implanted in the forearm muscles is uncomfortable, particularly when the hand is contorted into a fully flexed or extended position. We attempted to correct this by analyzing subject movements and removing movements that were outside of a specified range (Chapter 4). Future experiments that involve movements of the hand should investigate using a device which is physically displaced by the digit during movements to ensure that the full range of motion is reached such as the apparatus used by Li *et al.* (Li et al., 2000).

6.2.2 Musculoskeletal Biomimetic Model

A major area of future work is the implementation of controllers atop musculoskeletal biomimetic model (MBM). At the present time, the musculoskeletal model treats the fingers and finger muscle independently – there is no mechanical coupling between the fingers such as shared tendons or juncturae tendinum. Even passive movements of the fingers result in movements of neighboring digits (Lang & Schieber, 2004). Model performance could likely be further improved by adding these features, which would mimic the natural anatomy of the hand. Another major area of work for the MBM is development of a predictive model to simulate EMG activity from missing muscle locations. In Chapter 4, we showed generalized models of EMG activity for the extensors and flexors based on the movements of neighboring digits. It is conceivable that the inverse could be developed for the extrinsic finger muscles: the prediction of EMG activity based on the behavior of the neighboring digit muscles. While such a system is unlikely to be able to fully replace a hand, it is likely to at least provide some partial coverage and assist in whole-hand movements such as grasp.

Improvements aside, an area of interest in the future is to explore using the musculoskeletal model to simulate the intended movements of trans-radial amputee subjects. As kinematics would not be able to be recorded from these users, optimization would rely on comparing intended movement kinematics to predicted. This can be accomplished by instructing users to follow a motion and using the instructed kinematics as an input source, although some tests may be needed to identify how to compensate between possible delays between subject movements and intended kinematics. An alternative to this would be by recording the mirrored kinematics of the subject, as performed by Crouch and Huang in similar model-based work (Crouch & Huang, 2016).

I have presented intramuscular EMG data from the extrinsic hand muscles across a broad range of movements. With this data, I have shown how the mechanical coupling within the hand can contribute to modulation of the EMG activity of the extrinsic finger muscles. I have also shown how neural coupling is manifested in the EMG activity of the extrinsic finger muscles during the movements of neighboring digits. With these findings, I have demonstrated the viability of a high

DOF model-based prosthetic control system and developed an offline method of testing and simulating EMG-to-activation models. This approach may be used towards developing improved prosthetic control algorithms and identifying the important features of EMG activity necessary for prosthetic control.

Appendix A Supplementary Data

Appendix Table 1 List of movements performed for each subject

List of movements performed for each subject. For trial types 1-30 the wrist posture column indicates the static wrist posture for the entire trial, while the finger posture column indicates the position of the other fingers during the movement. For trial types 31-42 the wrist posture column indicates the wrist rotation posture for the entire trial, while the finger posture column indicates the position of all the fingers during the movement.

Trial #	Movement	Wrist Posture	Finger Posture
1	D2 Flexion/Extension	Neutral	Extended
2	D3 Flexion/Extension	Neutral	Extended
3	D4 Flexion/Extension	Neutral	Extended
4	D5 Flexion/Extension	Neutral	Extended
5	D1 Flexion/Extension	Neutral	Extended
6	D1 Abduction/Adduction	Neutral	Extended
7	D2 Flexion/Extension	Flexed	Extended
8	D3 Flexion/Extension	Flexed	Extended
9	D4 Flexion/Extension	Flexed	Extended
10	D5 Flexion/Extension	Flexed	Extended
11	D1 Flexion/Extension	Flexed	Extended
12	D1 Abduction/Adduction	Flexed	Extended
13	D2 Flexion/Extension	Extended	Extended
14	D3 Flexion/Extension	Extended	Extended
15	D4 Flexion/Extension	Extended	Extended
16	D5 Flexion/Extension	Extended	Extended
17	D1 Flexion/Extension	Extended	Extended
18	D1 Abduction/Adduction	Extended	Extended
19	D2 Flexion/Extension	Pronated	Extended
20	D3 Flexion/Extension	Pronated	Extended
21	D4 Flexion/Extension	Pronated	Extended
22	D5 Flexion/Extension	Pronated	Extended
23	D1 Flexion/Extension	Pronated	Extended
24	D1 Abduction/Adduction	Pronated	Extended
25	D2 Flexion/Extension	Supinated	Extended
26	D3 Flexion/Extension	Supinated	Extended
27	D4 Flexion/Extension	Supinated	Extended
28	D5 Flexion/Extension	Supinated	Extended
29	D1 Flexion/Extension	Supinated	Extended
30	D1 Abduction/Adduction	Supinated	Extended

Appendix Table 1 (Continued)

31	Wrist Flexion/Extension	Neutral	Flexed
32	Wrist Flexion/Extension	Pronated	Flexed
33	Wrist Flexion/Extension	Supinated	Flexed
34	Wrist Flexion/Extension	Neutral	Extended
35	Wrist Flexion/Extension	Pronated	Extended
36	Wrist Flexion/Extension	Supinated	Extended
37	Wrist Abduction/Adduction	Neutral	Flexed
38	Wrist Abduction/Adduction	Pronated	Flexed
39	Wrist Abduction/Adduction	Supinated	Flexed
40	Wrist Abduction/Adduction	Neutral	Extended
41	Wrist Abduction/Adduction	Pronated	Extended
42	Wrist Abduction/Adduction	Supinated	Extended

Bibliography

Acharya, S., Tenore, F., Aggarwal, V., Etienne-Cummings, R., Schieber, M. H., & Thakor, N. V. (2008). Decoding individuated finger movements using volume-constrained neuronal ensembles in the M1 hand area. *IEEE Transactions on Neural Systems and Rehabilitation Engineering*. https://doi.org/10.1109/TNSRE.2007.916269

Aggarwal, V., Acharya, S., Tenore, F., Shin, H. C., Etienne-Cummings, R., Schieber, M. H., & Thakor, N. V. (2008). Asynchronous decoding of dexterous finger movements using M1 neurons. *IEEE Transactions on Neural Systems and Rehabilitation Engineering*. https://doi.org/10.1109/TNSRE.2007.916289

Aggarwal, V., Tenore, F., Acharya, S., Schieber, M. H., & Thakor, N. V. (2009). Cortical decoding of individual finger and wrist kinematics for an upper-limb neuroprosthesis. *Proceedings of the 31st Annual International Conference of the IEEE Engineering in Medicine and Biology Society: Engineering the Future of Biomedicine, EMBC 2009*. https://doi.org/10.1109/IEMBS.2009.5334129

Ambike, S. S., Paclet, F., Latash, M. L., & Zatsiorsky, V. M. (2013). Grip-force modulation in multi-finger prehension during wrist flexion and extension. *Experimental Brain Research*. https://doi.org/10.1007/s00221-013-3527-z

An, K. N., Hui, F. C., Morrey, B. F., Linscheid, R. L., & Chao, E. Y. (2017). Muscles across the elbow joint: A biomechanical analysis. *Journal of Biomechanics*, *14*(10), 659–661. https://doi.org/10.1016/0021-9290(81)90048-8

Aratow, M., Ballard, R. E., Crenshaw, A. G., Styf, J., Watenpaugh, D. E., Kahan, N. J., & Hargens, A. R. (1993). Intramuscular pressure and electromyography as indexes of force during isokinetic exercise. *Journal of Applied Physiology*. https://doi.org/10.1152/jappl.1993.74.6.2634

Basmajian, J., & De Luca, C. J. (1985). *Muscles Alive, Their Functions Revealed by Electromyography*. Baltimore, MD, MD: Williams & Wilkins.

Beisteiner, R., Windischberger, C., Lanzenberger, R., Edward, V., Cunnington, R., Erdler, M., … Deecke, L. (2001). Finger somatotopy in human motor cortex. *NeuroImage*. https://doi.org/10.1006/nimg.2000.0737

Bell, D. G. (1993). The influence of air temperature on the EMG/force relationship of the quadriceps. *European Journal of Applied Physiology and Occupational Physiology*. https://doi.org/10.1007/BF00864225

Bickerton, L. E., Agur, A. M. R., & Ashby, P. (1997). Flexor Digitorum Superficialis: Locations of individual muscle bellies for botulinum toxin injections. *Muscle and Nerve*. https://doi.org/10.1002/(SICI)1097-4598(199708)20:8<1041::AID-MUS18>3.0.CO;2-Y

Birdwell, J. A., Hargrove, L. J., Kuiken, T. A., & Weir, R. F. f. (2013). Activation of individual extrinsic thumb muscles and compartments of extrinsic finger muscles. *Journal of Neurophysiology*, *110*(6), 1385–1392. https://doi.org/10.1152/jn.00748.2012

Birdwell, J. A., Hargrove, L. J., Weir, R. F., & Kuiken, T. A. (2015). Extrinsic finger and thumb muscles command a virtual hand to allow individual finger and grasp control. *IEEE Transactions on Biomedical Engineering*. https://doi.org/10.1109/TBME.2014.2344854

Blana, D., Chadwick, E. K., van den Bogert, A. J., & Murray, W. M. (2017). Real-time simulation of hand motion for prosthesis control. *Computer Methods in Biomechanics and Biomedical Engineering*. https://doi.org/10.1080/10255842.2016.1255943

Blana, D., Van den Bogert, A. J., Murray, W. M., Ganguly, A., Krasoulis, A., Nazarpour, K., & Chadwick, E. K. (2020). Model-based control of individual finger movements for prosthetic hand function. *IEEE Transactions on Neural Systems and Rehabilitation Engineering*.

Botte, M. J. (2003). *Surgical anatomy of the hand and upper extremity*. Lippincott Williams & Wilkins.

Buchanan, T. S., Lloyd, D. G., Manal, K., & Besier, T. F. (2004). Neuromusculoskeletal modeling: Estimation of muscle forces and joint moments and movements from measurements of neural command. *Journal of Applied Biomechanics*. https://doi.org/10.1123/jab.20.4.367

Burgar, C. G., Valero-Cuevas, F. J., & Hentz, V. R. (1997). Fine-wire electromyographic recording during force generation: Application to index finger kinesiologic studies. *American Journal of Physical Medicine and Rehabilitation*, *76*(6), 494–501. https://doi.org/10.1097/00002060-199711000-00012

Butler, T. J., Kilbreath, S. L., Gorman, R. B., & Gandevia, S. C. (2005). Selective recruitment of single motor units in human flexor digitorum superficialis muscle during flexion of individual fingers. *Journal of Physiology*, *567*(1), 301–309. https://doi.org/10.1113/jphysiol.2005.089201

Chase, R. A., & White, W. L. (1978). *Functional anatomy of the hand*. USA: Don Mills, Ont. : Southam Business Publications.

Christensen, H., Søgaard, K., Jensen, B. R., Finsen, L., & Sjøgaard, G. (1995). Intramuscular and surface EMG power spectrum from dynamic and static contractions. *Journal of Electromyography and Kinesiology*. https://doi.org/10.1016/S1050-6411(99)80003-0

Cipriani, C., Antfolk, C., Controzzi, M., Lundborg, G., Rosen, B., Carrozza, M. C., & Sebelius, F. (2011). Online myoelectric control of a dexterous hand prosthesis by transradial amputees. *IEEE Transactions on Neural Systems and Rehabilitation Engineering*. https://doi.org/10.1109/TNSRE.2011.2108667

Cipriani, C., Segil, J. L., Birdwell, J. A., & Weir, R. F. (2014). Dexterous control of a prosthetic hand using fine-wire intramuscular electrodes in targeted extrinsic muscles. *IEEE Transactions on Neural Systems and Rehabilitation Engineering*. https://doi.org/10.1109/TNSRE.2014.2301234

Clamann, H. P. (1969). Statistical Analysis of Motor Unit Firing Patterns in a Human Skeletal Muscle. *Biophysical Journal*. https://doi.org/10.1016/S0006-3495(69)86448-9

Cordella, F., Ciancio, A. L., Sacchetti, R., Davalli, A., Cutti, A. G., Guglielmelli, E., & Zollo, L. (2016). Literature review on needs of upper limb prosthesis users. *Frontiers in Neuroscience*. https://doi.org/10.3389/fnins.2016.00209

Crouch, D. L., & Huang, H. (2016). Lumped-parameter electromyogram-driven musculoskeletal hand model: A potential platform for real-time prosthesis control. *Journal of Biomechanics*. https://doi.org/10.1016/j.jbiomech.2016.10.035

Crouch, D. L., & Huang, H. (2017). Musculoskeletal model-based control interface mimics physiologic hand dynamics during path tracing task. *Journal of Neural Engineering*. https://doi.org/10.1088/1741-2552/aa61bc

Crouch, D. L., Pan, L., Filer, W., Stallings, J. W., & Huang, H. (2018). Comparing surface and intramuscular electromyography for simultaneous and proportional control based on a musculoskeletal model: A pilot study. *IEEE Transactions on Neural Systems and Rehabilitation Engineering*. https://doi.org/10.1109/TNSRE.2018.2859833

De Luca, C. J., Adam, A., Wotiz, R., Gilmore, L. D., & Nawab, S. H. (2006). Decomposition of surface EMG signals. *Journal of Neurophysiology*. https://doi.org/10.1152/jn.00009.2006

Dechent, P., & Frahm, J. (2003). Functional somatotopy of finger representations in human primary motor cortex. *Human Brain Mapping*. https://doi.org/10.1002/hbm.10084

Deeny, S., Chicoine, C., Hargrove, L. J., Parrish, T., & Jayaraman, A. (2014). A simple ERP method for quantitative analysis of cognitive workload in myoelectric prosthesis control and human-machine interaction. *PLoS ONE*. https://doi.org/10.1371/journal.pone.0112091

Delp, S. L., Anderson, F. C., Arnold, A. S., Loan, P., Habib, A., John, C. T., … Thelen, D. G. (2007). OpenSim: open-source software to create and analyze dynamic simulations of movement. *IEEE Transactions on Bio-Medical Engineering*. https://doi.org/10.1109/TBME.2007.901024

Duque, J., Masset, D., & Malchaire, J. (1995). Evaluation of handgrip force from EMG measurements. *Applied Ergonomics*. https://doi.org/10.1016/0003-6870(94)00003-H

Farina, D., Jiang, N., Rehbaum, H., Holobar, A., Graimann, B., Dietl, H., & Aszmann, O. C. (2014). The extraction of neural information from the surface EMG for the control of upper-limb prostheses: Emerging avenues and challenges. *IEEE Transactions on Neural Systems and Rehabilitation Engineering*. https://doi.org/10.1109/TNSRE.2014.2305111

Fligge, N., Urbanek, H., & Van der Smagt, P. (2013). Relation between object properties and EMG during reaching to grasp. *Journal of Electromyography and Kinesiology*. https://doi.org/10.1016/j.jelekin.2012.10.010

Fougner, A. L., Stavdahl, Ø., & Kyberd, P. J. (2014). System training and assessment in simultaneous proportional myoelectric prosthesis control. *Journal of NeuroEngineering and Rehabilitation*. https://doi.org/10.1186/1743-0003-11-75

Fougner, A. L., Stavdahl, O., Kyberd, P. J., Losier, Y. G., & Parker, P. A. (2012). Control of Upper Limb Prostheses: Terminology and Proportional Myoelectric Control—A Review. *IEEE Transactions on Neural Systems and Rehabilitation Engineering*. https://doi.org/10.1109/TNSRE.2012.2196711

Gentner, R., & Classen, J. (2006). Modular Organization of Finger Movements by the Human Central Nervous System. *Neuron*. https://doi.org/10.1016/j.neuron.2006.09.038

Gonzalez, R. V., Buchanan, T. S., & Delp, S. L. (1997). How muscle architecture and moment arms affect wrist flexion-extension moments. *Journal of Biomechanics*. https://doi.org/10.1016/S0021-9290(97)00015-8

Graziano, M. S. A., Cooke, D. F., Taylor, C. S. R., & Moore, T. (2004). Distribution of hand location in monkeys during spontaneous behavior. *Experimental Brain Research*. https://doi.org/10.1007/s00221-003-1701-4

Gritsenko, V., Hardesty, R. L., Boots, M. T., & Yakovenko, S. (2016). Biomechanical constraints underlying motor primitives derived from the musculoskeletal anatomy of the human arm. *PLoS ONE*. https://doi.org/10.1371/journal.pone.0164050

Hager-Ross, C., & Schieber, M. H. (2000). Quantifying the independence of human finger movements: Comparisons of digits, hands, and movement frequencies. *Journal of Neuroscience*. https://doi.org/10.1523/jneurosci.20-22-08542.2000

Hakonen, M., Piitulainen, H., & Visala, A. (2015). Current state of digital signal processing in myoelectric interfaces and related applications. *Biomedical Signal Processing and Control*. https://doi.org/10.1016/j.bspc.2015.02.009

Hargrove, L. J., Englehart, K., & Hudgins, B. (2006). The effect of electrode displacements on pattern recognition based myoelectric control. *Annual International Conference of the IEEE Engineering in Medicine and Biology - Proceedings*. https://doi.org/10.1109/IEMBS.2006.260681

Hargrove, L. J., Lock, B. A., & Simon, A. M. (2013). Pattern recognition control outperforms conventional myoelectric control in upper limb patients with targeted muscle reinnervation. *Proceedings of the Annual International Conference of the IEEE Engineering in Medicine and Biology Society, EMBS*. https://doi.org/10.1109/EMBC.2013.6609821

Hargrove, L. J., Miller, L. A., Turner, K., & Kuiken, T. A. (2017). Myoelectric Pattern Recognition Outperforms Direct Control for Transhumeral Amputees with Targeted Muscle Reinnervation: A Randomized Clinical Trial. *Scientific Reports*. https://doi.org/10.1038/s41598-017-14386-w

Harrison, V. F., & Mortensen, O. A. (1962). Identification and voluntary control of single motor unit activity in the tibialis anterior muscle. *The Anatomical Record*. https://doi.org/10.1002/ar.1091440205

Henzel, M. K., Munin, M. C., Niyonkuru, C., Skidmore, E. R., Weber, D. J., & Zafonte, R. D. (2010). Comparison of surface and ultrasound localization to identify forearm flexor muscles for botulinum toxin injections. *PM and R*. https://doi.org/10.1016/j.pmrj.2010.05.002

Hirt, B., Seyhan, H., & Wagner, M. (2016). *Hand and Wrist Anatomy and Biomechanics: A Comprehensive Guide*. Retrieved from https://books.google.com/books?id=3H5FDQAAQBAJ

Huang, H. P., & Chen, C. Y. (1999). Development of a myoelectric discrimination system for a multi-degree prosthetic hand. *Proceedings - IEEE International Conference on Robotics and Automation*. https://doi.org/10.1109/robot.1999.770463

Hudgins, B., Parker, P., & Scott, R. N. (1993). A New Strategy for Multifunction Myoelectric Control. *IEEE Transactions on Biomedical Engineering*. https://doi.org/10.1109/10.204774

Huesler, E. J., Maier, M. A., & Hepp-Reymond, M. C. (2000). EMG activation patterns during force production in precision grip. III. Synchronisation of single motor units. *Experimental Brain Research*. https://doi.org/10.1007/s002210000484

Ingram, J. N., Körding, K. P., Howard, I. S., & Wolpert, D. M. (2008). The statistics of natural hand movements. *Experimental Brain Research*. https://doi.org/10.1007/s00221-008-1355-3

Janssen, P., & Scherberger, H. (2015). Visual Guidance in Control of Grasping. *Annual Review of Neuroscience*. https://doi.org/10.1146/annurev-neuro-071714-034028

Jiang, N., Muceli, S., Graimann, B., & Farina, D. (2013). Effect of arm position on the prediction of kinematics from EMG in amputees. *Medical and Biological Engineering and Computing*. https://doi.org/10.1007/s11517-012-0979-4

Johanson, M. E., Skinner, S. R., Lamoreux, L. W., Helen, R. S., Moran, S. A., & Ashley, R. K. (1990). Phasic relationships of the extrinsic muscles of the normal hand. *Journal of Hand Surgery*. https://doi.org/10.1016/S0363-5023(09)90020-X

Johansson, R. S., Backlin, J. L., & Burstedt, M. K. O. (1999). Control of grasp stability during pronation and supination movements. *Experimental Brain Research*. https://doi.org/10.1007/s002210050813

Johnston, J. A., Bobich, L. R., & Santello, M. (2010). Coordination of intrinsic and extrinsic hand muscle activity as a function of wrist joint angle during two-digit grasping. *Neuroscience Letters*, *474*(2), 104–108.

Johnston, J. A., Winges, S. A., & Santello, M. (2005). Periodic modulation of motor-unit activity in extrinsic hand muscles during multidigit grasping. *Journal of Neurophysiology*. https://doi.org/10.1152/jn.01134.2004

Jones, L. A., & Lederman, S. J. (2007). Human Hand Function. In *Human Hand Function*. https://doi.org/10.1093/acprof:oso/9780195173154.001.0001

Kamavuako, E. N., Farina, D., Yoshida, K., & Jensen, W. (2009). Relationship between grasping force and features of single-channel intramuscular EMG signals. *Journal of Neuroscience Methods*. https://doi.org/10.1016/j.jneumeth.2009.09.006

Kamavuako, E. N., & Rosenvang, J. C. (2012). Hysteresis in the electromyography-force relationship: Toward an optimal model for the estimation of force. *Muscle and Nerve*, *46*(5), 755–758. https://doi.org/10.1002/mus.23393

Kamavuako, E. N., Rosenvang, J. C., Bog, M. F., Smidstrup, A., Erkocevic, E., Niemeier, M. J., … Farina, D. (2013). Influence of the feature space on the estimation of hand grasping force from intramuscular EMG. *Biomedical Signal Processing and Control*. https://doi.org/10.1016/j.bspc.2012.05.002

Kapelner, T., Sartori, M., Negro, F., & Farina, D. (2020). Neuro-Musculoskeletal Mapping for Man-Machine interfacing. *Scientific Reports*, *10*(1), 1–10.

Kapelner, T., Vujaklija, I., Jiang, N., Negro, F., Aszmann, O. C., Principe, J., & Farina, D. (2019). Predicting wrist kinematics from motor unit discharge timings for the control of active prostheses. *Journal of NeuroEngineering and Rehabilitation*. https://doi.org/10.1186/s12984-019-0516-x

Keen, D. A., & Fuglevand, A. J. (2003). Role of intertendinous connections in distribution of force in the human extensor digitorum muscle. *Muscle & Nerve*, *28*(5), 614–622.

Keen, D. A., & Fuglevand, A. J. (2004a). Common input to motor neurons innervating the same and different compartments of the human extensor digitorum muscle. *Journal of Neurophysiology*, *91*(1), 57–62. https://doi.org/10.1152/jn.00650.2003

Keen, D. A., & Fuglevand, A. J. (2004b). Distribution of motor unit force in human extensor digitorum assessed by spike-triggered averaging and intraneural microstimulation. *Journal of Neurophysiology*, *91*(6), 2515–2523.

Keir, P. J., Wells, R. P., & Ranney, D. A. (1996). Passive properties of the forearm musculature with reference to hand and finger postures. *Clinical Biomechanics*, *11*(7), 401–409.

Kilbreath, S. L., & Gandevia, S. C. (1994). Limited independent flexion of the thumb and fingers in human subjects. *The Journal of Physiology*, *479*(3), 487–497. https://doi.org/10.1113/jphysiol.1994.sp020312

Kilbreath, S. L., Gorman, R. B., Raymond, J., & Gandevia, S. C. (2002). Distribution of the forces produced by motor unit activity in the human flexor digitorum profundus. *The Journal of Physiology*, *543*(1), 289–296.

Kursa, K., Lattanza, L., Diao, E., & Rempel, D. (2006). In vivo flexor tendon forces increase with finger and wrist flexion during active finger flexion and extension. *Journal of Orthopaedic Research*. https://doi.org/10.1002/jor.20110

Lang, C. E., & Schieber, M. H. (2004). Human finger independence: limitations due to passive mechanical coupling versus active neuromuscular control. *Journal of Neurophysiology*, *92*(5), 2802–2810.

Latash, M. L., Scholz, J. P., & Schöner, G. (2002). Motor control strategies revealed in the structure of motor variability. *Exercise and Sport Sciences Reviews*. https://doi.org/10.1097/00003677-200201000-00006

Lehman, S. L., & Calhoun, B. M. (1990). An identified model for human wrist movements. *Experimental Brain Research*. https://doi.org/10.1007/BF00230116

Leijnse, J. N. A. L., Campbell-Kyureghyan, N. H., Spektor, D., & Quesada, P. M. (2008). Assessment of individual finger muscle activity in the extensor digitorum communis by surface EMG. *Journal of Neurophysiology*, *100*(6), 3225–3235. https://doi.org/10.1152/jn.90570.2008

Leijnse, J. N. A. L., Carter, S., Gupta, A., & McCabe, S. (2008). Anatomic basis for individuated surface EMG and homogeneous electrostimulation with neuroprostheses of the extensor digitorum communis. *Journal of Neurophysiology*. https://doi.org/10.1152/jn.00706.2007

Leijnse, J. N. A. L., Walbeehm, E. T., Sonneveld, G. J., Hovius, S. E. R., & Kauer, J. M. G. (1997). Connections between the tendons of the musculus flexor digitorum profundus involving the synovial sheaths in the carpal tunnel. *Cells Tissues Organs*, *160*(2), 112–122.

Leo, A., Handjaras, G., Bianchi, M., Marino, H., Gabiccini, M., Guidi, A., … Ricciardi, E. (2016). A synergy-based hand control is encoded in human motor cortical areas. *ELife*. https://doi.org/10.7554/eLife.13420

Leone, F., Gentile, C., Ciancio, A. L., Gruppioni, E., Davalli, A., Sacchetti, R., … Zollo, L. (2019). Simultaneous sEMg classification of hand/wrist gestures and forces. *Frontiers in Neurorobotics*. https://doi.org/10.3389/fnbot.2019.00042

Li, Z.-M. (2002). The influence of wrist position on individual finger forces during forceful grip. *Journal of Hand Surgery*. https://doi.org/10.1053/jhsu.2002.35078

Li, Z.-M., Latash, M. L., & Zatsiorsky, V. M. (1998). Force sharing among fingers as a model of the redundancy problem. *Experimental Brain Research*, *119*(3), 276–286.

Li, Z.-M., Zatsiorsky, V. M., & Latash, M. L. (2000). Contribution of the extrinsic and intrinsic hand muscles to the moments in finger joints. *Clinical Biomechanics*. https://doi.org/10.1016/S0268-0033(99)00058-3

Linburg, R. M., & Comstock, B. E. (1979). Anomalous tendon slips from the flexor pollicis longus to the flexor digitorum profundus. *Journal of Hand Surgery*. https://doi.org/10.1016/S0363-5023(79)80110-0

Lloyd, D. G., & Besier, T. F. (2003). An EMG-driven musculoskeletal model to estimate muscle forces and knee joint moments in vivo. *Journal of Biomechanics*. https://doi.org/10.1016/S0021-9290(03)00010-1

Lloyd, D. G., & Buchanan, T. S. (1996). A Model of Load Sharing Between Muscles and Soft Tissues at the Human Knee During Static Tasks. *Journal of Biomechanical Engineering*. https://doi.org/10.1115/1.2796019

Loren, G. J., Shoemaker, S. D., Burkholder, T. J., Jacobson, M. D., Friden, J., & Lieber, R. L. (1996). Human wrist motors: biomechanical design and application to tendon transfers. *Journal of Biomechanics*, *29*(3), 331–342.

Lynn, P. A., Bettles, N. D., Hughes, A. D., & Johnson, S. W. (1978). Influence of electrode geometry on bipolar recordings of the surface electromyogram. *Medical & Biological Engineering & Computing*. https://doi.org/10.1007/BF02442444

Malerich, M. M., Baird, R. A., McMaster, W., & Erickson, J. M. (1987). Permissible limits of flexor digitorum profundus tendon advancement—An anatomic study. *Journal of Hand Surgery*. https://doi.org/10.1016/S0363-5023(87)80156-9

Mason, C. R., Gomez, J. E., & Ebner, T. J. (2001). Hand synergies during reach-to-grasp. *Journal of Neurophysiology*. https://doi.org/10.1152/jn.2001.86.6.2896

Mateo, S., Revol, P., Fourtassi, M., Rossetti, Y., Collet, C., & Rode, G. (2013). Kinematic characteristics of tenodesis grasp in C6 quadriplegia. *Spinal Cord*. https://doi.org/10.1038/sc.2012.101

Mathiesen, J. R., Bøg, M. F., Erkocevic, E., Niemeier, M. J., Smidstrup, A., & Kamavuako, E. N. (2010). Prediction of grasping force based on eatures of surface and intramuscular EMG. *7th Semester Conference Paper*, 1–9.

McDonnall, D., Hiatt, S., Smith, C., & Guillory, K. S. (2012). Implantable multichannel wireless electromyography for prosthesis control. *Proceedings of the Annual International Conference of the IEEE Engineering in Medicine and Biology Society, EMBS*. https://doi.org/10.1109/EMBC.2012.6346188

Mcfarland, L. V., Winkler, S. L. H., Heinemann, A. W., Jones, M., & Esquenazi, A. (2010). Unilateral upper-limb loss: Satisfaction and prosthetic-device use in veterans and servicemembers from Vietnam and OIF/OEF conflicts. *Journal of Rehabilitation Research and Development*. https://doi.org/10.1682/JRRD.2009.03.0027

Merrill, D. R., Lockhart, J., Troyk, P. R., Weir, R. F., & Hankin, D. L. (2011). Development of an Implantable Myoelectric Sensor for Advanced Prosthesis Control. *Artificial Organs*. https://doi.org/10.1111/j.1525-1594.2011.01219.x

Mogk, J. P. M., & Keir, P. J. (2003). The effects of posture on forearm muscle loading during gripping. *Ergonomics*. https://doi.org/10.1080/0014013031000107595

Morse, J. L., Jung, M. C., Bashford, G. R., & Hallbeck, M. S. (2006). Maximal dynamic grip force and wrist torque: The effects of gender, exertion direction, angular velocity, and wrist angle. *Applied Ergonomics*. https://doi.org/10.1016/j.apergo.2005.11.008

Napier, J. R. (1960). Studies of the Hands of Living Primates. *Proceedings of the Zoological Society of London*. https://doi.org/10.1111/j.1469-7998.1960.tb05606.x

Nazemi, A., & Maleki, A. (2014). Artificial neural network classifier in comparison with LDA and LS-SVM classifiers to recognize 52 hand postures and movements. *Proceedings of the 4th International Conference on Computer and Knowledge Engineering, ICCKE 2014*. https://doi.org/10.1109/ICCKE.2014.6993343

Noce, E., Dellacasa Bellingegni, A., Ciancio, A. L., Sacchetti, R., Davalli, A., Guglielmelli, E., & Zollo, L. (2019). EMG and ENG-envelope pattern recognition for prosthetic hand control. *Journal of Neuroscience Methods*. https://doi.org/10.1016/j.jneumeth.2018.10.004

Overduin, S. A., d'Avella, A., Carmena, J. M., & Bizzi, E. (2014). Muscle synergies evoked by microstimulation are preferentially encoded during behavior. *Frontiers in Computational Neuroscience*. https://doi.org/10.3389/fncom.2014.00020

Overduin, S. A., D'Avella, A., Roh, J., & Bizzi, E. (2008). Modulation of muscle synergy recruitment in primate grasping. *Journal of Neuroscience*. https://doi.org/10.1523/JNEUROSCI.2869-07.2008

Paclet, F., & Quaine, F. (2012). Motor control theories improve biomechanical model of the hand for finger pressing tasks. *Journal of Biomechanics*. https://doi.org/10.1016/j.jbiomech.2012.01.038

Pan, L., Crouch, D. L., & Huang, H. (2019). Comparing EMG-based human-machine interfaces for estimating continuous, coordinated movements. *IEEE Transactions on Neural Systems and Rehabilitation Engineering*. https://doi.org/10.1109/TNSRE.2019.2937929

Pasquina, P. F., Evangelista, M., Carvalho, A. J., Lockhart, J., Griffin, S., Nanos, G., … Hankin, D. (2014). First-in-man demonstration of a fully implanted myoelectric sensors system to control an advanced electromechanical prosthetic hand. *Journal of Neuroscience Methods*. https://doi.org/10.1016/j.jneumeth.2014.07.016

Phinyomark, A., Quaine, F., Charbonnier, S., Serviere, C., Tarpin-Bernard, F., & Laurillau, Y. (2013). EMG feature evaluation for improving myoelectric pattern recognition robustness. *Expert Systems with Applications*. https://doi.org/10.1016/j.eswa.2013.02.023

Rayan, G. M., & Akelman, E. (2012). *The Hand: Anatomy, Examination, and Diagnosis*. Retrieved from https://books.google.com/books?id=eVTVkUAp7-4C

Reilly, K. T., Nordstrom, M. A., & Schieber, M. H. (2004). Short-term synchronization between motor units in different functional subdivisions of the human flexor digitorum profundus muscle. *Journal of Neurophysiology*. https://doi.org/10.1152/jn.00027.2004

Reilly, K. T., & Schieber, M. H. (2003). Incomplete functional subdivision of the human multitendoned finger muscle flexor digitorum profundus: An electromyographic study. *Journal of Neurophysiology*, *90*(4), 2560–2570. https://doi.org/10.1152/jn.00287.2003

Resnik, L., Huang, H., Winslow, A., Crouch, D. L., Zhang, F., & Wolk, N. (2018). Evaluation of EMG pattern recognition for upper limb prosthesis control: A case study in comparison with direct myoelectric control. *Journal of NeuroEngineering and Rehabilitation*. https://doi.org/10.1186/s12984-018-0361-3

Resnik, L., Klinger, S. L., & Etter, K. (2014). The DEKA Arm: Its features, functionality, and evolution during the veterans affairs study to optimize the DEKA Arm. *Prosthetics and Orthotics International*. https://doi.org/10.1177/0309364613506913

Roman-Liu, D., & Bartuzi, P. (2013). The influence of wrist posture on the time and frequency EMG signal measures of forearm muscles. *Gait and Posture*, *37*(3), 340–344. https://doi.org/10.1016/j.gaitpost.2012.07.027

Salonikidis, K., Amiridis, I. G., Oxyzoglou, N., De Villareal, E. S. S., Zafeiridis, A., & Kellis, E. (2009). Force variability during isometric wrist flexion in highly skilled and sedentary individuals. *European Journal of Applied Physiology*. https://doi.org/10.1007/s00421-009-1184-5

Santello, M., Flanders, M., & Soechting, J. F. (1998). Postural hand synergies for tool use. *Journal of Neuroscience*. https://doi.org/10.1523/jneurosci.18-23-10105.1998

Santello, M., Flanders, M., & Soechting, J. F. (2002). Patterns of hand motion during grasping and the influence of sensory guidance. *Journal of Neuroscience*. https://doi.org/10.1523/jneurosci.22-04-01426.2002

Sartori, M., Durandau, G., Došen, S., & Farina, D. (2018). Robust simultaneous myoelectric control of multiple degrees of freedom in wrist-hand prostheses by real-time neuromusculoskeletal modeling. *Journal of Neural Engineering*. https://doi.org/10.1088/1741-2552/aae26b

Savage, R. (1988). The influence of wrist position on the minimum force required for active movement of the interphalangeal joints. *Journal of Hand Surgery*. https://doi.org/10.1016/0266-7681(88)90082-4

Scheme, E., & Englehart, K. (2011). Electromyogram pattern recognition for control of powered upper-limb prostheses: State of the art and challenges for clinical use. *Journal of Rehabilitation Research and Development*. https://doi.org/10.1682/JRRD.2010.09.0177

Scheme, E., & Englehart, K. (2014). On the robustness of EMG features for pattern recognition based myoelectric control; a multi-dataset comparison. *2014 36th Annual International Conference of the IEEE Engineering in Medicine and Biology Society*, 650–653. IEEE.

Schenck, R. R. (1964). Variations of the extensor tendons of the fingers. *The Journal of Bone and Joint Surgery. American Volume*. https://doi.org/10.2106/00004623-196446010-00010

Schieber, M. H. (1991). Individuated finger movements of rhesus monkeys: A means of quantifying the independence of the digits. *Journal of Neurophysiology*. https://doi.org/10.1152/jn.1991.65.6.1381

Schieber, M. H. (1995). Muscular production of individuated finger movements: The roles of extrinsic finger muscles. *Journal of Neuroscience*.

Schieber, M. H. (1996). Individuated Finger Movements: Rejecting the Labeled-Line Hypothesis. *Hand and Brain*. https://doi.org/10.1016/B978-012759440-8/50008-6

Schieber, M. H., Gardinier, J., & Liu, J. (2001). Tension distribution to the five digits of the hand by neuromuscular compartments in the macaque flexor digitorum profundus. *Journal of Neuroscience*, *21*(6), 2150–2158.

Schieber, M. H., & Hibbard, L. S. (1993). How somatotopic is the motor cortex hand area? *Science*. https://doi.org/10.1126/science.8332915

Schieber, M. H., & Santello, M. (2004). Hand function: peripheral and central constraints on performance. *Journal of Applied Physiology*, *96*(6), 2293–2300. https://doi.org/10.1152/japplphysiol.01063.2003

Sears, H. H., & Shaperman, J. (1991). Proportional myoelectric hand control: An evaluation. *American Journal of Physical Medicine and Rehabilitation*. https://doi.org/10.1097/00002060-199102000-00005

Segil, J. L., Huddle, S. A., & Weir, R. F. F. (2017). Functional Assessment of a Myoelectric Postural Controller and Multi-Functional Prosthetic Hand by Persons with Trans-Radial Limb Loss. *IEEE Transactions on Neural Systems and Rehabilitation Engineering*. https://doi.org/10.1109/TNSRE.2016.2586846

Simon, A. M., Lock, B. A., Stubblefield, K. a, & Hargrove, L. J. (2011). Prosthesis-Guided Training Increases Functional Wear Time And Improves Tolerance To Malfunctioning Inputs Of Pattern Recognition–Controlled Prostheses. *Proc. MyoElectric Controls/Powered Prosthetics Symposium, MEC 11*.

Smith, L. H., Kuiken, T. A., & Hargrove, L. J. (2014). Real-time simultaneous and proportional myoelectric control using intramuscular EMG. *Journal of Neural Engineering*. https://doi.org/10.1088/1741-2560/11/6/066013

Smith, L. H., Kuiken, T. A., & Hargrove, L. J. (2016). Evaluation of linear regression simultaneous myoelectric control using intramuscular EMG. *IEEE Transactions on Biomedical Engineering*, *63*(4), 737–746. https://doi.org/10.1109/TBME.2015.2469741

Sobinov, A., Boots, M. T., Gritsenko, V., Fisher, L. E., Gaunt, R. A., & Yakovenko, S. (2019). Approximating complex musculoskeletal biomechanics using multidimensional autogenerating polynomials. *BioRxiv*. https://doi.org/10.1101/759878

Solomonow, M., Baratta, R. V., & D'Ambrosia, R. (1991). EMG-force relations of a single skeletal muscle acting across a joint: Dependence on joint angle. *Journal of Electromyography and Kinesiology*. https://doi.org/10.1016/1050-6411(91)90027-3

Takei, T., Confais, J., Tomatsu, S., Oya, T., & Seki, K. (2017). Neural basis for hand muscle synergies in the primate spinal cord. *Proceedings of the National Academy of Sciences of the United States of America*. https://doi.org/10.1073/pnas.1704328114

Takei, T., & Seki, K. (2010). Spinal interneurons facilitate coactivation of hand muscles during a precision grip task in monkeys. *Journal of Neuroscience*. https://doi.org/10.1523/JNEUROSCI.4297-10.2010

Tanaka, T., Amadio, P. C., Zhao, C., Zobitz, M. E., & An, K. N. (2005). Flexor digitorum profundus tendon tension during finger manipulation: A study in human cadaver hands. *Journal of Hand Therapy*. https://doi.org/10.1197/j.jht.2005.04.001

Taylor, C. L., & Schwarz, R. J. (1955). The anatomy and mechanics of the human hand. *Artificial Limbs*.

Tenore, F., Ramos, A., Fahmy, A., Acharya, S., Etienne-Cummings, R., & Thakor, N. V. (2007). Towards the control of individual fingers of a prosthetic hand using surface EMG signals. *Conference Proceedings : ... Annual International Conference of the IEEE Engineering in Medicine and Biology Society. IEEE Engineering in Medicine and Biology Society. Conference*.

Tortora, G. J., & Derrickson, B. H. (2018). *Principles of anatomy and physiology*. John Wiley & Sons.

touch bionics Product Catalog. (2015). touch bionics.

Valero-Cuevas, F. J. (2000). Predictive modulation of muscle coordination pattern magnitude scales fingertip force magnitude over the voluntary range. *Journal of Neurophysiology*. https://doi.org/10.1152/jn.2000.83.3.1469

van Beek, N., Stegeman, D. F., van den Noort, J. C., Veeger, D. J., & Maas, H. (2018). Activity patterns of extrinsic finger flexors and extensors during movements of instructed and non-instructed fingers. *Journal of Electromyography and Kinesiology*. https://doi.org/10.1016/j.jelekin.2017.02.006

van Duinen, H., Yu, W. S., & Gandevia, S. C. (2009). Limited ability to extend the digits of the human hand independently with extensor digitorum. *Journal of Physiology*. https://doi.org/10.1113/jphysiol.2009.177964

von Schroeder, H. P., & Botte, M. J. (1995). Anatomy of the extensor tendons of the fingers: Variations and multiplicity. *Journal of Hand Surgery*. https://doi.org/10.1016/S0363-5023(05)80053-X

Von Schroeder, H. P., & Botte, M. J. (2001). Anatomy and functional significance of the long extensors to the fingers and thumb. *Clinical Orthopaedics and Related Research*. https://doi.org/10.1097/00003086-200102000-00010

Wang, L., & Buchanan, T. S. (2002). Prediction of joint moments using a neural network model of muscle activations from EMG signals. *IEEE Transactions on Neural Systems and Rehabilitation Engineering*. https://doi.org/10.1109/TNSRE.2002.1021584

Weiss, E. J., & Flanders, M. (2004). Muscular and postural synergies of the human hand. *Journal of Neurophysiology*. https://doi.org/10.1152/jn.01265.2003

Werremeyer, M. M., & Cole, K. J. (1997). Wrist action affects precision grip force. *Journal of Neurophysiology*. https://doi.org/10.1152/jn.1997.78.1.271

White, M. M., Zhang, W., Winslow, A. T., Zahabi, M., Zhang, F., Huang, H., & Kaber, D. B. (2017). Usability Comparison of Conventional Direct Control Versus Pattern Recognition Control of Transradial Prostheses. *IEEE Transactions on Human-Machine Systems*. https://doi.org/10.1109/THMS.2017.2759762

Williams, T. W., Meier, R. H., & Atkins, D. J. (2004). Control of powered upper extremity prostheses. *Functional Restoration of Adults and Children with Upper Extremity Amputation*, *207*, 224.

Willison, R. G. (1964). Analysis of electrical activity in healthy and dystrophic muscle in man. *Journal of Neurology, Neurosurgery, and Psychiatry*. https://doi.org/10.1136/jnnp.27.5.386

Winges, S. A., Johnston, J. A., & Santello, M. (2006). Muscle-pair specific distribution and grip-type modulation of neural common input to extrinsic digit flexors. *Journal of Neurophysiology*. https://doi.org/10.1152/jn.00327.2006

Winges, S. A., & Santello, M. (2004). Common input to motor units of digit flexors during multi-digit grasping. *Journal of Neurophysiology*. https://doi.org/10.1152/jn.00516.2004

Young, A. J., Smith, L. H., Rouse, E. J., & Hargrove, L. J. (2013). Classification of simultaneous movements using surface EMG pattern recognition. *IEEE Transactions on Biomedical Engineering*. https://doi.org/10.1109/TBME.2012.2232293

Yu, W. S., van Duinen, H., & Gandevia, S. C. (2010). Limits to the control of the human thumb and fingers in flexion and extension. *Journal of Neurophysiology*. https://doi.org/10.1152/jn.00797.2009

Zajac, F. E. (1989). Muscle and tendon: properties, models, scaling, and application to biomechanics and motor control. *Critical Reviews in Biomedical Engineering*, *17*(4), 359–411.

Zatsiorsky, V. M., Li, Z.-M., & Latash, M. L. (2000). Enslaving effects in multi-finger force production. *Experimental Brain Research*, *131*(2).

Zhang, D., Zhao, X., Han, J., & Zhao, Y. (2014). A comparative study on PCA and LDA based EMG pattern recognition for anthropomorphic robotic hand. *Proceedings - IEEE International Conference on Robotics and Automation*. https://doi.org/10.1109/ICRA.2014.6907569

Ziegler-Graham, K., MacKenzie, E. J., Ephraim, P. L., Travison, T. G., & Brookmeyer, R. (2008). Estimating the Prevalence of Limb Loss in the United States: 2005 to 2050. *Archives of Physical Medicine and Rehabilitation*. https://doi.org/10.1016/j.apmr.2007.11.005